



## Project UpWind

Contract No.:  
019945 (SES6)

“Integrated Wind Turbine Design”



# Experiments and modelling of influence and interaction of temperature and frequency on fatigue life

AUTHOR:	Rogier Nijssen, Laurent Cormier
AFFILIATION:	Knowledge Centre Wind turbine Materials and Constructions
ADDRESS:	Kluisgat 5, 1771 MV Wieringerwerf, the Netherlands
TEL.:	+31 (0) 227-504927/49
EMAIL:	<a href="mailto:r.p.l.nijssen@wmc.eu">r.p.l.nijssen@wmc.eu</a>
FURTHER AUTHORS:	
REVIEWER:	
APPROVER:	

### Document Information

DOCUMENT TYPE	Test Report
DOCUMENT NAME:	Deliverable D 3.1.8 / WMC-2010-94
REVISION:	01
REV. DATE:	
CLASSIFICATION:	
STATUS:	Deliverable

## CONTENTS

1. Introduction .....	5
2. Test programme .....	5
3. Specimens and Test set-up .....	6
4. State of the art .....	8
4.1 Static behavior .....	8
4.1.1 Constituent scale effects .....	8
4.1.2 Laminate scale effects .....	9
4.2 Fatigue behavior .....	10
4.2.1 Fatigue Modelling .....	10
4.2.2 Effects of temperature .....	10
4.2.3 Effects of frequency .....	11
4.2.4 Combined temperature and frequency effects .....	11
5. Results and Discussion .....	14
5.1 Static tests .....	14
5.1.1 Tension .....	14
5.1.2 Compression .....	17
5.2 Fatigue tests .....	19
5.2.1 R = 0.1 .....	19
5.2.2 R = -1 .....	23
5.3 Influence of temperature .....	26
5.4 Influence of frequency .....	29
6. Concluding remarks .....	33
7. Acknowledgement .....	33
8. References .....	33
ANNEX A Selected specimen pictures before testing .....	36
ANNEX B Measurement summaries .....	50
ANNEX C Selected specimen pictures after testing .....	66

## LIST OF FIGURES

Figure 1: Reference specimen (planform code R08).....	6
Figure 2: Test set-up using Zwick 220 kN (left) and ZB 100 kN maximum capacity test frames next to Espec external climate chamber .....	7
Figure 3: Analytical evaluation of the amount of cycles to failure with increasing loading frequency [19] .....	12
Figure 4: Analytical evaluation of damage growth per cycle with increasing loading frequency [19] .....	12
Figure 5: S-N curves by Mandell and Meier.....	13
Figure 6: Geometry type 1A defined in ISO 527 standard (dimensions in mm) .....	13
Figure 7: Average tensile strengths at -40 °C, 23 °C and 60 °C.....	16
Figure 8: Average tensile moduli at -40 °C, 23 °C and 60 °C .....	17
Figure 9: Average compressive strengths at -40 °C, 23 °C and 60 °C.....	18
Figure 10: Average compressive moduli at -40 °C, 23 °C and 60 °C.....	19
Figure 11: S-N diagram for R=0.1 fatigue at -40 °C, 23 °C and 60 °C. ....	27
Figure 12: S-N diagram for R=-1 fatigue at -40 °C, 23 °C and 60 °C. ....	27
Figure 13: Life vs. temperature for tension-tension fatigue at R=0.1.....	28
Figure 14: Life vs. temperature for tension-compression fatigue at R=-1.....	29
Figure 15: S-N diagram for R=0.1 fatigue at intermediate (CAM) and low (CA) frequencies.....	30
Figure 16: S-N diagram for R=0.1 fatigue at high (CAH) and low (CA) frequencies. ....	30
Figure 17: S-N diagram for R=-1 fatigue at high (CAH) and low (CA) frequencies. ....	31
Figure 18: Life-frequency diagram for R=0.1 fatigue. ....	32
Figure 19: Life-frequency diagram for R=-1 fatigue. ....	32

## LIST OF TABLES

Table 1: Test programme for temperature and frequency effect .....	5
Table 2: Reference material constituent specifications .....	6
Table 3: Maximum stress and E-modulus as a function of temperature (of short glass fibre reinforced polyamide 6) [21].....	14
Table 4: Fatigue strength at 10 <sup>6</sup> cycles and slope (k) of the S-N curve (of short glass fibre reinforced polyamide 6) [21].....	14
Table 5: Tensile test results .....	15
Table 6: Average mechanical properties for tensile tests .....	16
Table 7: Compressive tests results .....	17
Table 8: Average mechanical properties for compressive tests .....	18
Table 9: Tension-tension fatigue test results at room temperature (23 °C).....	19
Table 10: Tension-tension fatigue test results at room temperature -40 °C .....	21
Table 11: Tension-tension fatigue test results at room temperature 60 °C .....	22
Table 12: Tension-compression fatigue test results at room temperature (23 °C).....	24
Table 13: Tension-compression fatigue test results at -40 °C .....	25
Table 14: Tension-compression fatigue test results at 60 °C .....	26

STATUS, CONFIDENTIALITY AND ACCESSIBILITY						
Status		Confidentiality			Accessibility	
<b>S0</b>	Approved/Released	<b>R0</b>	General public	<b>x</b>	Private web site	
<b>S1</b>	Reviewed	<b>R1</b>	Restricted to project members		Public web site	
<b>S2</b>	Pending for review	<b>R2</b>	Restricted to European. Commission		Paper copy	
<b>S3</b>	Draft for comments	<b>R3</b>	Restricted to WP members + PL			

RECORD OF CHANGES			
Rev	Date	Author	Description
00	22/12/2010	R. Nijssen	Initial draft version
01	10/02/2011	R. Nijssen, L. Cormier	Final version

# 1. INTRODUCTION

This report describes the tests carried out within UPWIND WP3, subtask 3.1, aimed at providing data for better understanding and modeling of the alleged temperature and frequency effect in composite materials in fatigue. The majority of the work was carried out in the laboratory of WMC between 2006 and 2011.

In previous projects, e.g. the OPTIMAT programme [1], testing at a higher frequency was shown to lead to lower lifetimes. This was attributed to internal heating of the laminate, through visco-elastic effects and friction, combined with the poor heat conductivity of glass/epoxy laminates.

To optimise fatigue data collection in the OPTIMAT programme, the fatigue test frequencies were related to load level following a strain range related rule [2], and since then, measurement of the external temperature near the tab during a fatigue test has been performed consistently during UPWIND.

Nevertheless, at the time it was not in the scope of the OPTIMAT project to de-couple the alleged effects of temperature and frequency on the fatigue life. To this end, a dedicated test programme was foreseen within the UPWIND project [3].

The objective of this work is to qualify and quantify the effect of temperature and frequency on fatigue life of the UPWIND reference material.

An extensive test program was carried out in a test frame equipped with climate facility, so that the test conditions and loading frequencies could be independently controlled. The results from these tests are documented in this report.

# 2. TEST PROGRAMME

The original tentative test programme is outlined in the WP 3.1 detailed plan of action [3]. Also indicated is the actual test programme that was conducted.

**Table 1: Test programme for temperature and frequency effect**

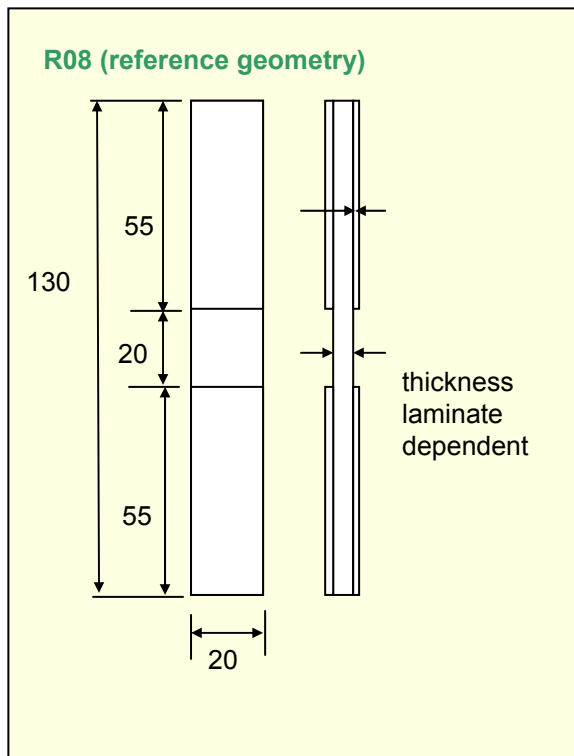
Loading type	Condition	Target N	Frequency
Static	Room Temperature, -40°C, +60°C	<b>1</b>	<b>1 mm/min</b>
R=0.1	Room Temperature, -40°C, +60°C	<b>10000</b>	<b>2, 8, 24</b>
	Room Temperature, -40°C, +60°C	<b>1000000</b>	<b>6, 8, 24</b>
R=-1	Room Temperature, -40°C, +60°C	<b>10000</b>	<b>1, 24</b>
	Room Temperature, -40°C, +60°C	<b>1000000</b>	<b>3, 24</b>

### 3. SPECIMENS AND TEST SET-UP

The UPWIND reference specimen constituent material, lay-up, and specimen geometry are shown in Table 2, and in Figure 1.

**Table 2: Reference material constituent specifications**

Matrix	Resin	Hardener	Mixing ratio	Density	Curing conditions
	L135i	134i 137i	-	100/30 by weight	1.15 (cured)
Reinforcement	Construction	Areal weight [g/m <sup>2</sup> ]	Tolerance [±%]		Material
	<i>total</i>	963	5		UD
	<i>0°</i>	864	5		PPG2002 2400 tex
	<i>90°</i>	40	5		OC 111A 200 tex
	<i>90°</i>	41	5		PPG2002 68 tex
<i>stitching</i>	18	5		PES	



**Figure 1: Reference specimen (planform code R08)**

A picture of the test set-ups used at WMC in this project is shown in Figure 2. Tests at -40° were also performed at VTT, Finland.



**Figure 2: Test set-up using Zwick 220 kN (left) and ZB 100 kN maximum capacity test frames next to Espec external climate chamber**

Part of the tests was performed on the Zwick 220 kN maximum capacity test frame, but the majority was carried out in the ZB 100 kN test frame.

The test set-up consists of a servo-hydraulic test frame. The test area is enclosed in an insulating box. Measures were taken to thermally insulate the grips from the moving actuator and load cell, as well as measures to provide corrosion protection. The test area obtains cooled, heated and/or humidified air from the adjacent Espec external climate chamber. This air is circulated through the system, and the settings of the external climate chamber are adjusted based on the temperature measurements in the test area.

The mounting procedure was the same for all specimens. First, the specimen is gripped in the lower grips, the specimen is allowed to reach test conditions, and the strain gauges are balanced. Subsequently, the top grips are closed. This allows measurement of bending due to curvature or grip misalignment.

Static tests are carried out at a constant grip displacement rate of 1 mm/min, in displacement control mode. Fatigue tests are carried out at load control mode. Load and displacements are recorded from the test frame load cell and actuator LVDT displacement sensor, respectively. Temperature is measured by a temperature sensor bonded to the side of the specimen, close to the gripped area.

Prior to the fatigue tests, a 'slow' cycle was carried out, to obtain quasi-static data recorded at 50 Hz. The information in these files was used to obtain values for the (initial) stiffness from the strain gauges' and load cell signals. In static tests, data was recorded at the same data acquisition rate. In fatigue tests, the periodic maxima and minima were recorded at logarithmically increasing intervals.

The room temperature tests were typically not carried out with the Espec climate chamber.

Pictures of specimens before testing are shown in ANNEX A. Examples of static and fatigue measurements are shown in ANNEX B.

## 4. STATE OF THE ART

A brief review of relevant literature is presented herein. First, published work on the effects of temperature on static strength are presented. The state of the art relating to temperature and frequency effects on the fatigue behavior of composite materials is then discussed.

### 4.1 STATIC BEHAVIOR

Effect of high temperatures on polymer matrix composite material properties have been the subject of several research since the early days of advanced composites. However, study of the effects of low, but non-cryogenic, temperatures on the mechanical properties of laminates and on bonded joints enjoyed much less attention. A paper from Liu and Kharbari suggests that the need for further research in the area of hygrothermal effects, including cold temperature, are significant before composites can be widely used in common structures. As a result, it is suggested that this topic be further investigated [4].

Temperature can affect composite material properties at several scales. For example, it can create internal stresses at constituent level or at ply level. Therefore, thermal effects on static properties are first discussed with a focus on the microstructural or constituent level behavior. Then considerations for laminate scale and macroscopic scale are presented. Note that this literature review focuses on the thermal effects on properties of thermoset matrix composite systems.

#### 4.1.1 Constituent scale effects

Although most inorganic fibers are not very sensitive to the range of temperatures applicable to polymer composites, the matrix is sensitive to thermal conditions. In general, a thermoset polymer system is in a glassy (stiff and brittle) state if its temperature is below a threshold usually known as the glass transition temperature ( $T_g$ ). If the temperature approaches this threshold, the polymer's stiffness rapidly declines and its internal damping increases until the material reaches a state where viscous effects are dominant. This condition is known as the rubbery state. It is however worth noting that some polymers also show an increase in internal damping at specific low temperatures. These temperatures are usually referred to as  $T_\beta$  and  $T_\gamma$ . These changes in material behavior are believed to be the results of molecular chains arrangements. At elevated temperatures, dilatations allow for increased chain mobility, resulting in a loss of modulus and increase in internal damping. On the other hand, low temperature reduces chain mobility, thus resulting in increased stiffness, strength and brittleness. Lower temperature transitions are not very well understood but are also believed to be due to chain rearrangement [5][6].

An empirical relation, modeled after tests on six epoxy resin systems, was proposed by Chamis to evaluate the mechanical properties of polymers under the influence of temperature (under  $T_g$ ) and absorbed moisture (Equation 1) [7][8].

#### Equation 1

$$F_m = \frac{P}{P_0} = \left[ \frac{T_{gw} - T}{T_{g0} - T_0} \right]^{1/2}$$

Where

- $F_m$  = Matrix property retention factor;
- $P$  = Matrix degraded property;
- $P_0$  = Matrix initial property;
- $T_{gw}$  = Moisture degraded glass transition temperature (°F);
- $T$  = Actual temperature (°F);
- $T_{g0}$  = Nominal glass transition temperature (°F);
- $T_0$  = Reference temperature (°F);

and where :

#### Equation 2

$$T_{gw} = (0,005 * M_r^2 - 0,10 * M_r + 1) * T_{g0}$$

with  $M_r$  = Mass fraction of absorbed moisture in the matrix.



Equation 1 suggests a linear change in polymer mechanical properties with temperature. However, literature suggests that while close to  $T_G$ , properties may vary abruptly but linearly between an upper and a lower threshold. Outside these bounds, mechanical properties are expected to display a slower variation, although possibly still linear [6]. Therefore, the validity of Chamis' model for low temperatures far from  $T_G$  may be questioned.

Like all other materials, composite constituents undergo dimensional changes when exposed to a temperature increase or decrease. However, composite material themselves are heterogeneous and all phases may not react the same way to the thermal loading. Moreover, these phases are usually solidly bonded together and must remain under dimensional equilibrium. Therefore, internal strains will arise from temperature changes in composites. These are in addition to any pre-existing strains due to matrix shrinkage during polymerization or external loads. Usually, fibers can be expected to have a coefficient of thermal expansion (CTE) about an order of magnitude lower than matrices and some fibers, like carbon and aramid, may have anisotropic behavior and/or negative CTE. [6].

Lord and Dutta, have proposed a micromechanics model to evaluate the fiber and matrix axial stresses due to temperature changes ( $\sigma^T$ ). According to this equation, constituent stresses are a function of their respective modulus (E), CTE ( $\alpha$ ) and of the fiber volume fraction ( $v_f$ ) as per Equation 3 and Equation 4, where subscript f and m respectively indicate fiber and matrix properties. It is suggested that the reference temperature for the (thermal) stress free state should be close to  $T_G$  because during polymerization and later cool down, the matrix can still relieve thermal stresses until  $T_G$  is reached [9].

### Equation 3

$$\sigma_{1m}^T = E_m (\alpha_m - \alpha_c) \Delta T = \frac{E_m E_f v_f (\alpha_m - \alpha_f) \Delta T}{E_f v_f + E_m (1 - v_f)} = \frac{E_m E_f v_f (\alpha_m - \alpha_f) (T_0 - T)}{E_f v_f + E_m (1 - v_f)}$$

### Equation 4

$$\sigma_{1f}^T = -\frac{v_m}{v_f} \sigma_{1m}^T$$

According to Equation 3 and Equation 4, a temperature raise would therefore induce compressive stresses in the matrix and tensile stresses in the fibers while a cool down would induce tensile stress in the matrix and compressive stresses in the fibers. This last remarks then brings the concern that, being slender columns, fibers may buckle if a sufficiently low temperature is reached, in which case, compressive properties of the composite may be significantly degraded.

#### 4.1.2 Laminate scale effects

At the laminate scale, changes in matrix properties should result in laminate properties changes. Modified matrix properties from Equation 1 may be used in the classical laminate theory (CLT) to estimate the material properties. However, it was shown that this approach may not yield adequate results for unidirectional laminates at low temperatures [10]. In this research, tensile, compressive and short beam shear tests were performed at room and -40 °C and an increase in strength was noted at low temperatures, while tensile modulus stayed unaltered. In most cases the changes were shown to be higher than what Equation 1 and the CLT suggested.

The literature review presented in [10] also shows that there is important variability in the conclusions from research on the effect of low temperatures on composites. Different authors conclusions range from suggesting a slight degradation of the material to stating that there is a significant performance improvement. This is thought to be the result of the large number of material constituents, architectures and conditions that are studied.

Macroscopic effects of high temperatures on the mechanical properties of unidirectional E glass-epoxy laminates ( $v_f=65\%$ ) under static loading were studied by Aktas and Karakuzu [11]. They performed tensile and compressive tests, both in the longitudinal and transverse fiber directions, as well as interlaminar and intralaminar shear properties measurements. Test at temperatures ranged from 20 °C to 100 °C in 20 °C increments.

Their work showed unidirectional composites lose strength and stiffness as temperature increase. More specifically, in the fiber direction, modulus remains quite constant up to 60 °C after which temperature, it drop significantly until halved at 100 °C. On the other hand, transverse and shear modulus decrease gradually from 20 °C to 100 °C, temperature where they are more than halved. Poisson's ratio on the other hand seems to remain unchanged by increasing temperature. Longitudinal tensile and compressive strength as well as transverse compressive strength also gradually decrease as temperature increases. Both inter and intralaminar shear strengths also showed a strong negative dependence on temperature, with significantly reduced performance from 40 °C. Transverse tensile strength seems unaffected by a temperature increase. Although no explanation for this specific characteristic is given, one might suggest that transverse tensile failure is brittle and that higher temperature reduce the matrix brittleness, counteracting the expected matrix loss of strength.

Kinsella et al. also present test results for S glass-epoxy unidirectional composites tested between -55 °C and 8 °C [12]. Quasi-static tensile, compressive tests on 0°, ±45° and 90° laminates were performed. These results show that at -55 °C, tensile strength was improved by about 10%. Compressive and shear strength improved by a slightly higher proportion, more in the 15% range. At 80 °C, tensile strength and compressive strengths were reduced by a similar amount while shear strength was reduced by close to 25%. Tensile and compressive modulus remained relatively unaltered by these temperature changes. On the other hand, shear modulus was increased by about 20% at cold temperature and reduced by almost 30% at 80 °C.

## 4.2 FATIGUE BEHAVIOR

The topic of environmental effects on fatigue behavior of composite materials is still not fully addressed. For example, Kharbari suggests that the study of hygrothermal effects on composite materials should focus on adhesive joint and fatigue properties [13]. However, fatigue testing of composite is time consuming due to frequency limitations imposed by hysteretic heating occurring in polymer composite materials. A short review on fatigue modeling and on the effects of temperature, frequency and their combination on fatigue properties of polymer composites is therefore presented.

### 4.2.1 Fatigue Modelling

In time different approaches were developed to analyze fatigue life. Among those analytical, experimental and statistical approaches, the most commonly used is probably Wöhler (S-N) curve [14].

For fatigue under CA loading, the stress-life relation approach is a commonly used technique. The stress-life is implemented by including both the applied stress (S) and the number of cycles to failure (N) at that specific stress level into a graph known as the S-N curve. In an S-N curve the applied stress is plotted on the vertical axis versus the number of cycles to failure on the horizontal axis.

The regression line to be straight when both axes have a logarithmic scale. An S-N curve is characterized by Equation 5 and should intercept the vertical axis at the materials ultimate tensile strength.

#### Equation 5

$$\log N = a \log S + b$$

Where N is the life in cycle, S is the maximum stress and a and b are slope and intercept parameters.

### 4.2.2 Effects of temperature

Hygrothermal effects on fatigue life behaviour of polymer composites was studied by Hai C. Tang et al. [15]. In this paper, a model for predicting the fatigue life of fiber-reinforced polymeric composites was established and verified. Fatigue experiments are made on a glass fiber-vinyl ester composite in air, fresh water and salt water at 30°C. The flat panels consist of a cross-ply laminate made from UD (Uni Directional; most fibers in loading direction) roving and an off-axis random mat of continuous fibers. The specimens are cut into rectangular shapes, 200mm long, 25mm wide and 3.2mm thick.

Fatigue experiments are conducted in a tension-tension mode with a stress ratio of R=0.1. Maximum applied load ranges from 35% to 70% of ultimate tensile strength and frequency is set at 10 Hz for

studying temperature effect. All experiments are conducted at three temperatures: 4 °C, 30 °C and 60°C.

Results from these tests show that for this particular material, the fatigue life at 60°C is about the same as that at 30°C, but the fatigue life at 4°C is significantly longer than that at 30°C. The slope of the S-N curve is also steeper at higher temperatures.

In [16] a short elaboration is given about the research after the fatigue life of the UD material at Room Temperature and 60 °C. The tensile-tensile ( $R = 0.1$ ) fatigue conditions do not show obvious difference in fatigue life at considered conditions. All the data of fatigue life for extreme conditions are within confidence limits of the reference data set. However the data of fatigue life at 60 °C are consistently below the regression line of the reference conditions. The high temperature had little effect on Young's Modulus and strength, but did reduce the fatigue life.

Effects of cold temperatures on the fatigue behavior of polymer matrix composite is very scarcely documented. Work from Bureault and Denault 2004 focused on the effect of temperatures of -40 to 50 on the fatigue behavior of two composite materials. The first composite is a 2-2 glass tweed in a polyester matrix and the second laminate is a biaxial glass fabric in polypropylene resin. Both laminates were of 60 % fiber weight fraction. Tensile fatigue tests were performed at  $R=0.1$  and a frequency of 5 Hz. According to their results, S-N curves for the glass-polyester were superimposed when normalized by the static strength at the respective temperature while polypropylene matrix composite showed a small improvement in fatigue life [17].

#### 4.2.3 Effects of frequency

The possibility of using high-frequency loading for accelerating fatigue tests of polymer composite materials is discussed by R. Apinis [11]. The results of this research are compared with those found in conventional low-frequency loadings. Results are given for an LM-L1 UD glass-fiber plastic in loadings with frequencies of 17 and 400 Hz and  $R = -1$ . These results confirm that it is possible to accelerate the fatigue testing of polymer composite material by considerably increasing the loading frequency. The necessary condition for using this method is an intense cooling of specimens to prevent them from vibration heating. For achieving the same temperature modes of testing, the specimens during the high-frequency loading were cooled with jets of water. To prevent the material from the action of moisture, the surface of specimens was covered with a thin layer of wax.

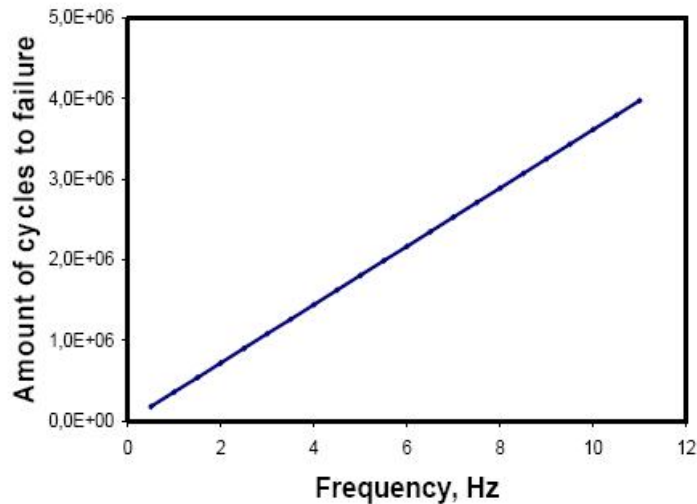
#### 4.2.4 Combined temperature and frequency effects

The results of different researches considering the effect of frequency on the fatigue (T-T and T-C) behaviour were summarized by [18] as follows: *“At low frequency ranges where there is negligible heat dissipation, as the load frequency increases, cycles to failure increase also. As higher frequency ranges are considered this increase is at a slower rate. When there is excessive heat dissipation however, a reverse trend can be observed”*.

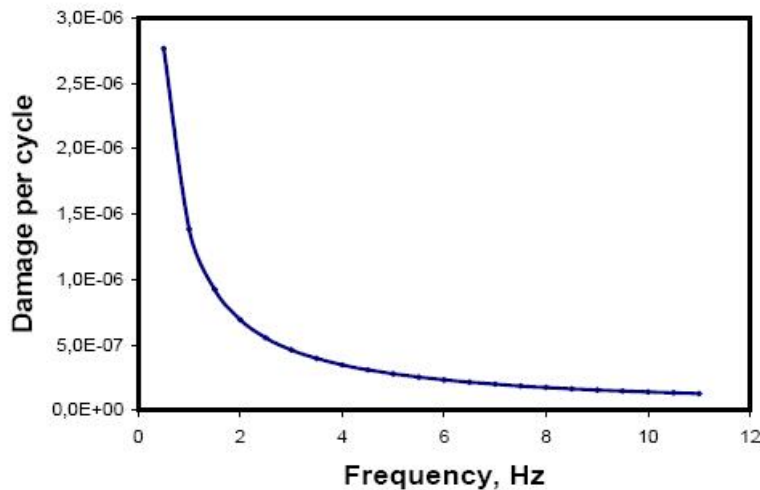
The lifetime of a specimen under constant load is dependent on applied stress and temperature. Apparently if considering a more complex case of multi-step loading, a failure of a material is not a step-wise event after a lapse of time, but a continuous process of the defect accumulation and degradation at the lower scale level. The failure does not occur after each loading step (since the duration of the steps is much lower than the time-to-failure for a given constant loading). However, such multi-step loading can lead to the failure as well as one long step loading. The residual lifetime of a specimen under loading decreases due to the formation of defects [19].

Considering fatigue, the cyclic tension-tension loading curve can be represented as a multi-step loading as well. A half-cycle curve can be discretized into several steps, for determining the damage increase for each step. A decreasing correlation exists between the damage growth rate in each cycle and the frequency of loading. This means that the number of cycles to failure increases with increasing the loading frequency (Figure 3). Figure 4 shows the damage growth per cycle decreases with increasing loading frequency.

In this analytical approach it is stated that: *“the total time to failure is constant, the frequency of loading does not affect the total time to failure”* [19].



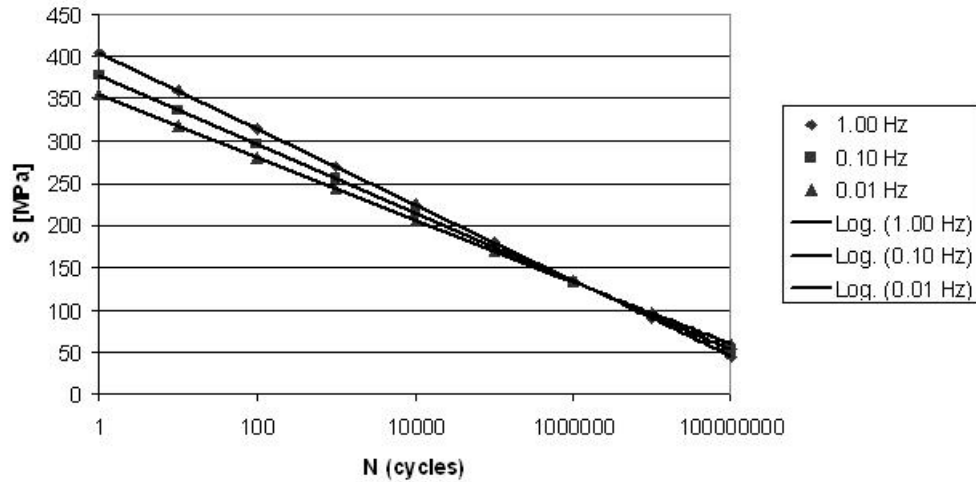
**Figure 3: Analytical evaluation of the amount of cycles to failure with increasing loading frequency [19]**



**Figure 4: Analytical evaluation of damage growth per cycle with increasing loading frequency [19]**

The model is applicable to the case when neither dynamic effects nor heat dissipation influence the damage growth in the materials. To verify the analytical kinetic model of fatigue damage from [19], its results were compared to the experiments by Mandell and Meier [20].

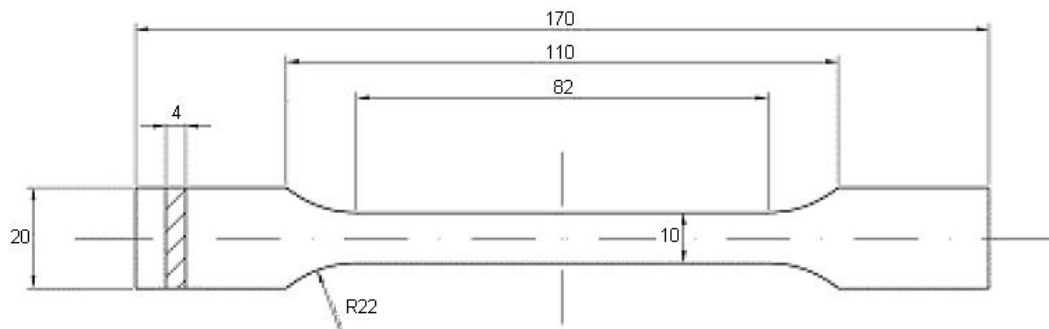
Mandell and Meier studied tension load frequency effects for cross-ply E-glass/epoxy laminates, carrying out tests at low frequencies of 0.01, 0.1 and 1 Hz (to prevent any hysteretic heating) and observed that the number of cycles to failure increased at higher load frequencies. The plates were subject to square and spike loadings. They noted, “*at higher frequencies there is an interaction of heating and mechanical effects, which was intentionally avoided here*”. In Figure 5 the S-N curves obtained by Mandell and Meier for the different frequencies are presented [20].



**Figure 5: S-N curves by Mandell and Meier**

It shows that the number of cycles to failure increases almost linearly with increasing loading frequency. In the case of polymer composite materials, an increase in the loading frequency also leads to an intense heating of the material, owing to the high hysteretic losses and the poor heat conductivity of the material. This internal heating can skew test results by causing a thermal degradation of the material. Therefore, internal heat generation can become a problem for testing composite materials at higher frequencies. However, this effect can possibly be eliminated either by intense cooling of the specimen or by selecting its dimensions such that the natural cooling is sufficient [21]. Nonetheless, only a limited amount of information is available about combined temperature and frequency effects on the fatigue behaviour of composites.

One example of publication in this field is that of A. Bernasconi et al. [21] whose research focused on the temperature and frequency effects on fatigue behaviour of short glass fibre reinforced (30% weight) polyamide-6. The E-type glass fibers have a nominal fiber diameter of 10  $\mu\text{m}$  and an aspect ratio (relationship between length and diameter) ranging from 30 to 50. Injection molding technique was employed for the preparation of specimens. Specimen shape and dimensions correspond to those of type 1A samples defined in ISO 527 standard [22] (see Figure 6 for dimensions).



**Figure 6: Geometry type 1A defined in ISO 527 standard (dimensions in mm)**

Tensile strength and fatigue tests were performed at 23°C and 50°C. Fatigue tests were conducted in load control mode with sinusoidal tension-tension load cycles at 2 Hz and 4 Hz. The stress ratio, defined as by Equation 6 was equal to  $R = 0.1$

**Equation 6 Stress ratio**

$$R_{stress} = \frac{\sigma_{min}}{\sigma_{max}}$$

Where: R is the stress ratio

$\sigma_{\max}$  is the maximum applied stress per cycle  
 $\sigma_{\min}$  is the minimum applied stress

As shown in Table 3, the result of an increment in temperature during quasi-static tensile tests is a decrease of both ultimate tensile strength and elastic modulus .

**Table 3: Maximum stress and E-modulus as a function of temperature (of short glass fibre reinforced polyamide 6) [21]**

23°C		50°C	
$\sigma_{\max}$	E	$\sigma_{\max}$	E
109 MPa	5800 MPa	84 MPa	4300 MPa

Results of fatigue tests evidenced the influence of both external and self-heating on the fatigue life of specimens. External heating is the temperature rise of a specimen caused by an external source, while self-heating of specimens is the temperature rise within the specimen caused by internal friction and resistance between inter-laminar interfaces. Besides concluding on the dependency of temperature and frequency (Table 4) it shows no modification in cyclic behaviour and failure mechanism.

**Table 4: Fatigue strength at  $10^6$  cycles and slope (k) of the S-N curve (of short glass fibre reinforced polyamide 6) [21]**

T	f	$\sigma$	k
23°C	2 Hz	56.0 MPa	18.9
23°C	4 Hz	52.5 MPa	20.7
50°C	4 Hz	47.5 MPa	18.5

The results of fatigue tests reported in S-N curves show frequency effects are comparable to temperature effects. Both effects lead to a reduction of fatigue strength [21]. The self-heating effect therefore seems to be comparable to the effect of external temperature and it has to be taken into account during fatigue research.

## 5. RESULTS AND DISCUSSION

All UPWIND temperature and frequency results presented here are in the OPTIDAT database [23]. In the following chapters, the results are summarised in tabular form and figures.

Measurement summaries are documented in ANNEX B. Typical failure modes are shown in ANNEX C.

### 5.1 STATIC TESTS

The static test program includes tension and compression tests performed at -40 °C, 23 °C and 60 °C. Results are first presented for tensile tests, with a short discussion of the results. Compressive tests are then summarized and discussed.

#### 5.1.1 Tension

Tensile tests are performed on at least six specimens at -40 °C, 23 °C and 60 °C. Axial load, displacement and strains are measured while stresses are calculated based on the average cross-section in the middle of each specimen and tensile modulus is calculated from the slope of the stress-strain curve between 500  $\mu\epsilon$  and 2500  $\mu\epsilon$ . Tensile test results are presented in Table 5.

**Table 5: Tensile test results**

Specimen ID	Test frame	Max load [kN]	Cross section [mm <sup>2</sup> ]	$\sigma_{11max}$ [MPa]	$E_{11avg}$ [GPa]	$T_{avg}$ [°C]
BL08R08	Instron 100 kN	52.90	58.67	902	38.0	23.2
BS23R08	Schenck 100 kN	54.30	60.62	896	37.1	25.1
BS24R08	Instron 100 kN	52.00	60.34	862	37.4	23.4
BT03R08	Schenck 100 kN	51.70	57.03	907	40.5	25.7
BT06R08	Schenck 100 kN	51.80	56.73	913	38.9	25.7
BT28R08	Instron 100 kN	53.10	56.88	934	40.0	23.9
BU08R08	Instron 100 kN	56.10	57.83	970	38.9	23.2
BU13R08	Instron 100 kN	50.90	60.64	839	37.5	24.2
BU20R08	Schenck 100 kN	55.70	58.71	949	37.4	25.5
DS24R08	Schenck 100 kN	52.02	60.80	856	37.2	28.7
DS28R08	Schenck 100 kN	56.36	60.46	932	37.3	26.5
LN02R08	ZB 100 kN	56.57	58.17	973		N/A*
LN11R08	ZB 100 kN	57.67	59.85	964		N/A
DQ16R08	ZB 100 kN	43.83	58.34	751	35.9	59.5
DV08R08	ZB 100 kN	44.25	59.99	738	35.7	N/A
DV27R08	ZB 100 kN	46.78	60.60	772	35.7	59.5
DW10R08	ZB 100 kN	42.80	59.13	724	34.7	N/A
ET13R08	ZB 100 kN	44.49	59.54	747	35.0	60.4
ET15R08	ZB 100 kN	44.88	61.36	731	34.6	60.0
EV03R08	ZB 100 kN	43.17	59.00	732	34.9	60.0
EV19R08	ZB 100 kN	43.20	61.37	704	34.3	60.3
DW22R08	ZB 100 kN	60.19	59.54	1011	38.2	-39.5
ET03R08	ZB 100 kN	63.61	59.58	1067	36.9	-39.7
ET20R08	ZB 100 kN	60.11	60.61	992	36.8	-39.3
EV02R08	ZB 100 kN	64.02	58.93	1086	37.0	39.7
EV14R08	ZB 100 kN	61.67	59.63	1034	36.7	-39.4
EV24R08	ZB 100 kN	61.17	58.95	1038	36.5	-40.1
*no reliable temperature measurement available						

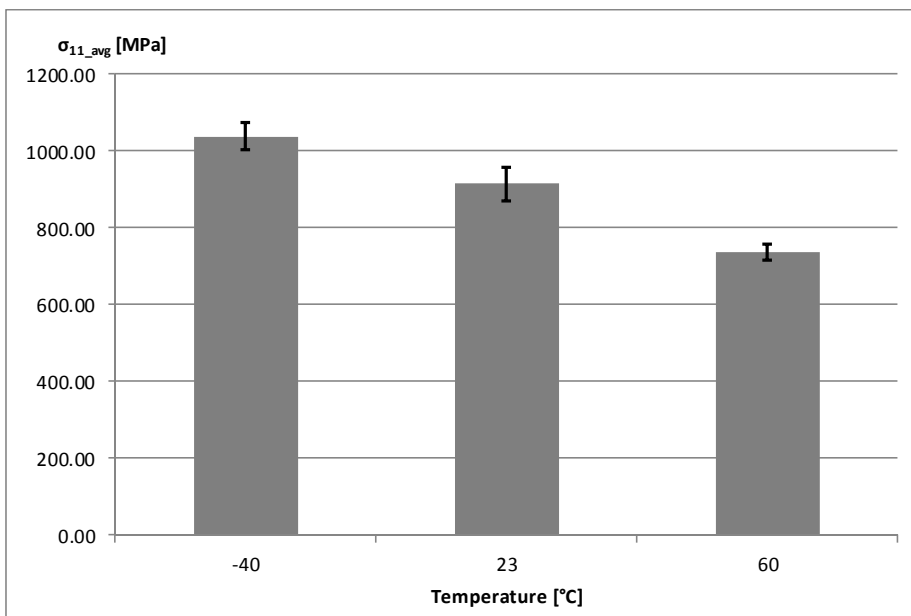
Statistics on the strength and modulus obtained from these results are presented in Table 6.

**Table 6: Average mechanical properties for tensile tests**

Temperature [°C]	$\sigma_{11avg}$ [MPa]	$\sigma_{11}$ St Dev [MPa]	$\sigma_{11}$ CV [%]	$d\sigma_{11}$ [%]
Ambient	915	44	4.8	0
60	737	20	2.7	-19.4
-40	1038	35	3.4	13.4
Temperature [°C]	$E_{11AVG}$ [GPa]	$E_{11}$ St Dev. [GPa]	$E_{11}$ CV [%]	$dE_{11}$ [%]
Ambient	38.2	1.20	3.15	0
60	35.1	0.59	1.69	-8.1
-40	37.0	0.60	1.62	-3.1

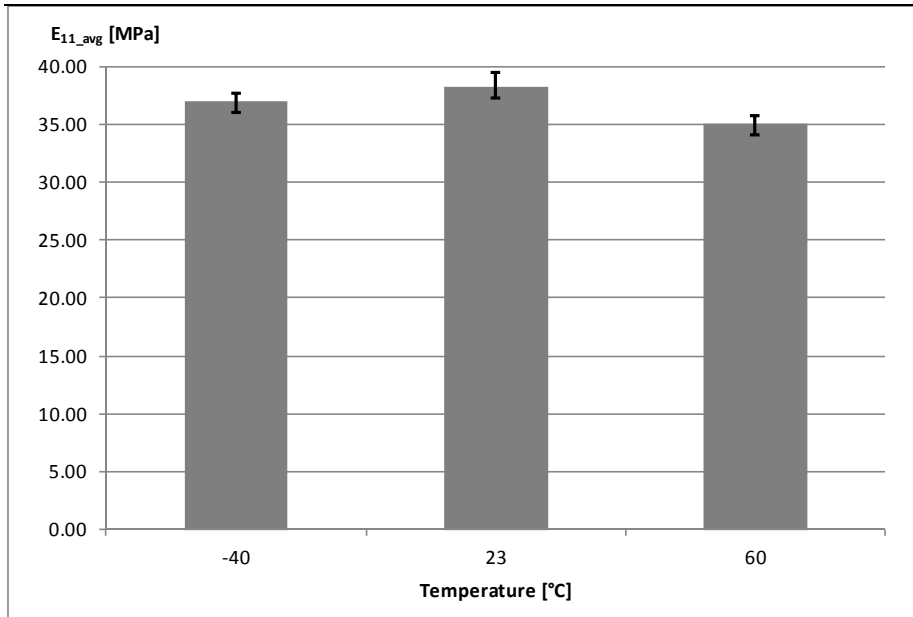
$\sigma_{11}$  St Dev=standard deviation  
 $\sigma_{11}$  CV=coefficient of variation  
 $d\sigma_{11}$ =difference in % w.r.t. reference

According to these results, a temperature of 60 °C induces a significant drop of the laminate tensile strength (-19.4 %), while at -40 °C, the tensile strength is improved by 13.4 %. On the other hand, although tensile modulus appears to remain quite constant with a decrease of temperature, a reduction of 8.1 % is observed at 60 °C. In order to provide better visualization of these differences, Figure 7 and Figure 8 respectively show the average tensile strengths and moduli in graphical form.



**Figure 7: Average tensile strengths at -40 °C, 23 °C and 60 °C.**





**Figure 8: Average tensile moduli at -40 °C, 23 °C and 60 °C**

### 5.1.2 Compression

Compressive tests are also performed on at least six specimens at -40 °C, 23 °C and 60 °C. Axial load, displacement and strains are measured while stresses are calculated based on the average cross-section of each specimen and modulus is calculated from the slope of the stress-strain curve between -500  $\mu\epsilon$  and -2500  $\mu\epsilon$ . Compressive test results are presented in Table 7, while Table 8 shows some statistics obtained from this dataset.

**Table 7: Compressive tests results**

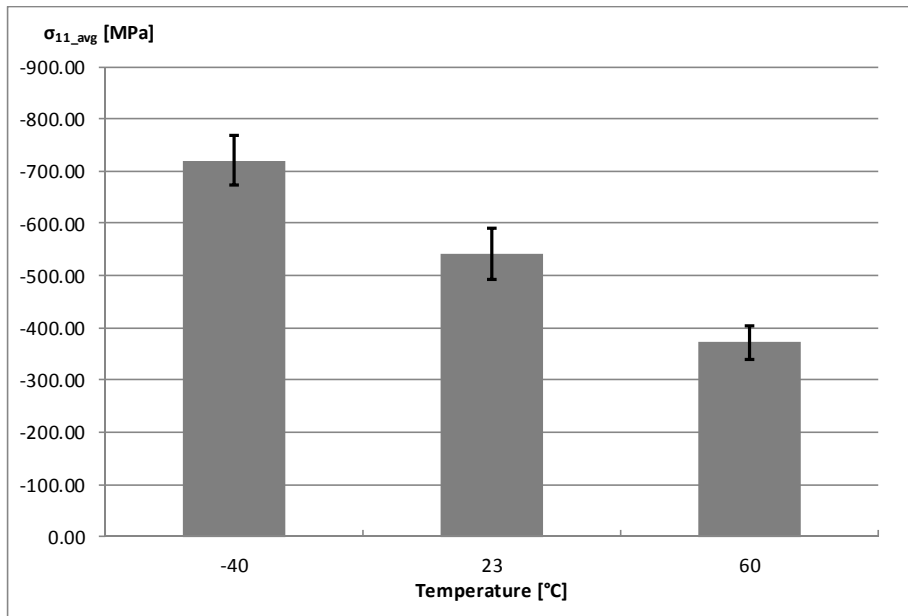
Specimen ID	T <sub>avg</sub> [°C]	Test frame	Min load [kN]	Cross section [mm <sup>2</sup> ]	$\sigma_{11min}$ [MPa]	E <sub>11</sub> [GPa]
BL09R08	24.5	Instron 100 kN	-31.5	58.39	-539	37.9
BS21R08	24.2	Instron 100 kN	-34.0	61.16	-556	36.4
BT04R08	27.0	Schenck 100 kN	-32.1	56.64	-567	38.4
BT07R08	23.5	Instron 100 kN	-33.3	57.10	-583	38.0
BU06R08	23.3	Instron 100 kN	-30.9	58.35	-530	37.5
BU14R08	27.1	Schenck 100 kN	-24.2	60.60	-399	38.1
BU19R08	24.0	Instron 100 kN	-33.0	59.51	-555	36.0
BU23R08	27.8	Schenck 100 kN	-33.2	58.42	-568	37.1
DS06R08	25.3	Schenck 100 kN	-33.7	60.41	-558	38.0
DS14R08	25.1	Schenck 100 kN	-34.2	60.82	-562	36.9
DS18R08	26.4	Schenck 100 kN	-33.1	60.53	-546	N/A
DQ27R08	58.7	ZB 100 kN	-23.4	60.67	-386	34.4
DV25R08		ZB 100 kN	-22.9	60.59	-378	34.9
DW02R08	59.3	ZB 100 kN	-21.1	61.23	-345	34.6
DW24R08		ZB 100 kN	-22.1	59.20	-374	35.6
ET10R08	59.7	ZB 100 kN	-21.0	60.53	-347	34.8
ET17R08	59.5	ZB 100 kN	-20.4	61.23	-333	34.5
EV01R08	59.2	ZB 100 kN	-26.2	60.31	-434	35.3

Specimen ID	T <sub>avg</sub>	Test frame	Min load	Cross section	σ <sub>11min</sub>	E <sub>11</sub>
EV09R08	59.6	ZB 100 kN	-23.8	62.28	-382	34.4
DP26R08	-39.4	ZB 100 kN	-45.7	60.12	-760	37.4
DQ24R08	-39.6	ZB 100 kN	-39.3	60.43	-651	35.6
DV21R08	-39.1	ZB 100 kN	-43.9	60.57	-725	37.3
DW07R08	-39.7	ZB 100 kN	-44.2	59.11	-747	38.6
ET07R08	-40.3	ZB 100 kN	-44.9	58.90	-762	38.3
EV05R08	-40.0	ZB 100 kN	-40.0	59.61	-671	37.0

**Table 8: Average mechanical properties for compressive tests**

Temperature [°C]	σ <sub>11avg</sub> [MPa]	σ <sub>11</sub> St Dev [MPa]	σ <sub>11</sub> CV [%]	dσ <sub>11</sub> [%]
Ambient	-542	50	-9.1	0
60	-372	32	-8.5	-31.3
-40	-719	48	-6.6	32.7
Temperature [°C]	E <sub>11avg</sub> [GPa]	E <sub>11</sub> St Dev. [GPa]	E <sub>11</sub> CV [%]	dE <sub>11</sub> [%]
Ambient	37.4	0.8	2.1	0
60	34.8	0.4	1.3	-7.0
-40	37.4	1.1	2.8	-0.2

Results presented in Table 8 show that compressive properties are strongly affected by temperature conditions. At 60 °C, strength is reduced by more than 30 % while a 7 % decrease in modulus is noted. At -40 °C, strength is improved by about 30 %. However, modulus is not significantly affected by the low temperature. In order to provide a relative vision of these differences, Figure 9 and Figure 10 respectively show the average compressive strengths and moduli in graphical form.



**Figure 9: Average compressive strengths at -40 °C, 23 °C and 60 °C.**

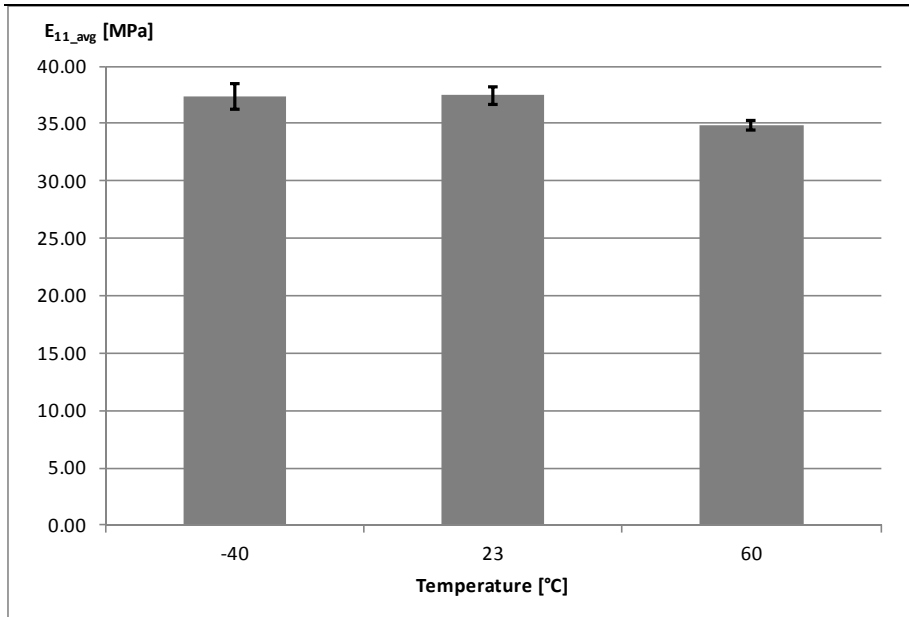


Figure 10: Average compressive moduli at -40 °C, 23 °C and 60 °C.

## 5.2 FATIGUE TESTS

Fatigue tests are performed at -40 °C, 23 °C and 60 °C. Frequencies depend on the load level as described in Table 1. For each environmental condition, a minimum of five tests were performed at each of the two main load levels. For room temperature, all available data points from tests performed at WMC on the ZB 100 kN and Zwick 250 kN specimens are accounted for. In Table 9 to Table 14, these test frames will simply be referred to as ZB and Zwick.

In the following section, results are presented by load ratio ( $R = \text{minimum cyclic load}/\text{maximum cyclic load}$ ). The output data for tension-tension fatigue tests at  $R = 0.1$  is first presented with a focus on temperature effects and on frequency effects. Results of tension-compression fatigue at  $R = -1$  are then presented in the same order for effect of temperature and frequency. Finally, analysis of the data is performed in order to provide tentative explanations of the observed tendencies.

### 5.2.1 R = 0.1

This section provides a synthesis of the test results from each specimen tested in tensile fatigue at  $R = 0.1$ . Tables are provided with measured and inferred values for tests at ambient temperature, at low temperatures and at high temperatures.

#### 5.2.1.1 Room temperature

Table 9 provides a summary of measurements and test results for tests at room temperature and  $R=0.1$ .

Table 9: Tension-tension fatigue test results at room temperature (23 °C)

Specimen	Cross section	Test frame	Grip bolt torque	$F_{max}$	$\sigma_{max}$	f	Cycles to failure	$E_{avg}$	$T_{S\_avg}$
	[mm <sup>2</sup> ]		[Nm]	[kN]	[MPa]	[Hz]	[N]	[GPa]	[°C]
DC04R08	59.25	ZB	80	20	338	24	63370	x*	29.8
DC14R08	62.32	ZB	80	20	321	24	250860	x	33.5
DC15R08	60.10	ZB	80	20	333	24	209888	x	27.1
DD07R08	63.17	ZB	80	20	317	24	331881	x	x**

Specimen	Cross section	Test frame	Grip bolt torque	$F_{max}$	$\sigma_{max}$	f	Cycles to failure	$E_{avg}$	$T_{S_{avg}}$
DD12R08	62.91	ZB	80	20	318	24	300341	37.9	29.8
DD22R08	61.24	ZB	60	20	327	24	279915	x	26.9
DD28R08	62.21	ZB	80	20	321	24	419144	x	27.3
DC09R08	58.58	ZB	80	32	546	24	977	x	26.9
DC11R08	60.10	ZB	80	32	532	24	1597	x	28.7
DC12R08	61.14	ZB	80	32	523	24	1507	x	30.7
DD13R08	62.73	ZB	80	32	510	24	3115	36.1	22.6
DD21R08	61.07	ZB	80	32	524	24	1911	36.7	24.5
DD27R08	61.64	ZB	75	32	519	24	2187	36.4	24.7
CM09R08	58.77	Zwick	200	20	340	8	1069571	37.2	27.1
DA07R08	60.58	Zwick	200	20	330	8	550296	37.6	24.7
DA11R08	61.19	Zwick	200	20	327	8	543671	36.3	25.5
CW02R08	60.04	Zwick	275	20	333	8	105178	36.5	27.4
CW28R08	62.19	Zwick	275	20	322	8	1139574	36.8	26.2
CB11R08	60.62	Zwick	275	32	528	8	6390	37.1	25.6
CB15R08	59.50	Zwick	275	32	538	8	15848	40.1	26.2
CB21R08	61.55	Zwick	275	32	520	8	8423	35.1	26.6
CB29R08	59.73	Zwick	275	32	536	8	10714	37.3	28.6
CW19R08	61.19	Zwick	275	32	523	8	1673	35.7	28.3
BJ10R08	60.75	ZB	60	18	296	6	3456926	37.0	27.3
CM22R08	60.99	Zwick	275	18	295	6	3320841	37.3	25.1
BJ04R08	60.23	ZB	50	20	332	6	665216	33.5	29.3
BJ05R08	60.32	ZB	60	20	332	6	827289	x	29.9
DC22R08	59.01	Zwick	500	20	339	6	654378	37.2	28.6
DP10R08	60.25	Zwick	500	20	332	6	235752	25.6	31.9
DQ08R08	59.32	Zwick	500	20	337	6	891024	38.1	32.1
DQ29R08	60.86	ZB	60	20	329	6	985334	36.7	28.1
DV20R08	60.94	Zwick	500	20	328	6	1073158	36.9	32.4
DV22R08	60.71	ZB	60	20	329	6	908888	37.2	30.6
DW13R08	59.76	ZB	60	20	335	6	427068	36.8	32.1
LN06R08	56.89	ZB	75	20	352	6	670926	39.0	x
LN09R08	59.06	ZB	70	20	339	6	1421057	38.3	x
LN16R08	57.31	ZB	75	20	349	6	2063590	39.7	x
AQ11R08	54.52	ZB	60	24	440	3	66181	x	26.1
BJ01R08	59.27	ZB	60	24	405	3	139126	x	27.5
BJ12R08	60.89	ZB	60	24	394	3	157004	x	28.8
BJ15R08	61.48	ZB	60	24	390	3	151302	x	30.2

Specimen	Cross section	Test frame	Grip bolt torque	$F_{max}$	$\sigma_{max}$	f	Cycles to failure	$E_{avg}$	$T_{S_{avg}}$
CB01R08	60.73	Zwick	275	32	527	4	25210	39.4	26.7
CB03R08	61.23	Zwick	275	32	523	4	12195	36.0	25.3
FL15R08	60.04	Zwick	275	32	533	4	3314	38.0	25.2
BJ06R08	60.85	ZB	80	32	526	2	18663	x	27.4
BJ13R08	60.90	ZB	80	32	525	2	15868	x	26.2
FL09R08	59.40	Zwick	275	32	539	2	4631	37.6	25.2
FL13R08	59.96	Zwick	275	32	534	2	2365	38.5	26.1
FL14R08	60.05	Zwick	275	32	533	2	4132	38.1	26
DC07R08	58.42	Zwick	500	32	548	2	4508	38.5	27.5
DP08R08	59.65	Zwick	500	32	536	2	5311	38.2	31.9
DP14R08	60.58	ZB	75	32	528	2	6900	36.5	30
DQ06R08	59.74	Zwick	500	32	536	2	3484	35.0	31.5
DQ23R08	60.78	ZB	75	32	526	2	10875	37.1	28.7
DW12R08	59.39	ZB	75	32	539	2	7071	37.0	27.1
LN04R08	55.89	ZB	75	32	573	2	7891	39.3	x
LN17R08	57.38	ZB	75	32	558	2	6908	38.7	x
LN21R08	59.30	ZB	75	32	540	2	11909	38.4	x
BJ09R08	60.46	ZB	80	32	529	1	15717	x	23.4

Actual specimen temperatures were often higher than the target temperature of 23 °C. It is also worth noting that the difference between mean and maximum temperature seems to be more important at elevated frequency.

The necessary grip bolt torques are different for the Zwick and ZB test frames because of differences in the configuration of the grips. The Zwick test frame uses a single 30 mm bolt with trapezoidal thread and 3mm pitch. The ZB uses two M12 bolts. In the course of the test programme, some wear was induced in the grip surfaces of the Zwick, requiring much higher clamping pressures. Because of this and availability / planning, it was decided to move to the ZB machine.

#### 5.2.1.2 -40°

Table 10 provides a summary of measurements and test results for tests performed at -40 °C and R = 0.1. As for ambient temperature tests, some variation of the actual specimen temperature is noted and grip pressures used on the ZB and Zwick machine differ significantly. However, the difference between mean and maximum specimen temperatures seems to be less than for tests performed at 23 °C.

**Table 10: Tension-tension fatigue test results at room temperature -40 °C**

Specimen	A	Test frame	Grip bolt torque	$F_{max}$	$\sigma_{max}$	f	Cycles to failure	$E_{avg}$	$T_{S_{avg}}$
	[mm <sup>2</sup> ]		[Nm]	[kN]	[MPa]	[Hz]	[N]	[GPa]	[°C]
DQ07R08	59.98	ZB	80	20	333	24	494106	38.9	-37.9
DV13R08	60.53	ZB	80	20	330	24	331378	37.4	-37.8
DV24R08	60.22	ZB	80	20	332	24	879008	37.8	-39.9
DW15R08	59.05	ZB	80	20	339	24	755885	37.9	-33.5
DW17R08	61.44	ZB	80	20	326	24	796028	37.3	-35.9

Specimen	A	Test frame	Grip bolt torque	F <sub>max</sub>	σ <sub>max</sub>	f	Cycles to failure	E <sub>avg</sub>	T <sub>S_avg</sub>
DP18R08	60.38	ZB	80	32	530	24	6278	37.5	-34.9
DP28R08	59.90	ZB	80	32	534	24	5647	38.0	-32.6
DQ21R08	61.24	ZB	80	32	523	24	5355	38.1	-39.9
DV14R08	60.69	ZB	80	32	527	24	5162	37.8	-34.1
DW03R08	61.46	ZB	80	32	521	24	3116	36.7	-36.9
DW06R08	59.41	ZB	80	32	539	24	2287	38.9	-37.7
CW12R08	61.27	Zwick	350	20	326	8	652871	36.6	-39.9
CW18R08	61.36	Zwick	350	20	326	8	568236	39.3	-39.2
CW03R08	61.05	Zwick	350	32	524	8	1826	38.4	-38.4
CW06R08	61.37	Zwick	350	32	521	8	6515	37.7	-31.6
CW23R08	61.88	Zwick	550	32	517	8	8823	36.7	-40.8
DA05R08	61.73	Zwick	300	32	518	8	5490	38.2	-38.5
CW04R08	61.36	Zwick	350	20	326	6	518328	37.3	-38.4
CW09R08	62.03	Zwick	500	20	322	6	435011	37.5	-36.9
CW25R08	61.69	Zwick	350	20	324	6	375470	36.5	-39.6
DP03R08	60.52	ZB	80	20	330	6	635945	36.5	-32.1
DQ09R08	59.47	ZB	80	20	336	6	252451	38.0	-37.8
CW01R08	59.63	Zwick	550	32	537	2	8584	39.2	-34.8
CW05R08	61.41	Zwick	350	32	521	2	6138	36.5	-40.5
CW20R08	61.80	Zwick	350	32	518	2	7574	37.2	-40.5
DA10R08	60.49	Zwick	300	32	529	2	9561	38.3	-40.6
FL02R08	62.04	Zwick	250	32	516	2	6812	x	-37.5

### 5.2.1.3 +60°

Results from tests performed at R = 0.1 at a temperature of 60 °C are summarized in Table 11. Apart from measurements on a few tests, data suggests that temperature control was more consistent with the target temperature than for ambient and low temperature tests. However, relatively high grip pressures were needed on the Zwick test frame due to wear of the grips. No high frequency tests were performed at elevated temperature.

**Table 11: Tension-tension fatigue test results at room temperature 60 °C**

Specimen	A	Test frame	Grip bolt torque	F <sub>max</sub>	σ <sub>max</sub>	f	Cycles to failure	E <sub>avg</sub>	T <sub>S_avg</sub>
	[mm <sup>2</sup> ]		[Nm]	[kN]	[MPa]	[Hz]	[N]	[GPa]	[°C]
FL04R08	60.34	Zwick	135	18	298	6	482006	x	61.3
DD03R08	62.28	Zwick	450	20	321	6	15568	x	60.1

Specimen	A	Test frame	Grip bolt torque	F <sub>max</sub>	σ <sub>max</sub>	f	Cycles to failure	E <sub>avg</sub>	T <sub>S av</sub> g°
DQ13R08	59.79	ZB	80	20	335	6	90091	36.8	66.2
DV03R08	60.60	ZB	80	20	330	6	223419	37.9	62.6
DW26R08	60.10	ZB	80	20	333	6	151104	x	62.9
FL16R08	59.22	Zwick	135	20	338	3	211520	x	60.2
FL10R08	59.90	Zwick	170	24	401	3	14136	x	59.2
CM12R08	59.05	Zwick	275	32	542	2	1045	36.9	61.1
DA03R08	62.12	Zwick	275	32	515	2	565	16.8	59.4
DA08R08	60.10	Zwick	275	32	532	2	360	36.2	60.7
DD09R08	63.94	Zwick	300	32	500	2	1385	x	60.2

## 5.2.2 R = -1

This section provides a synthesis of the test results from each specimen tested in tension-compression fatigue at R = -1. Tables are provided with measured and inferred values for tests at ambient temperature, at low temperatures and at high temperature. Tests for R = -1 were all performed on the same test frame, the ZB 100 kN, in order to eliminate potential variations in specimen longevity that could be induced by differences in grip action and grip pressure.

### 5.2.2.1 Room temperature

Table 12 provides a summary of the available data for all specimens tested in tension-compression fatigue (R = -1) at ambient temperature (23 °C).

**Table 12: Tension-compression fatigue test results at room temperature (23 °C)**

Specimen	Cross section [mm <sup>2</sup> ]	Test frame	Grip bolt torque [Nm]	F <sub>max</sub> [kN]	σ <sub>max</sub> [MPa]	f [Hz]	Cycles to failure [N]	E <sub>avg</sub> [GPa]	T <sub>S_avg</sub> [°C]	T <sub>S_max</sub> [°C]
DP17R08	60.55	ZB	60	14	231	24	262719	36.6	36.7	40.5
DP20R08	60.60	ZB	60	14	231	24	273697	37.0	33.4	35.7
DQ15R08	60.53	ZB	60	14	231	24	41488	36.6	x	x
DQ25R08	60.64	ZB	60	14	231	24	135385	37.5	35.5	39.2
DV15R08	60.61	ZB	60	14	231	24	105751	37.6	40.7	44.2
DW14R08	59.23	ZB	60	14	236	24	4948	36.9	37	40.3
DP12R08	60.00	ZB	60	24	400	24	274	36.9	26.2	26.3
DQ30R08	61.05	ZB	60	24	393	24	502	36.5	28.3	30.1
DV06R08	60.43	ZB	60	24	397	24	462	36.8	31.8	36.2
DV17R08	60.85	ZB	60	24	394	24	415	36.4	30.3	34.1
DW16R08	60.07	ZB	60	24	400	24	290	37.5	28.7	29.8
DW23R08	59.07	ZB	60	24	406	24	338	37.6	30.8	34.7
BS11R08	60.44	ZB	50	12	199	3	1961631	35.5	25.2	28.2
BS22R08	60.90	ZB	60	14	230	3	656467	32.1	27.1	28.8
DC16R08	59.22	ZB	80	14	236	3	555020	37.6	29.4	32.6
LN05R08	54.61	ZB	60	14	256	3	1077613	40.0	25.9	29.7
LN14R08	57.35	ZB	60	14	244	3	899773	38.5	x	x
LN20R08	58.45	ZB	60	14	240	3	1655954	39.3	x	x
BT13R08	57.29	ZB	60	20	349	3	3029	x	28.4	29.3
DC17R08	57.71	ZB	80	20	347	3	3285	37.8	28.8	29.4
DC18R08	59.39	ZB	80	20	337	3	2170	38.3	28.7	29.2
DC05R08	60.00	ZB	80	24	400	1	192	38.7	28.9	29.6
DC08R08	58.20	ZB	80	24	412	1	413	39.2	28.3	29.1
DC19R08	59.23	ZB	60	24	405	1	462	39.5	26.2	28
DP04R08	59.99	ZB	60	24	400	1	1645	38.4	23.3	23.6
DQ04R08	59.97	ZB	60	24	400	1	176	39.3	22.8	23
LN03R08	58.29	ZB	65	24	412	1	23024	39.4	24.5	26.4
LN10R08	59.72	ZB	65	24	402	1	27052	37.9	25.5	26.5
LN13R08	58.21	ZB	65	24	412	1	11157	38.2	23	23.7
LN15R08	58.45	ZB	65	24	411	1	18585	39.2	26.4	27.5
LN18R08	57.18	ZB	65	24	420	1	19081	39.1	26.8	27.8
LN19R08	57.93	ZB	65	24	414	1	22183	39.7	24.5	24.8

Specimen temperature during the tests performed at room temperature turned out to be higher than the target environment temperature of 23 °C. Although low frequency tests show better agreement between the target and the actual temperature, high frequency tests reached much higher specimen temperatures. Moreover, the difference between the mean and maximum temperature of high frequency test specimens appears to be higher than for those tested at lower rates.



Fatigue life at higher loads and low frequency also show large scatter, although the data points seem to be relatively grouped in two clusters.

### 5.2.2.2 -40°

Measured and inferred data from fully reversed tension-compression tests at -40 °C are given in Table 13.

**Table 13: Tension-compression fatigue test results at -40 °C**

Specimen	A	Test frame	Grip bolt torque	F <sub>max</sub>	σ <sub>max</sub>	f	Cycles to failure	E <sub>avg</sub>	T <sub>S_avg</sub>
	[mm <sup>2</sup> ]		[Nm]	[kN]	[MPa]	[Hz]	[N]	[GPa]	[°C]
DP21R08	60.75	ZB	80	14	230	24	702027	x	-37.6
DQ19R08	61.09	ZB	80	14	229	24	647166	38.4	-38.7
DQ26R08	60.43	ZB	80	14	232	24	712086	37.5	-36.3
DV29R08	60.66	ZB	80	14	231	24	677804	37.9	-40.8
DW01R08	60.32	ZB	80	14	232	24	26464	37.6	-42.3
DW21R08	59.81	ZB	80	14	234	24	258457	38.8	-39.0
DP24R08	59.84	ZB	80	24	401	24	831	38.0	-37.9
DQ03R08	59.90	ZB	80	24	401	24	1159	38.7	-37.1
DV05R08	60.22	ZB	80	24	399	24	827	38.1	-40.1
DV18R08	60.56	ZB	80	24	396	24	932	37.6	-40.5
DW19R08	61.68	ZB	80	24	389	24	720	38.4	-36.8
DW25R08	59.94	ZB	80	24	400	24	802	38.5	-37.4
DP25R08	60.02	ZB	80	14	233	3	780659	37.7	-38.5
DQ14R08	60.41	ZB	80	14	232	3	317655	38.9	-41.0
DQ20R08	61.14	ZB	80	14	229	3	158410	x	x
DQ22R08	61.09	ZB	80	14	229	3	622230	37.2	-41.3
DV11R08	60.09	ZB	80	14	233	3	607278	37.7	-40.8
DV12R08	60.11	ZB	80	14	233	3	624205	39.0	x
DV26R08	60.30	ZB	80	14	398	3	623128	37.9	-37.8
DW30R08	59.86	ZB	80	14	234	3	540344	37.8	-40.3
DP29R08	60.31	ZB	80	24	398	1	11767	37.9	-41.0
DQ17R08	60.82	ZB	80	24	395	1	11797	39.0	-39.4
DV01R08	60.16	ZB	80	24	399	1	11751	37.9	-39.7
DV02R08	60.08	ZB	80	24	400	1	15183	38.1	-40.6
DW04R08	61.12	ZB	80	24	393	1	14868	38.7	-40.1
DW27R08	60.47	ZB	80	24	397	1	16842	38.5	-40

In general, specimen temperature were closer to the target environment.

### 5.2.2.3 +60°

Table 14 provides information on the fully reversed fatigue loading tests performed at high temperatures

**Table 14: Tension-compression fatigue test results at 60 °C**

Specimen	A	Test frame	Grip bolt torque	F <sub>max</sub>	σ <sub>max</sub>	f	Cycles to failure	E <sub>avg</sub>	T <sub>S_avg</sub>	T <sub>S_max</sub>
	[mm <sup>2</sup> ]		[Nm]	[kN]	[MPa]	[Hz]	[N]	[GPa]	[°C]	[°C]
DQ28R08	61.01	ZB	60	10	164	3	3064340	x	56	62.5
DV16R08	61.33	ZB	60	10	163	3	2841534	x	62.6	64.2
DW20R08	60.38	ZB	60	10	166	3	1018115	35.5	59.9	61.6
DC23R08	58.29	ZB	60	11	189	3	907	x	61.1	62
DP11R08	59.89	ZB	60	11	184	3	1436	x	60.6	61.5
DV28R08	60.78	ZB	60	11	181	3	1348647	x	61.8	63.6
DP05R08	59.28	ZB	60	12	202	3	960	36.2	60.7	61.3
DQ12R08	59.38	ZB	60	12	202	3	369	37.3	59.4	60.5
DV10R08	60.11	ZB	60	12	200	3	30255	35.8	63.1	64.3
DW29R08	59.65	ZB	60	12	201	3	634	35.9	60.4	61
DP09R08	60.03	ZB	60	14	233	3	150	36.0	60.9	61.6
DQ05R08	59.80	ZB	60	14	234	3	177	35.3	61.1	62
DV23R08	60.35	ZB	60	14	232	3	1131	36.5	62.3	63.6
DW28R08	59.84	ZB	60	14	234	3	853	36.3	60.7	61.4

For tests performed at 60 °C, the loads used had to be reduced because the specimen was weakened. Even though the maximum stress associated to the ±24 kN loading is only about half the measured compressive strength of the specimen, this load level proved to be too high for reliable fatigue testing at 60 °C.

### 5.3 INFLUENCE OF TEMPERATURE

In order to allow for an easier analysis of the extreme temperature fatigue behavior of the unidirectional (UD) E-glass/epoxy composite under investigation, results are presented in stress-life (S-N) diagrams. The assumption that the fatigue behavior varies linearly in the log-log stress-life space is made for modeling purposes.

Figure 11 shows the fatigue life curves obtained for test performed in tension-tension at R = 0.1. According to these results, a temperature of -40 °C appears to have an insignificant effect on the fatigue life of the laminate being studied. On the other hand, tests performed at 60 °C are shown to have an average fatigue life about a decade shorter than that of a similar specimen loaded at ambient temperature. The slope of the fatigue curve at high temperature however, seems to remain unchanged.

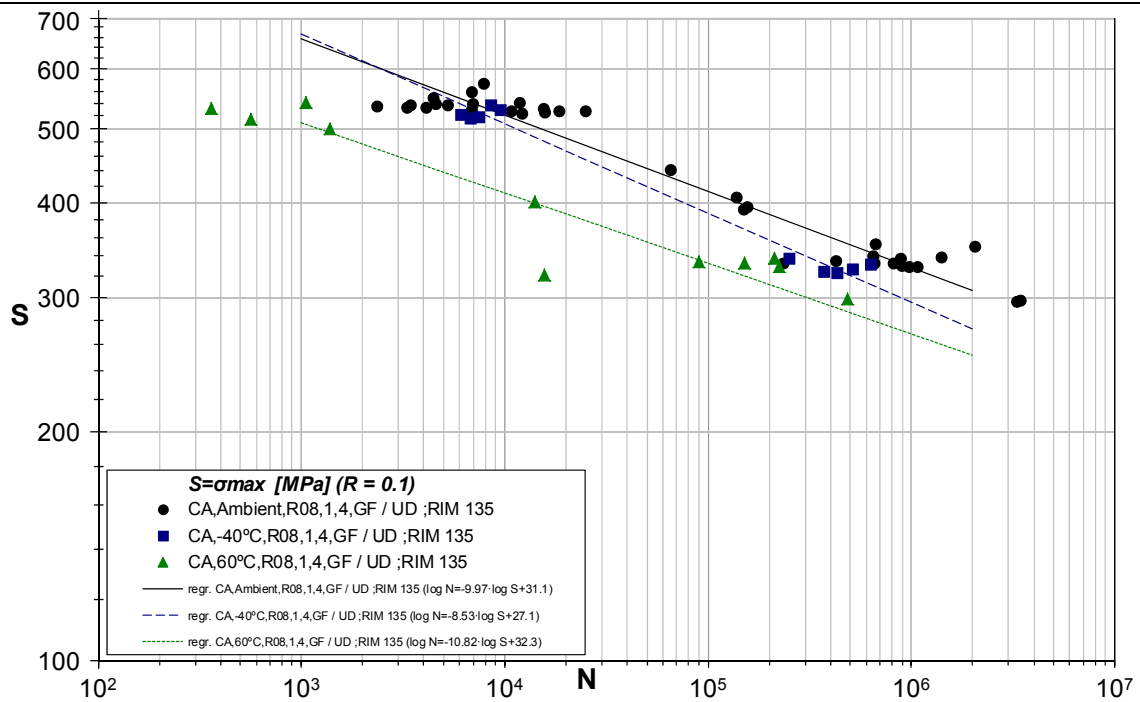


Figure 11: S-N diagram for R=0.1 fatigue at -40 °C, 23 °C and 60 °C.

The S-N curves for fully reversed loading fatigue at the same temperatures are plotted in Figure 12. As for tensile fatigue, the effects of a temperature of -40 °C are not significant since the data points all fall well within the scatter of the reference condition (ambient temperature). However, scatter of the room temperature test is quite high, mainly for elevated loads.

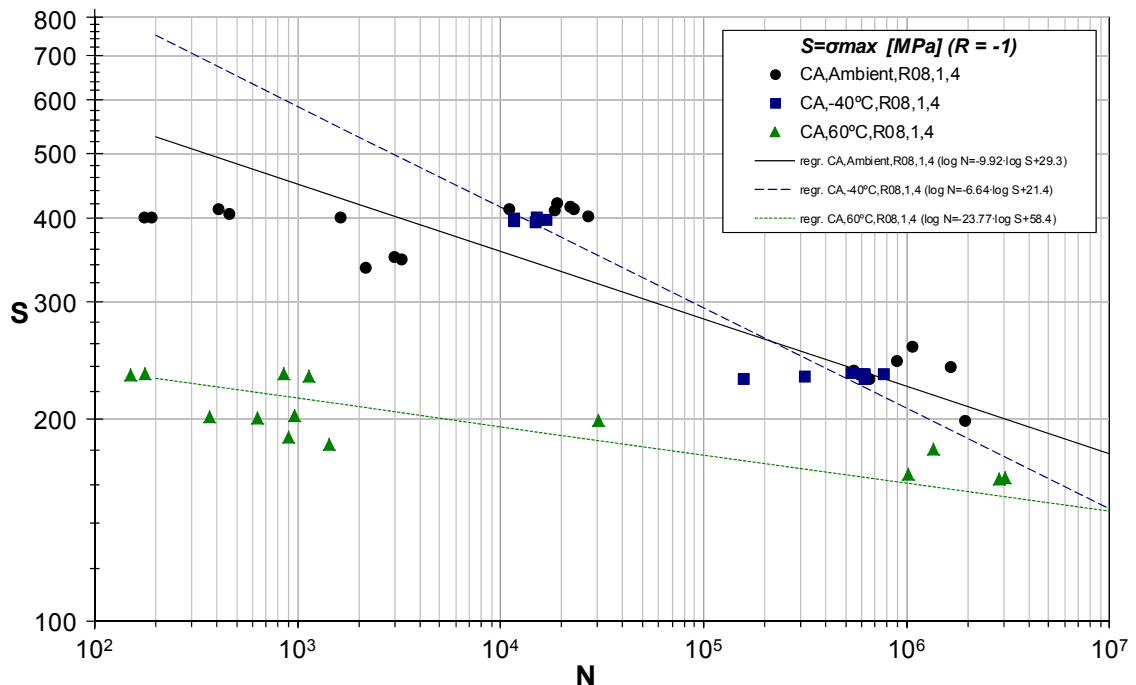
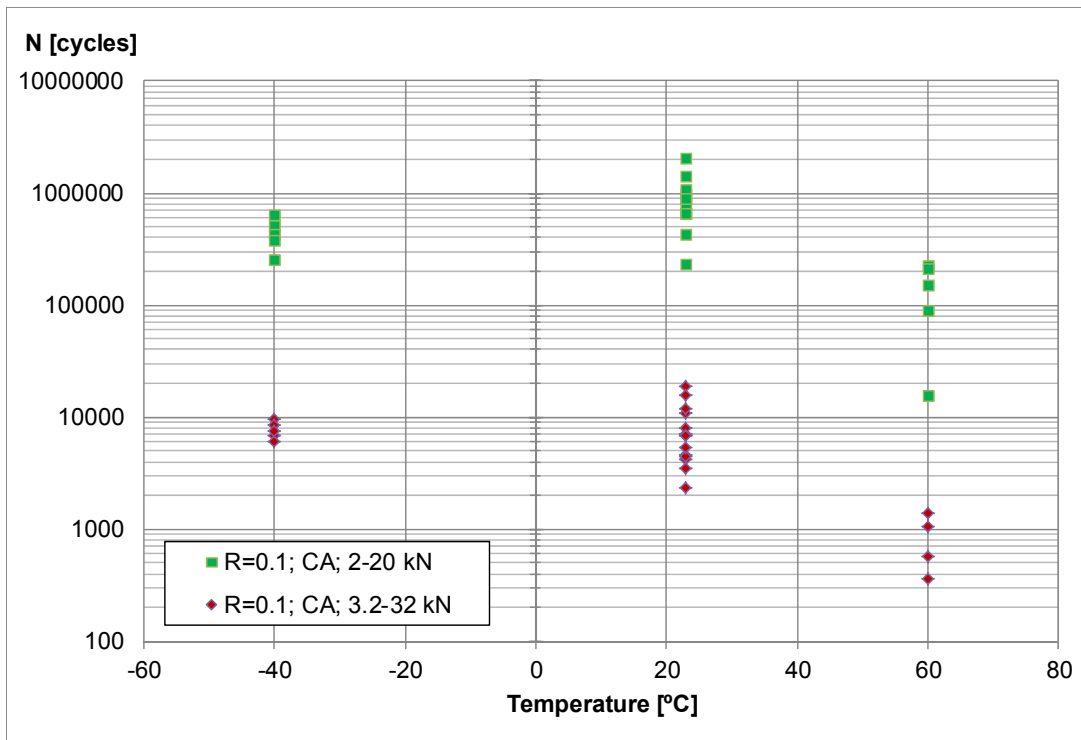


Figure 12: S-N diagram for R=-1 fatigue at -40 °C, 23 °C and 60 °C.

On the other hand, results from tests performed at 60 °C show a reduction in life of about three decades for a  $\pm 200$  MPa reversed loading and the specimen was unable to withstand fatigue loading at the planned 400 MPa load level. Therefore, it seems that a temperature of 60 °C is highly detrimental to the fatigue behavior of the laminate under examination.

Moreover, the slope is reduced compared to that of the ambient temperature condition. Therefore, the life is also much more sensitive to small variations in load level. Note that both curves ( $R = 0.1$  and  $R = -1$ ) show an increase in slope at  $-40\text{ }^{\circ}\text{C}$ . This may suggest that even though life expectancies for the composite exposed to low temperature do not change, the latter may be a little less sensitive to load fluctuation than at room temperature.

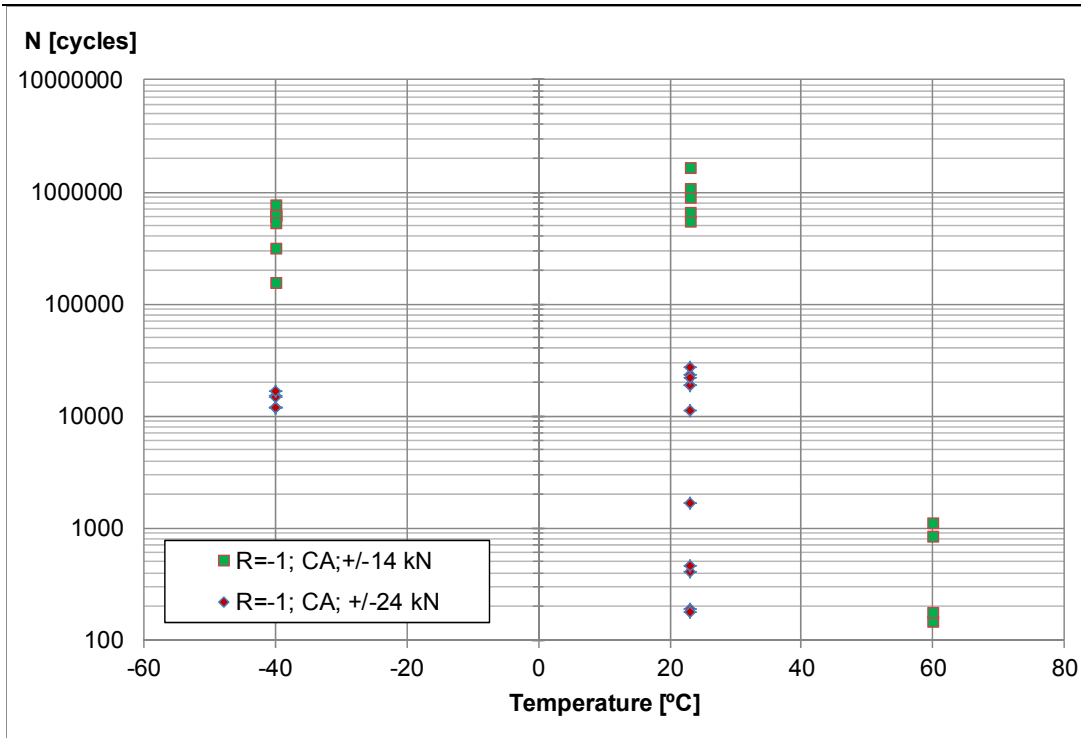
The fatigue life of specimen is also plotted against temperature for the low and high reference loads at  $R=0.1$  and  $R=-1$ . Figure 13 illustrates the behavior of the tension-tension fatigue test specimens while Figure 14 describes that of the fully reversed tension-compression fatigue.



**Figure 13: Life vs. temperature for tension-In tension fatigue at  $R=0.1$ .**

Results shown in Figure 13 illustrate again that the tension-tension fatigue strength of the E-glass/epoxy laminate under study is degraded at a temperature of  $60\text{ }^{\circ}\text{C}$ . At this temperature, specimen life is reduced by about an order of magnitude independently from the load level.

In the case of low temperatures, although the average specimen life is similar to that at room temperature, scatter seems to be somewhat lower and there is a slight tendency for life at low loads to be lower. However, considering the scatter of the reference condition, this tendency may not be significant at the loads that were studied.



**Figure 14: Life vs. temperature for tension-compression fatigue at R=-1.**

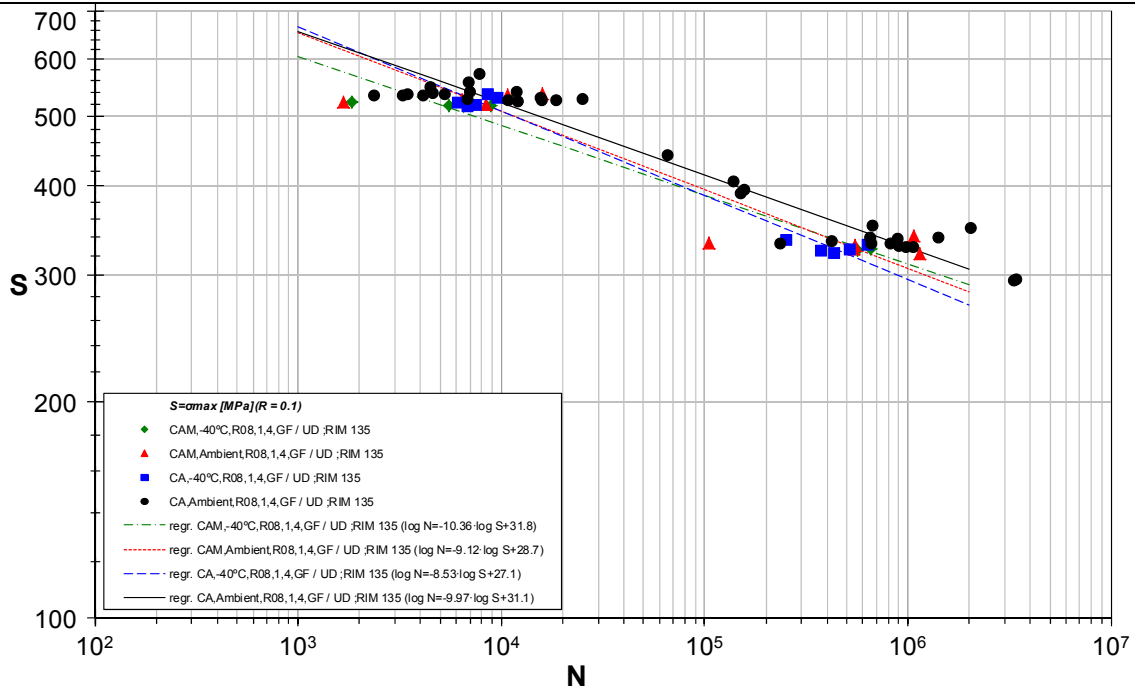
From Figure 14, the effect of high temperature on the fatigue life of the laminate is also very clear. For example, it is evident that at 60 °C, fatigue strength was reduced in such a way that specimens from the lower load level ( $\pm 14$  kN) only showed life equivalent to the weakest specimens tested at room temperature, but at a higher ( $\pm 24$  kN). Moreover, at 60 °C, the specimen was weakened in such a way that fatigue tests at this higher load level could not be reliably performed.

For tests at -40 °C, results from Figure 14 suggest that life of the specimens seem to be similar to those at room temperature.

## 5.4 INFLUENCE OF FREQUENCY

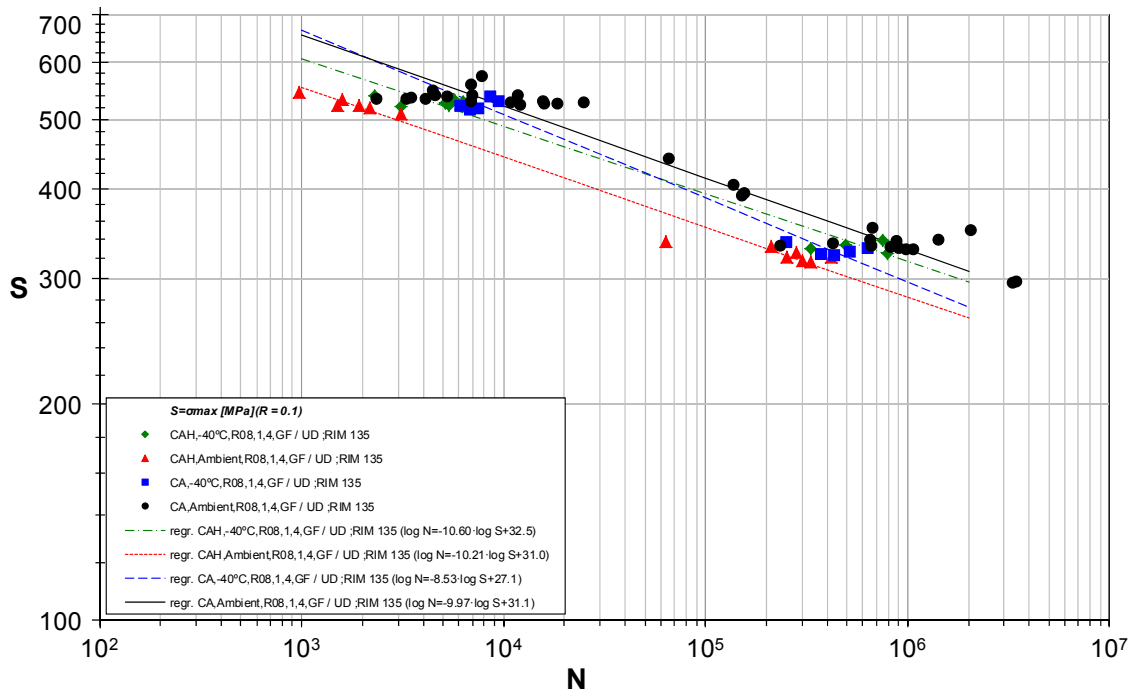
The effect of test frequencies on the fatigue life of the laminate is studied at ambient and -40 °C. For the reference condition, identified as CA, the test frequency is related to the actual load applied on the specimen as described in the methodology. For intermediate frequency (CAM), the test is conducted at 8 Hz, while elevated frequency (CAH) are made at 24 Hz. Intermediate and high frequencies are not related to the load level. Intermediate frequency tests are only performed at R = 0.1.

The S-N curves for R=0.1 at intermediate and elevated frequencies are respectively shown in Figure 15 and Figure 16.



**Figure 15: S-N diagram for R=0.1 fatigue at intermediate (CAM) and low (CA) frequencies.**

From the results shown in Figure 15, most data points for tests at intermediate frequency fall well within the dispersion of the baseline frequency test, although on the lower side. This suggests that for the unidirectional laminate being studied, a frequency of 8 Hz does not seem to significantly affect fatigue life of the specimen at tested at room or at low temperature.

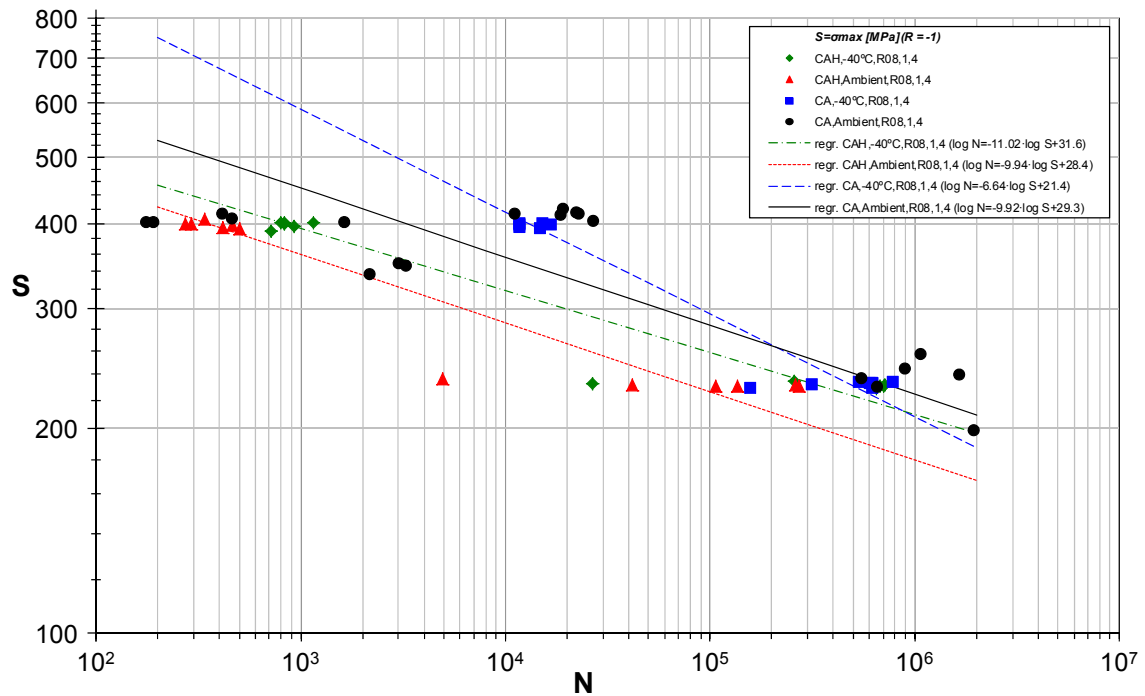


**Figure 16: S-N diagram for R=0.1 fatigue at high (CAH) and low (CA) frequencies.**

On the other hand, if the load frequency is increased to 24 Hz, life of specimens tested at room temperature are reduced. According to results presented in Figure 16, life of the high frequency specimen is reduced by almost a decade. The slope of the S-N curve is not influenced by the test frequency.

When tests are conducted at  $-40\text{ }^{\circ}\text{C}$ , the frequency effect appears to be reduced to a negligible level, as evidenced by specimens fatigue lives falling within the scatter of the reference condition and being well matched to the low temperature results at low frequencies. This suggests that the life reduction observed at ambient temperature may be the result of internal heat generation reaching an undesirable level.

Test results for high frequency tests performed at  $R=-1$  are presented as S-N curves in Figure 17. These results show that the general trends are the same as for tests conducted at a load ratio of  $R=0.1$ . However, scatter is much more important for fully reversed fatigue.



**Figure 17: S-N diagram for  $R=-1$  fatigue at high (CAH) and low (CA) frequencies.**

Therefore, even though the trend line of the fatigue lives at ambient temperature and high frequency is about an order of magnitude lower than for low frequencies, at high load levels it still lays within the scatter of the reference condition. Nonetheless, it could easily be argued that the life reduction is significant since the slope of both curves are similar and lower load results show a clearer trend toward life reduction.

Results for the  $-40\text{ }^{\circ}\text{C}$  results prove to be more equivocal. Taken in isolation, results from  $-40\text{ }^{\circ}\text{C}$  would suggest that the combination of low temperature and high loading rate produce a reduction of the specimen life of the order of a decade, while at lower loads, life would converge to a similar level. On the other hand, it was initially stated that lower temperature of the order of  $-40\text{ }^{\circ}\text{C}$  does not have a significant effect on fatigue life in tension fatigue. If one compares the low temperature results to those of the reference condition, the reduction in fatigue life is insignificant. Slopes of both curves for high frequency tests remain similar to the reference condition at ambient temperature.

In order to relate effect of frequency on the fatigue life of the specimens, data points may also be plotted in a life-frequency diagram. In such a diagram, the fatigue life each data point from a specific load level is plotted against the test loading frequency. In this manner, frequency effects may be isolated. Figure 18 and Figure 19 respectively show the life-frequency plots for  $R=0.1$  and  $R=-1$  tests.





In the case of fully reversed fatigue, frequency effect seems to be more important than for tension-tension loading. In the case of  $R=-1$  performed at room temperature, tests performed at high frequency (24 Hz) provide lives that are within the limits of the reference conditions results scatter. However, it is clear from Figure 19 that the specimen consistently failed in the lower region of the range.

At the lower temperature of  $-40\text{ }^{\circ}\text{C}$ , observations from the life-frequency diagram suggest that there could be a load-temperature-frequency interrelation. For high loads at low temperatures, there is a significant reduction of observed lives at 24 Hz. This is however not the case at lower loads where measured lives are quite similar independently of loading frequency.

## 6. CONCLUDING REMARKS

An extensive test programme was carried out in an attempt to de-couple the effects of testing frequency and testing temperature on fatigue life. The results described in this document give rise to the hypothesis that the lower lifetimes in fatigue at higher frequencies can be attributed for the largest part to the frequency-induced temperature of the specimen, not to the frequency per se.

In addition, the results show that for this particular specimen/laminate combination, the fatigue life obtained at  $-40\text{ }^{\circ}\text{C}$  is representative of the fatigue life at room temperature, regardless of testing frequency, within the range of frequencies tested here. This gives room for speculation on the possibility of accelerated testing, although a more thorough study of the fatigue failure mechanism should be pursued.

The results described in this report are a useful description of fatigue behaviour in  $R=0.1$  and  $R=-1$  fatigue, at  $-40\text{ }^{\circ}\text{C}$ , Room temperature, and  $+60\text{ }^{\circ}\text{C}$ . In addition, they are relevant for interpretation of fatigue test results on thick laminates, and general constant life diagram, particularly in the regions of high mean stress fatigue.

Most specimens failed in the tab area, which is the expected failure mode for the reference specimen. However, for the  $+60\text{ }^{\circ}$  tests, grip failures were more pronounced.

The method of local temperature measurement employed in this work has several drawbacks. First of all, temperature measurement is local, where for a better correlation of failure mode and location, lifetime, and temperature, a full-field temperature measurement would be recommended.

Second, the temperature measurement is superficial and the actual temperature (distribution) inside the specimen can only be derived accurately from finite element modelling in combination with multiple location or full-field temperature measurement.

## 7. ACKNOWLEDGEMENT

The work reported here was partially carried out in the framework of the EU-FP6 funded UPWIND project, contract number SES6-019945

## 8. REFERENCES

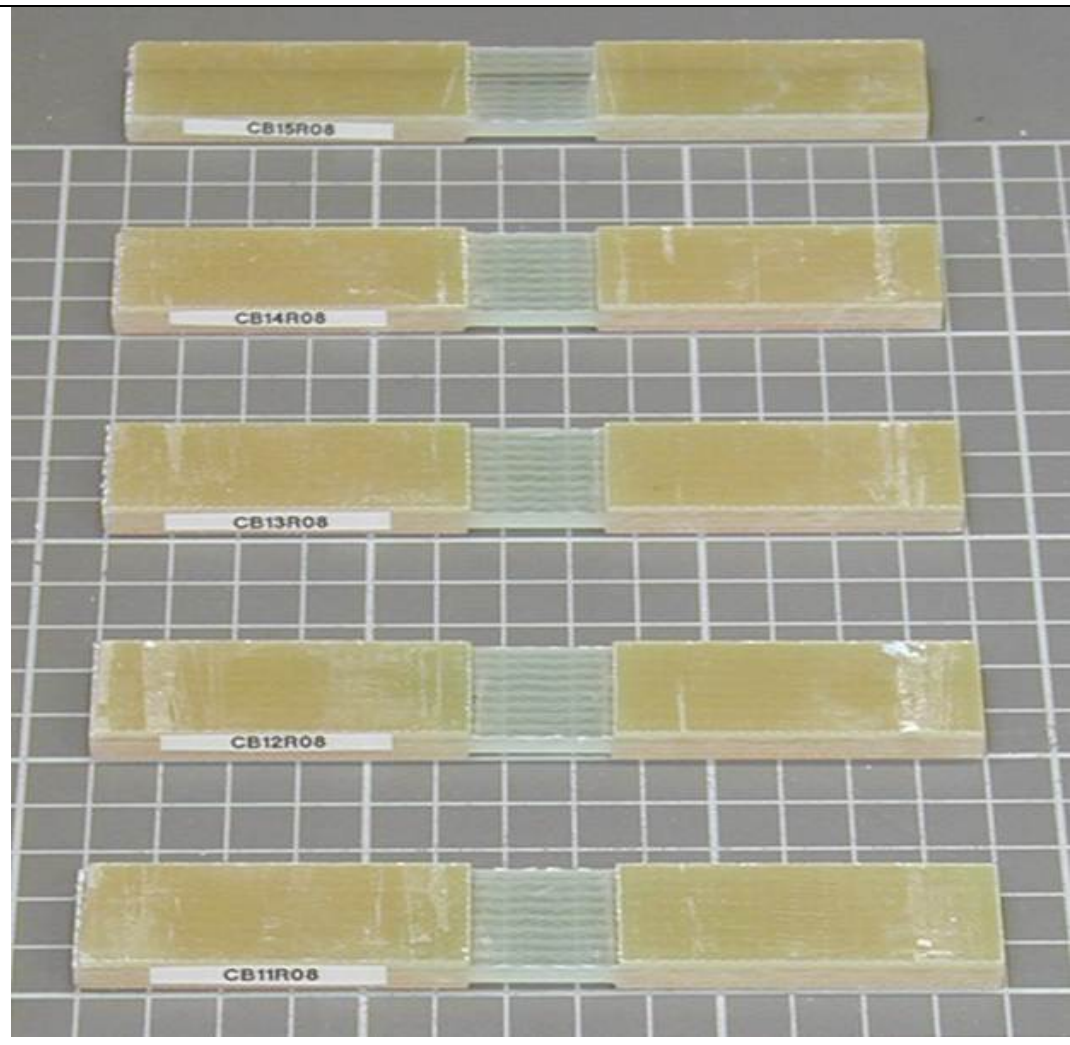
- [1] [www.wmc.eu/optimatblades.php](http://www.wmc.eu/optimatblades.php)
- [2] Krause, O., and Philippidis, Th., 'General test specification', OPTIMAT document OB\_TC\_R014 rev. 005, September 2005
- [3] Janssen, L.G.J., van Wingerde, A., Mishnaevsky, L., Philippidis, Th., 'Detailed Plan of Action, WP 3 'Rotor Structures and Materials', ECN-X--06-135, Deliverable 3.4.1
- [4] Liu, J. J. et Karbhari, V. M. (2007). Performance and design of fibre-reinforced polymer composites at cold temperatures : current status and future needs. International Journal of Materials and Product Technology, 28(1) :1–7.

- 
- [5] Adams, R. D. et Singh, M. M. (2001). Low temperature transitions in fibre reinforced polymers. *Composites Part A : Applied Science and Manufacturing*, 32(6) :797– 814.
  - [6] Dutta, Piyush K. 1998. « Thermo-mechanical behavior of polymer composites. ». In *Advanced multilayered and fibre-reinforced composites; Proceedings of the NATO Advanced Research Workshop*, (Kiev, Ukraine; 2-6 June 1997). p. 541-554. Pays-Bas.
  - [7] Chamis, C. C. (1983). Simplified Composite Micromechanics Equations for Hygral, Thermal and Mechanical Properties. Rapport technique NAS 1.15 :83320, NASA Glenn Research Center.
  - [8] Chamis, C. C. (1984). Simplified composite micromechanics equations for strength, fracture toughness and environmental effects. Rapport technique NAS 1.15 :83696, NASA Glenn Research Center.
  - [9] Lord, H. W. et Dutta, P. K. (1988). On the Design of Polymeric Composite Structures for Cold Regions Applications. *Journal of Reinforced Plastics and Composites*, 7(5) :435–458.
  - [10] Laurent Cormier and Simon Joncas. Effects of cold temperature, moisture and freeze-thaw cycles on the mechanical properties of unidirectional glass fiber-epoxy composites. In *51st AIAA/ASME/ASCE/AHS/ASC Structures, Structural Dynamics and Materials Conference*, Orlando, FL, United states, 2010.
  - [11] Apinis, R. Acceleration of fatigue tests of polymer composite materials by using high-frequency loadings, *Mechanics of Composite Materials*, Vol. 40, No. 2, 2004.
  - [12] Michael Kinsella, Dennis Murray, David Crane, John Mancinelli, and Mark Kranjc. Mechanical properties of polymeric composites reinforced with high strength glass fibers. volume 33, pages 1644 – 1657, Seattle, WA, United states, 2001.
  - [13] Karbhari, V. M., Chin, J. W., Hunston, D., Benmokrane, B., Juska, T., Morgan, R., Lesko, J. J., Sorathia, U., et Reynaud, D. (2003). Durability gap analysis for fiber- reinforced polymer composites in civil infrastructure. *Journal of Composites for Construction*, 7(3) :238–247.
  - [14] Wohler, A. (1871). Tests to Determine the Forces Acting on Railway Carriage Axles and the Capacity of Resistance of the Axles. *English Abstract Engineering*, 2 :199.
  - [15] Tang, Hai C. et al. Temperature effects on fatigue of polymer composites.
  - [16] Megnis, M., Brøndsted, P. and Eriksen, K.P., Effects of extreme conditions on properties of the reference material, Optimat blades TG3, OB\_TG3\_R015 rev.002.
  - [17] Bureau, M. N. et Denault, J. (2004). Fatigue Resistance of Continuous Glass Fiber-Polypropylene Composites : Temperature Dependence. *Polymer Composites*, 25 :622–629.
  - [18] Hahn, H.T. and Turkgenç, O., The effect of loading parameters on fatigue of composite laminates: part IV information systems, 2000, contract report DOT/FAA/AR-00/48
  - [19] Mishnaevsky Jr L., and Brøndsted, P., Micromechanical Modelling of Strength and Damage of Fiber Reinforced Composites, Annual Report on EU FP6 Project UpWind Integrated Wind Turbine Design (WP 3.2), Period: 1.4.2006-30.3.2007
  - [20] Mandell, J.F. and Meier, U., Effects of stress ratio, frequency and loading time on the tensile fatigue of glass-reinforced epoxy, Long-term behaviour of composites, ASTM STP 813, T.K. O'Brien, Ed., Philadelphia, 1983, pp. 55-77.
  - [21] Bernasconi, A. et al. Temperature and frequency effect on the fatigue behaviour of short glass fibre reinforced polyamide.
  - [22] ISO 527-2. Plastics - Determination of tensile properties - part 2: Test conditions for moulding and extrusion plastics, 1993.
  - [23] OptiDAT database edition 2011, February 10, 2011, [www.upwind.eu](http://www.upwind.eu)

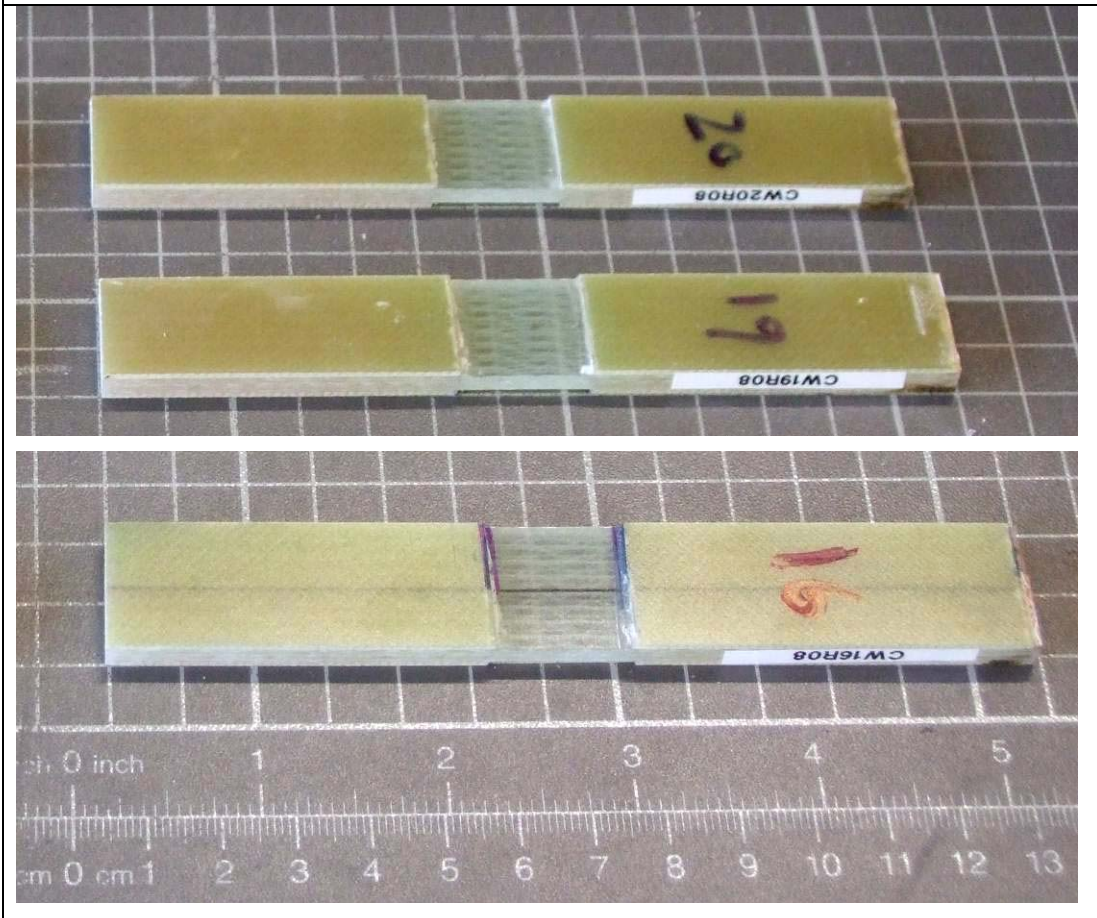


**ANNEX A Selected specimen pictures before testing**

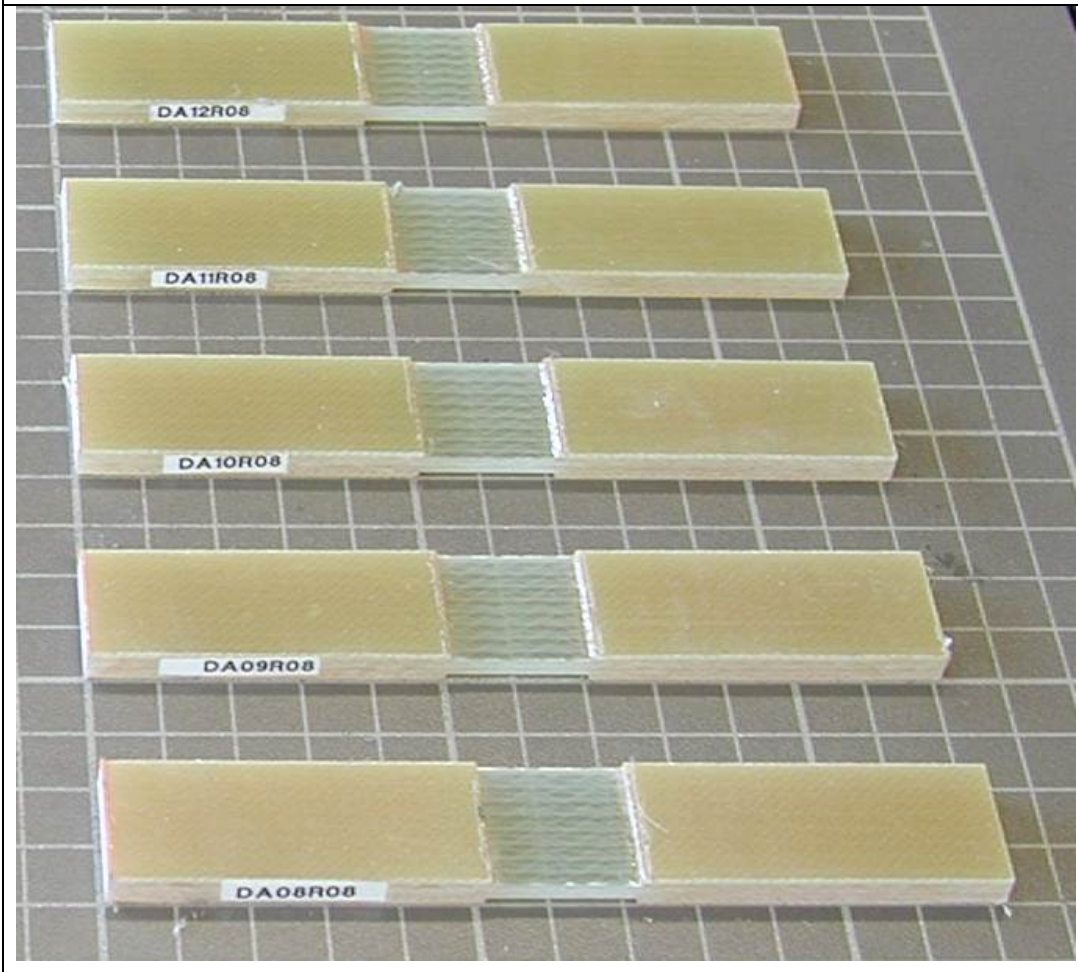
CB11R08 – CB15R08



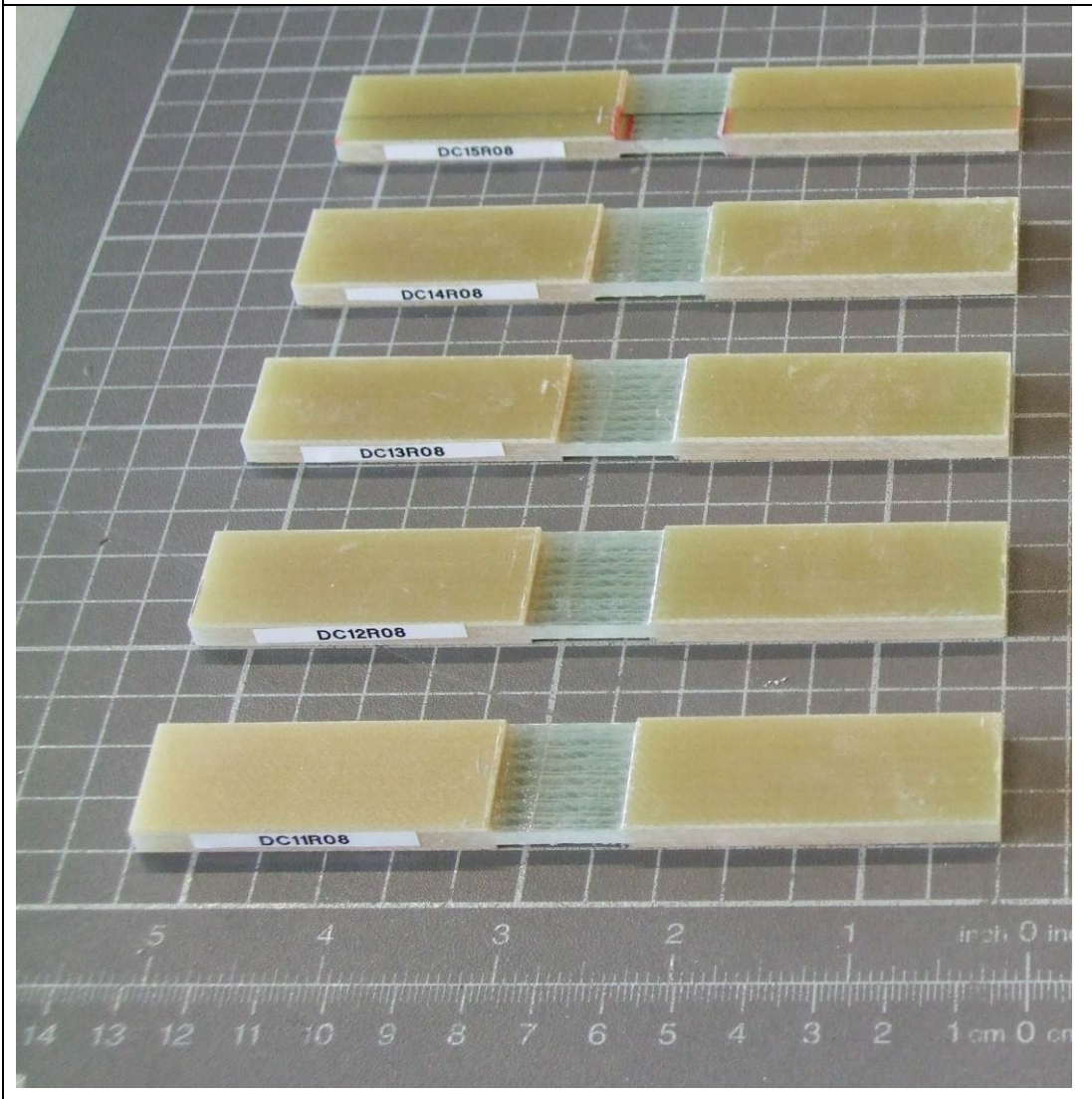
CW16R08 – CV19R08 – CW20R08



DA08R08 – DA12R08



DC11R08 – DC15R08

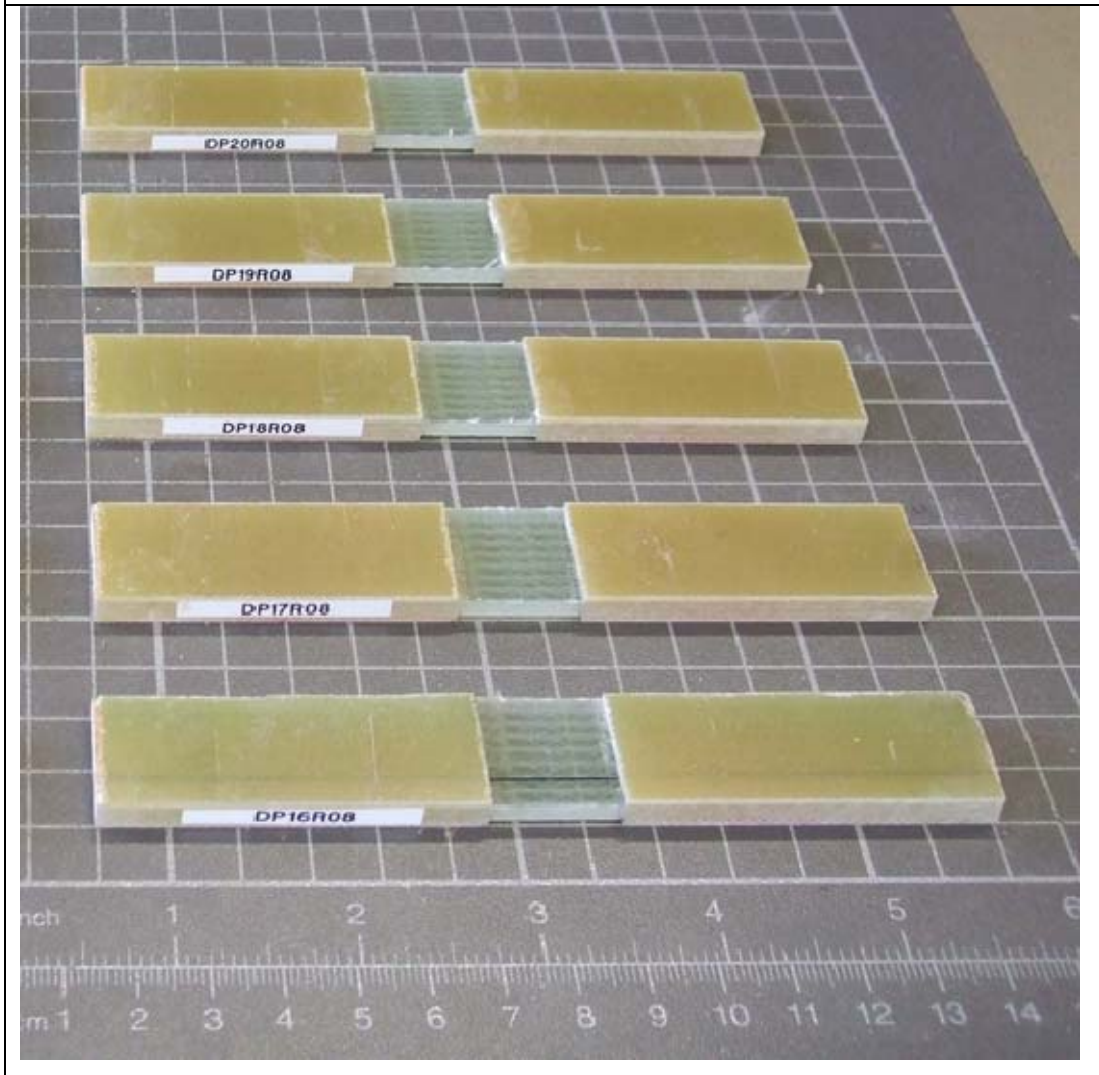


DD25R08 – DD27R08 – DD28R08

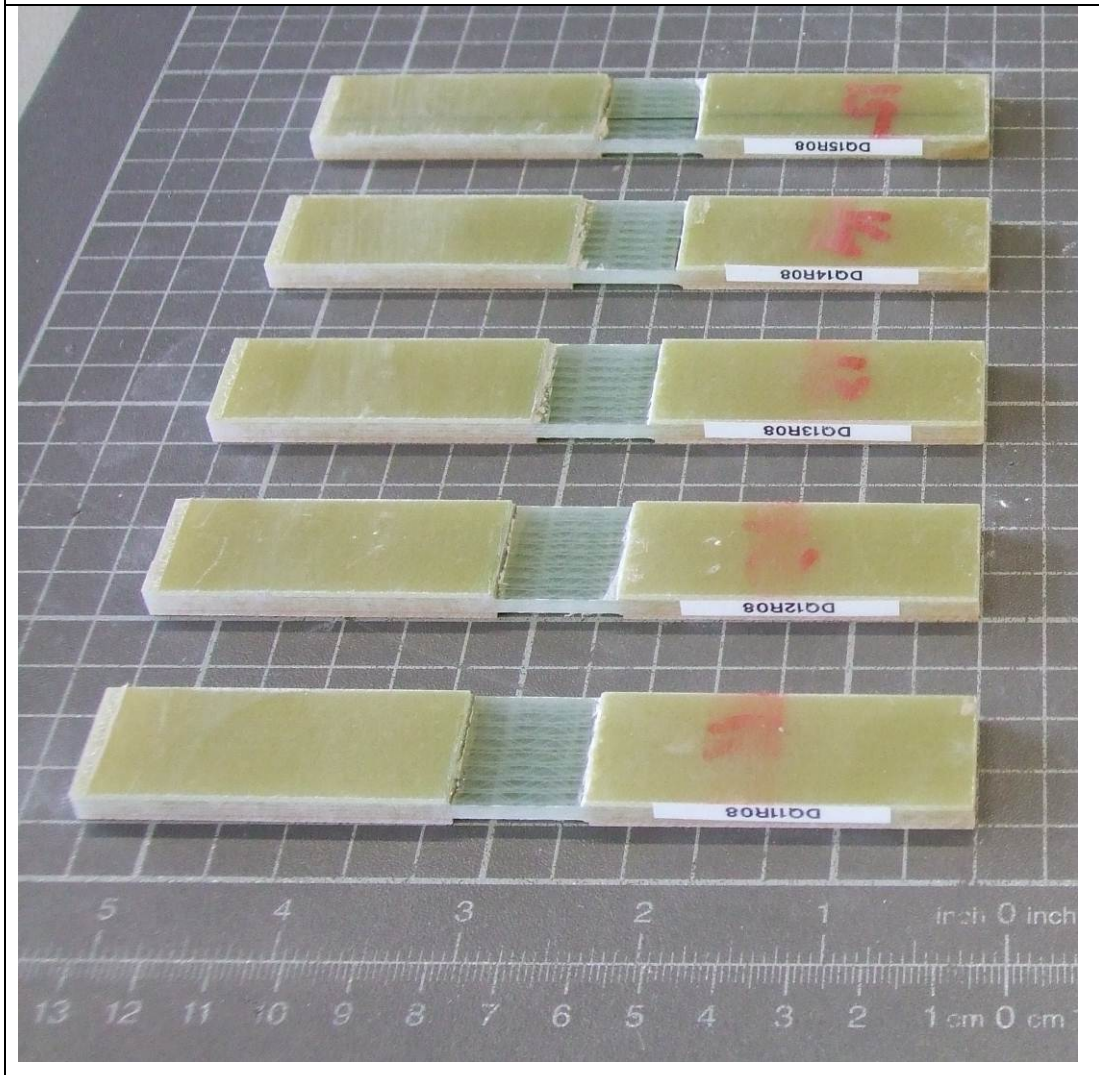




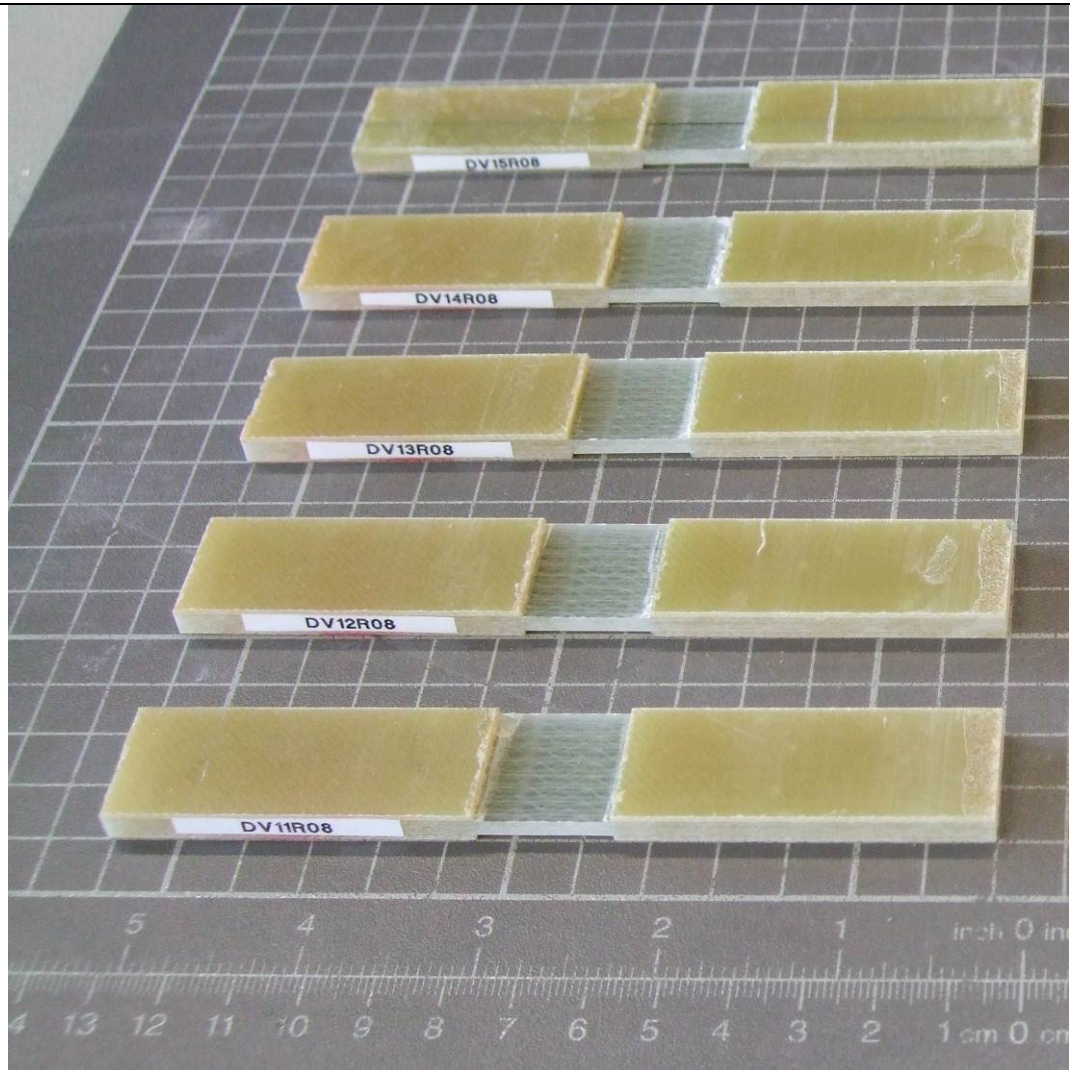
DP16R08 – DP20R08



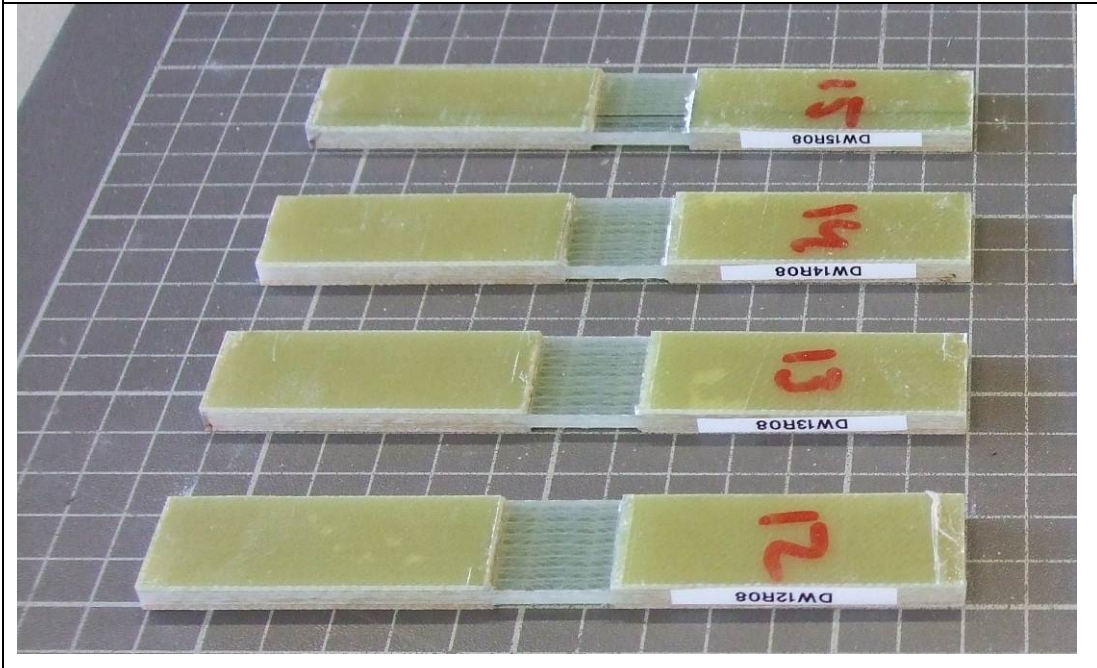
DQ11R08 – DQ15R08



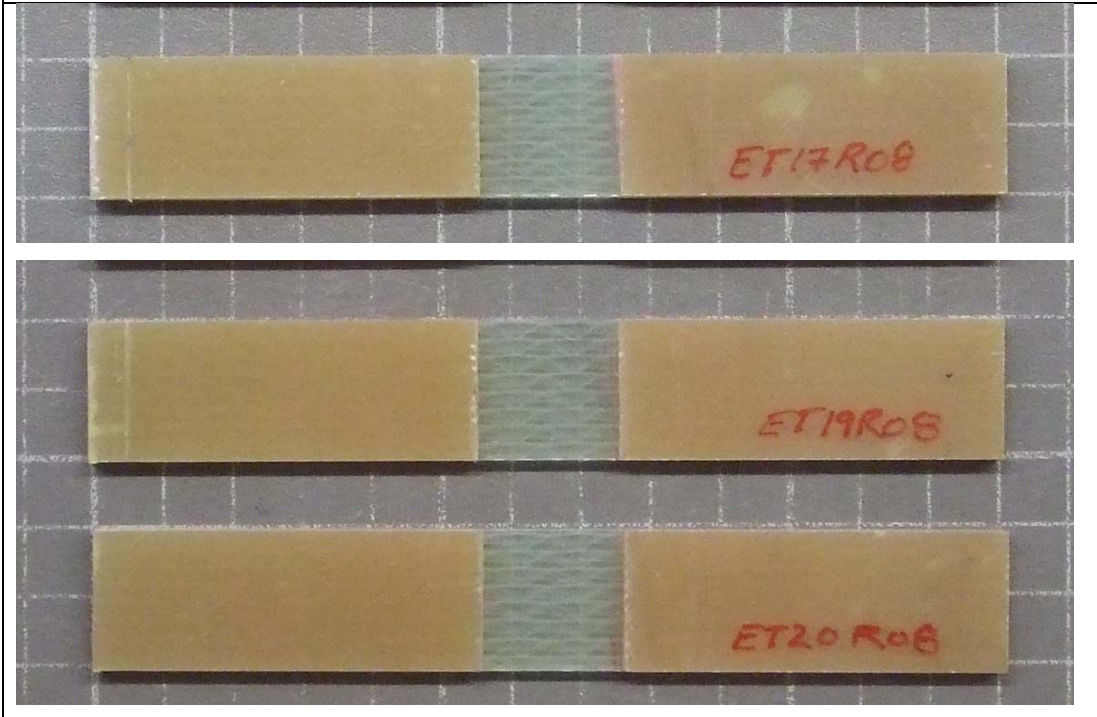
DV11R08 – DV15R08



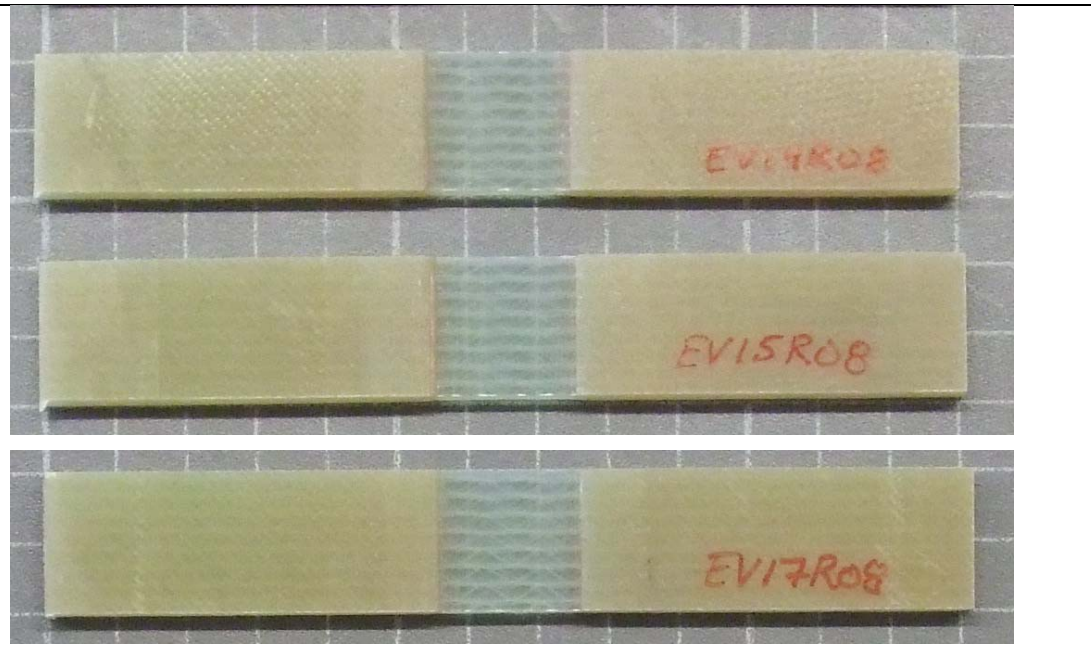
DW12R08 – DW15R08



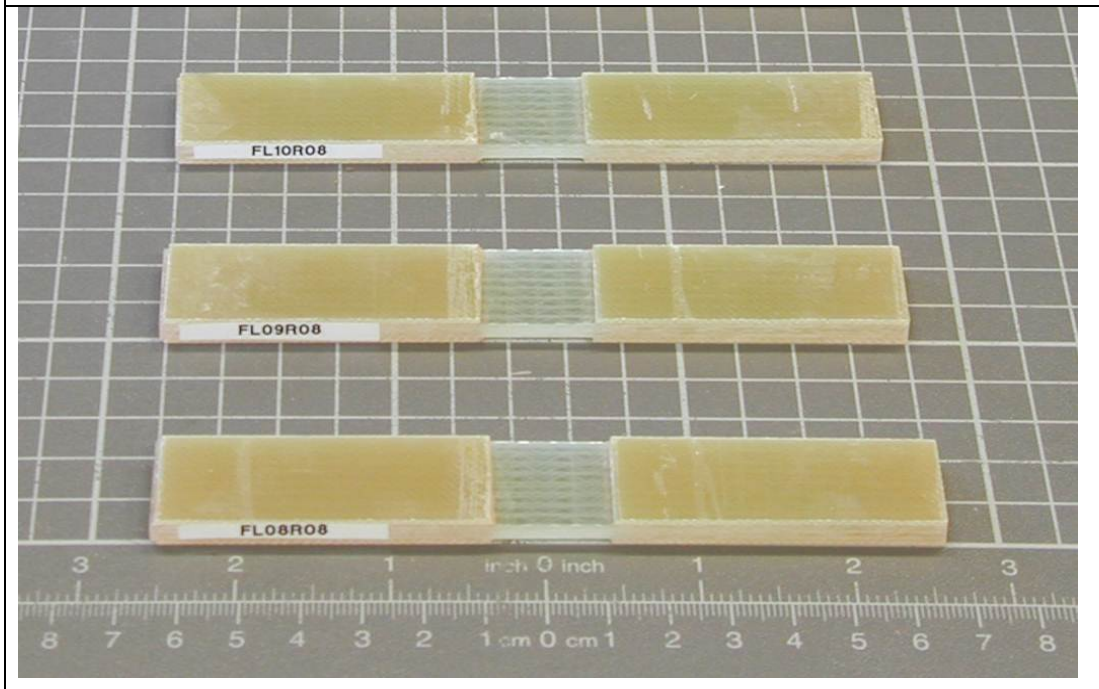
ET17R08 – ET19R08 – ET20R08



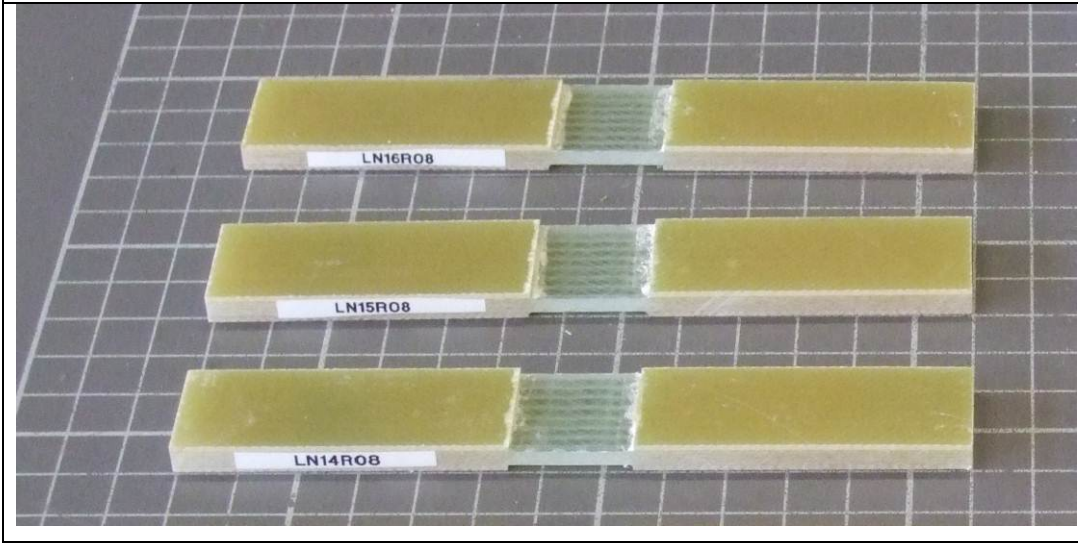
EV14R08 – EV15R08 – EV17R08



FL08R08 – FL10R08



LN14R08 – LN16R08





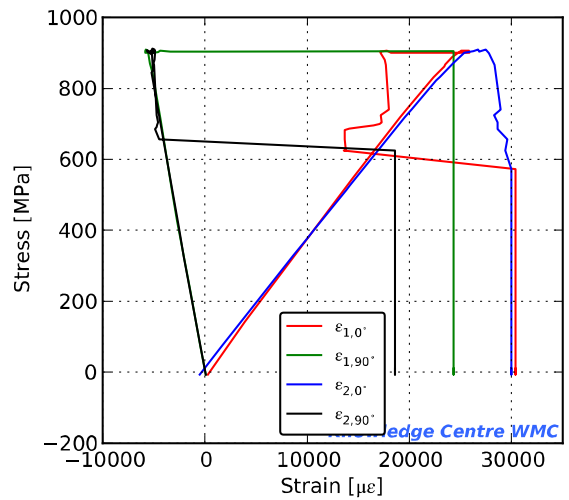
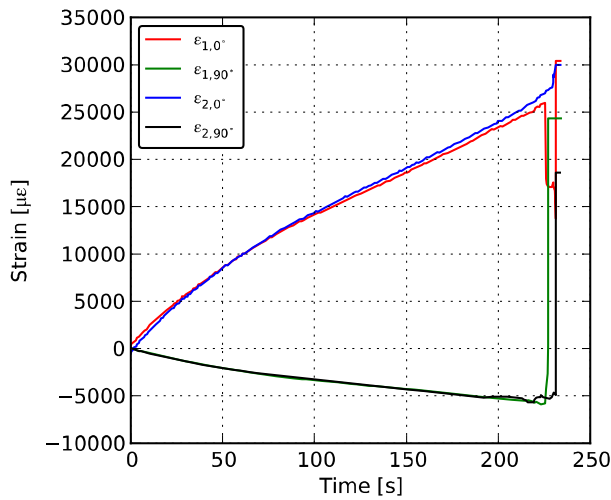
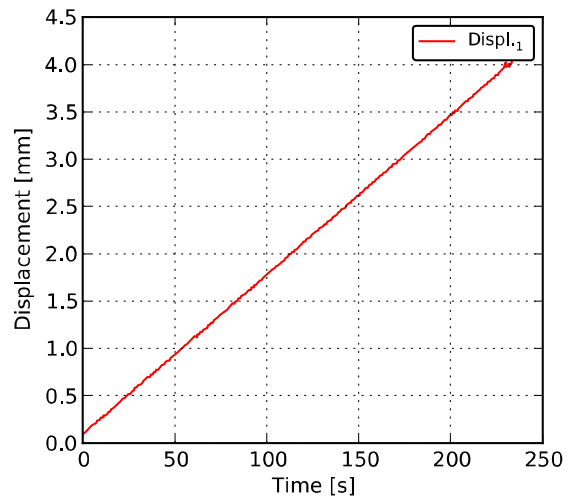
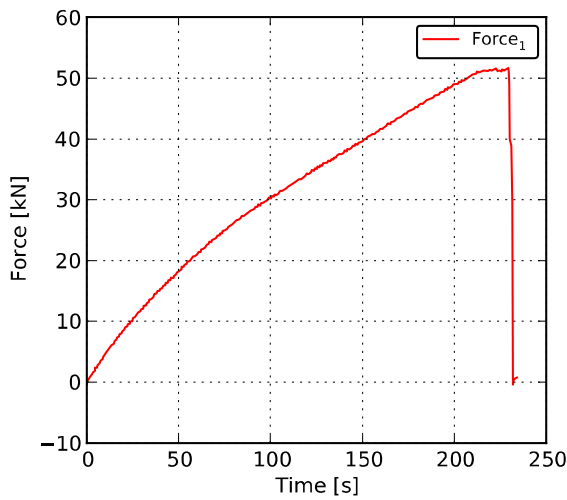


## ANNEX B Measurement summaries

23 °C Static tension

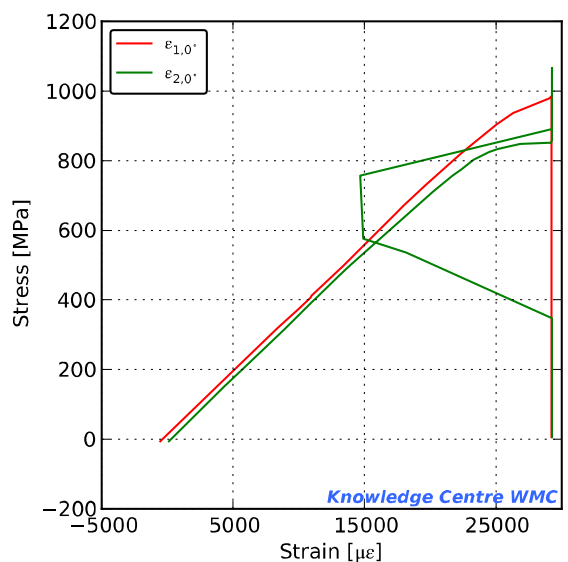
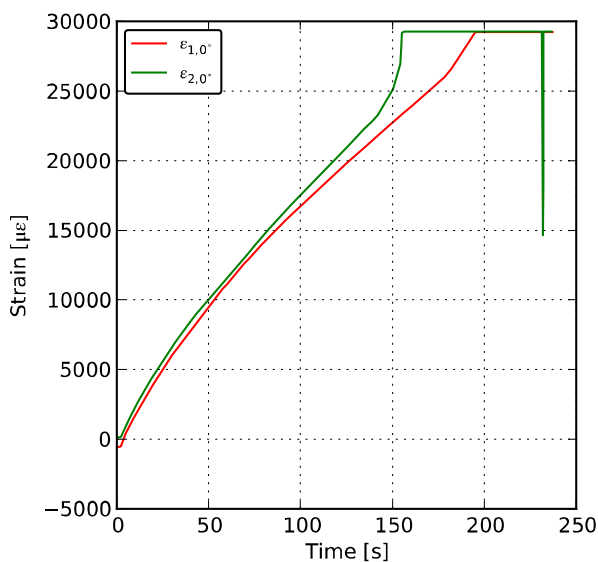
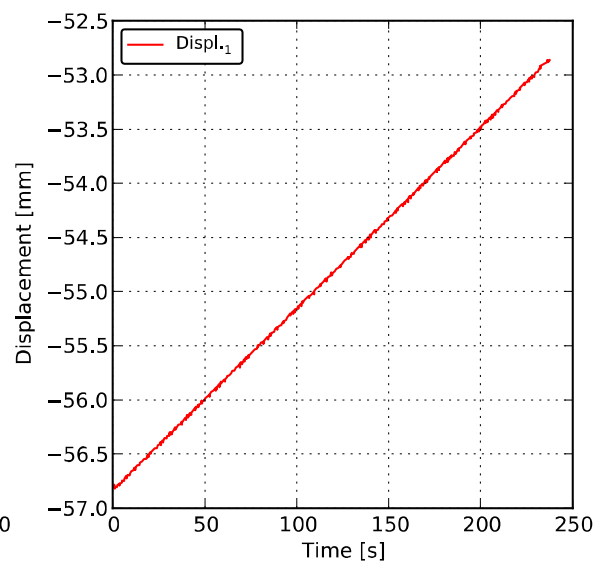
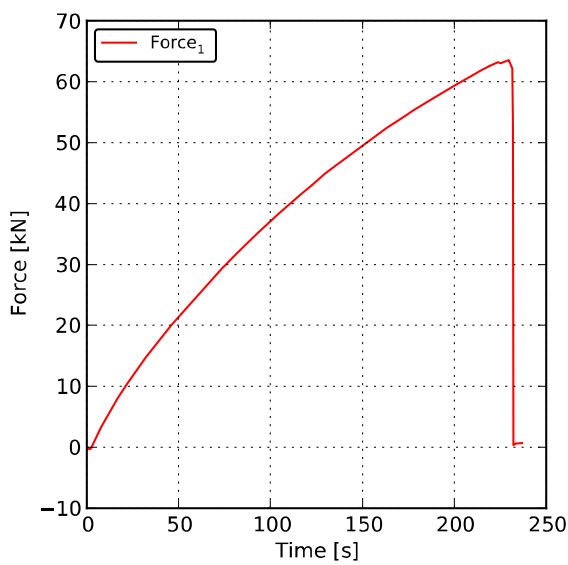
Test results for specimen: BT06R08

Channel	Maximum	Minimum	at max. Force
Force <sub>1</sub> [kN ]	51.82	-0.40	51.82
Displ. <sub>1</sub> [mm]	4.03	0.08	3.97
$\epsilon_{1,0^\circ}$ [ $\mu\epsilon$ ]	30403	251	17110
$\epsilon_{1,90^\circ}$ [ $\mu\epsilon$ ]	24346	-5983	24346
$\epsilon_{2,0^\circ}$ [ $\mu\epsilon$ ]	29982	-544	27614
$\epsilon_{2,90^\circ}$ [ $\mu\epsilon$ ]	18620	-5696	-5156
$\sigma_1$ [MPa]	913.4	-7.1	913.4
Temperature	Maximum	Minimum	Average
Temp. <sub>2</sub> [ ° C]	26.1	25.3	25.5
$E_{1t}$ [MPa]	40944	Young's Modulus front (tension)	
$E_{2t}$ [MPa]	36478	Young's Modulus back (tension)	
$\nu_{1t}$	0.264	Poisson's Ratio front (tension)	
$\nu_{2t}$	0.247	Poisson's Ratio back (tension)	



Test results for specimen: ET03R08

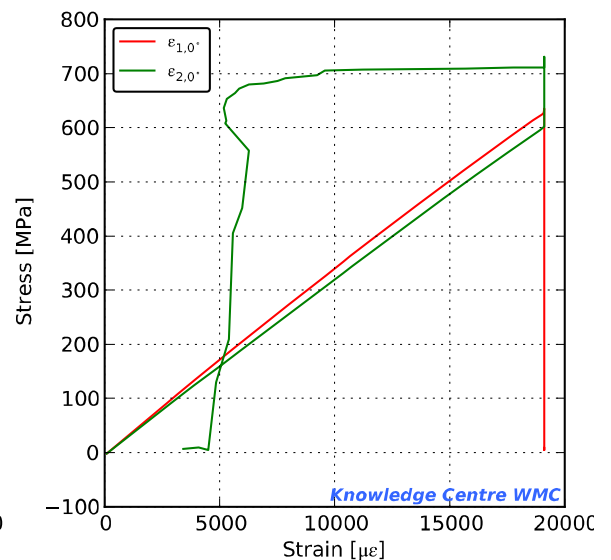
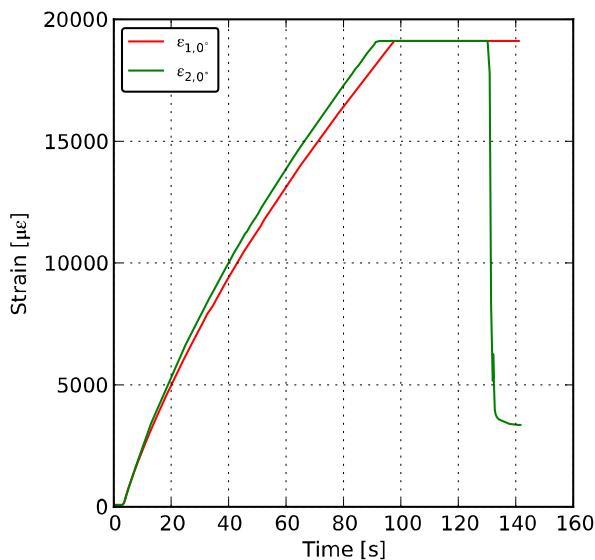
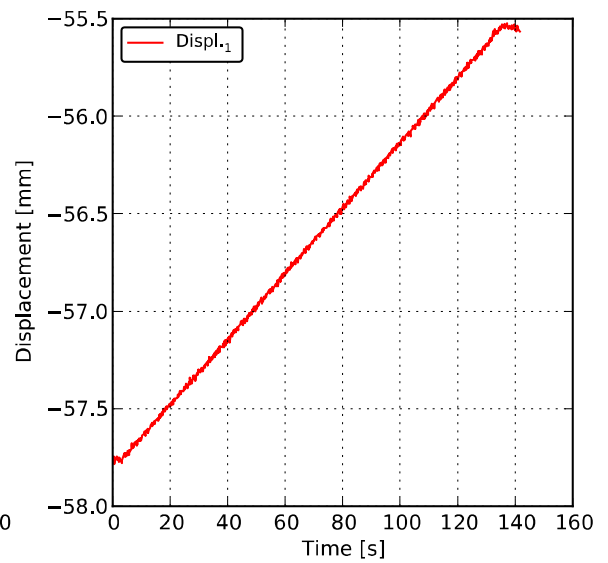
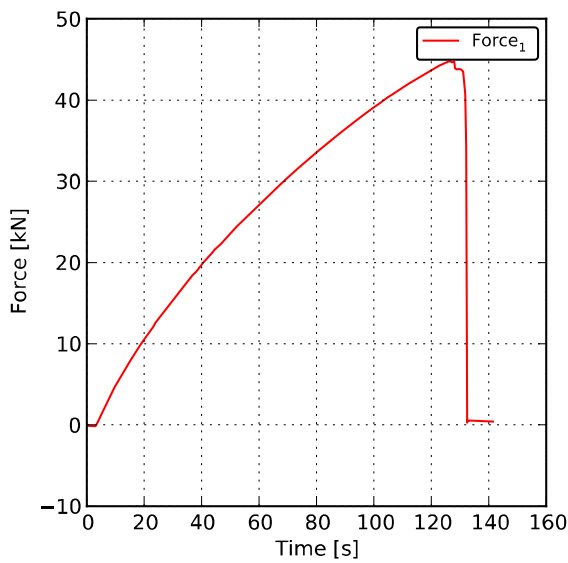
Channel	Maximum	Minimum	at max. Force
Force <sub>1</sub> [kN ]	63.59	-0.43	63.59
Displ. <sub>1</sub> [mm]	-52.86	-56.82	-53.00
$\epsilon_{1,0^\circ}$ [ $\mu\epsilon$ ]	29225	-587	29225
$\epsilon_{2,0^\circ}$ [ $\mu\epsilon$ ]	29285	65	29285
$\sigma_1$ [MPa]	1067.3	-7.2	1067.3
Temperature	Maximum	Minimum	Average
Temp. <sub>2</sub> [° C]	-39.5	-39.9	-39.7
$E_{1t}$ [MPa]	36471	Young's Modulus front (tension)	
$E_{2t}$ [MPa]	37476	Young's Modulus back (tension)	



Knowledge Centre WMC

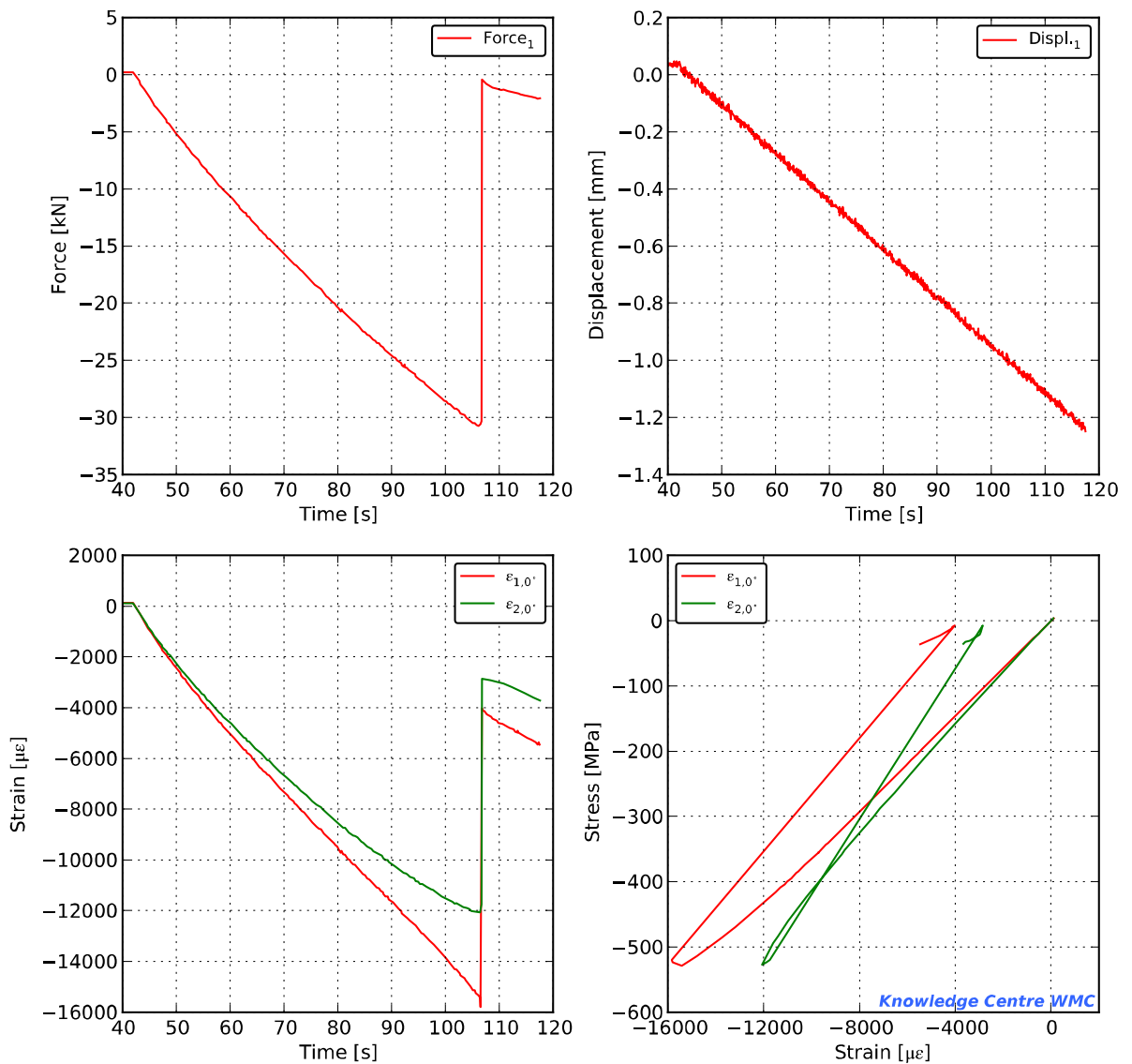
Test results for specimen: ET15R08

Channel	Maximum	Minimum	at max. Force
Force <sub>1</sub> [kN ]	44.86	-0.28	44.86
Displ. <sub>1</sub> [mm]	-55.52	-57.78	-55.71
$\epsilon_{1,0^\circ}$ [ $\mu\epsilon$ ]	19118	5	19118
$\epsilon_{2,0^\circ}$ [ $\mu\epsilon$ ]	19113	10	19113
$\sigma_1$ [MPa]	731.2	-4.6	731.2
Temperature	Maximum	Minimum	Average
Temp. <sub>2</sub> [ ° C]	60.2	59.8	60.0
$E_{1t}$ [MPa]	35743	Young's Modulus front (tension)	
$E_{2t}$ [MPa]	33479	Young's Modulus back (tension)	



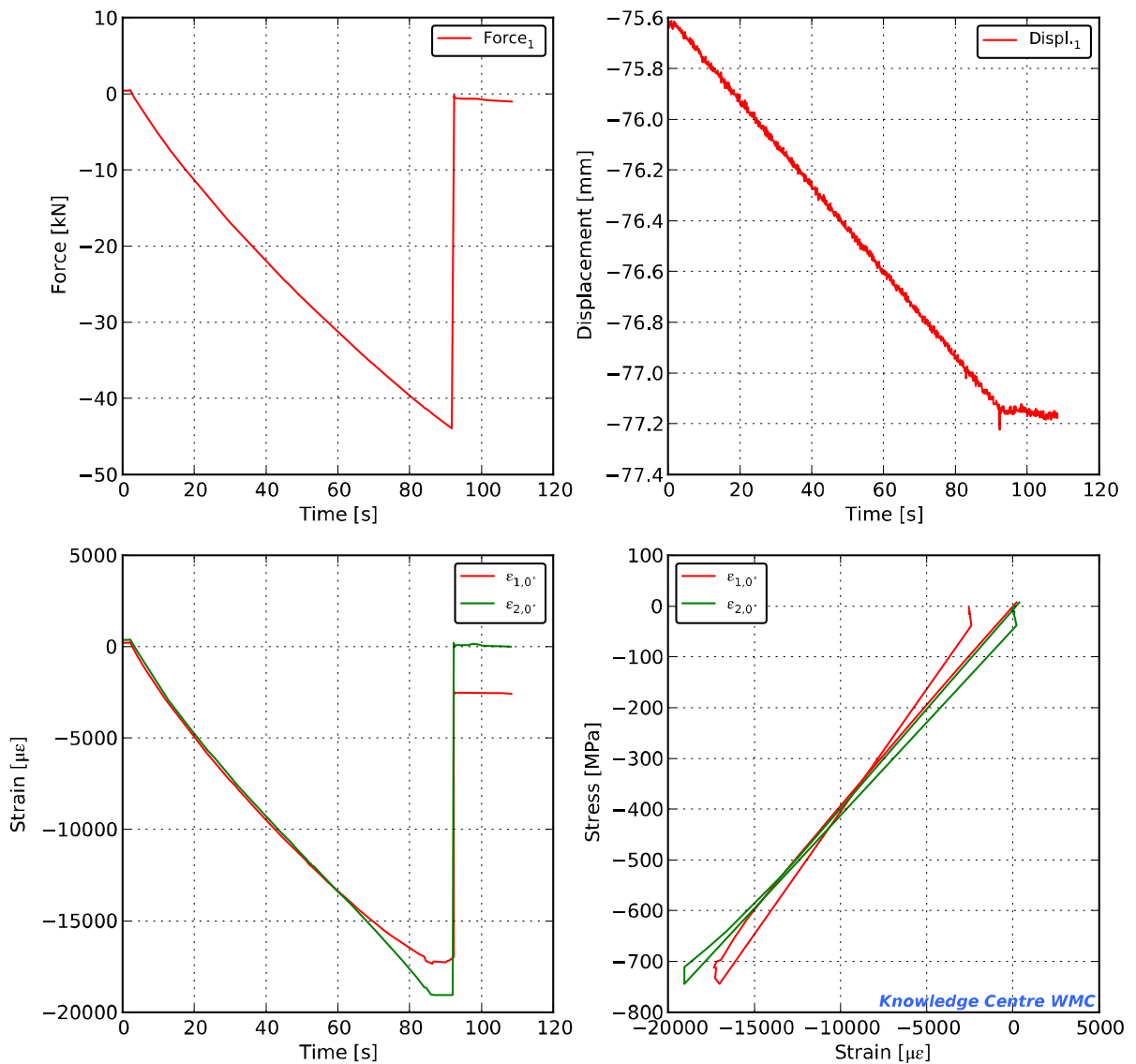
Test results for specimen: BU06R08

Channel	Maximum	Minimum	at max. Force
Force <sub>1</sub> [kN]	0.25	-30.93	-30.93
Displ. <sub>1</sub> [mm]	0.05	-1.25	-1.06
ε <sub>1,0°</sub> [με]	131	-15854	-15459
ε <sub>2,0°</sub> [με]	112	-12097	-12097
σ <sub>1</sub> [MPa]	4.2	-530.1	-530.1
Temperature	Maximum	Minimum	Average
Temp. <sub>2</sub> [°C]	23.6	23.0	23.3
E <sub>1c</sub> [MPa]	35722	Young's Modulus front (comp.)	
E <sub>2c</sub> [MPa]	39305	Young's Modulus back (comp.)	



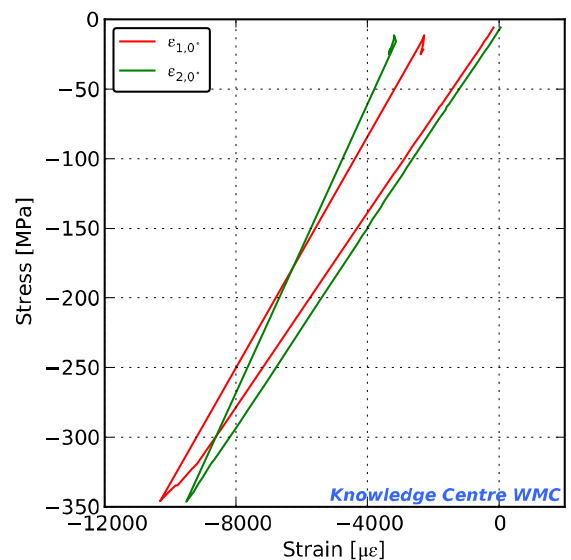
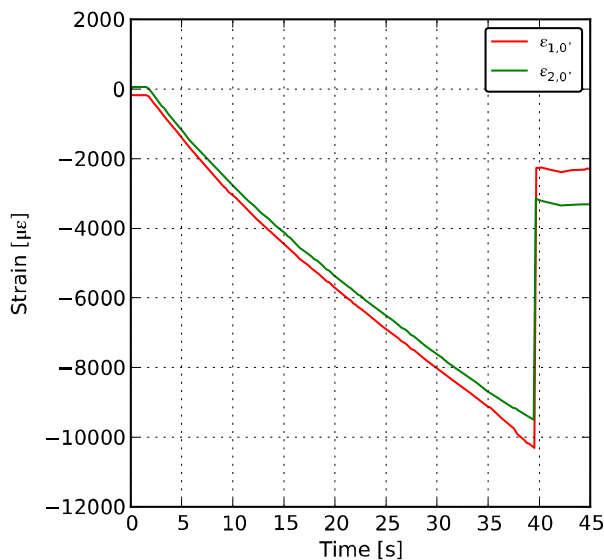
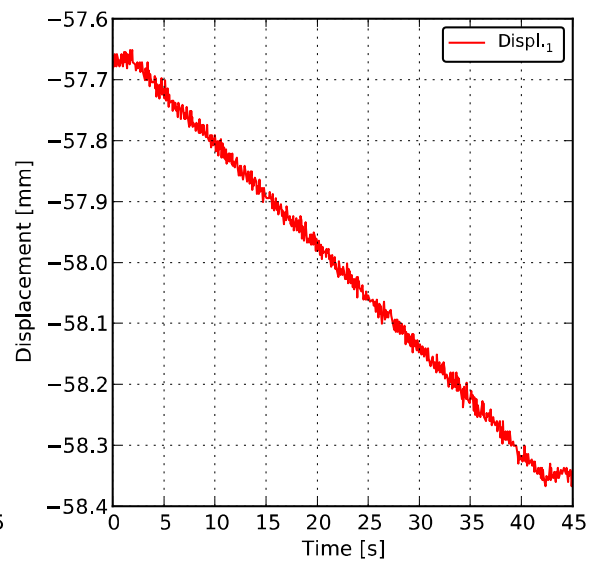
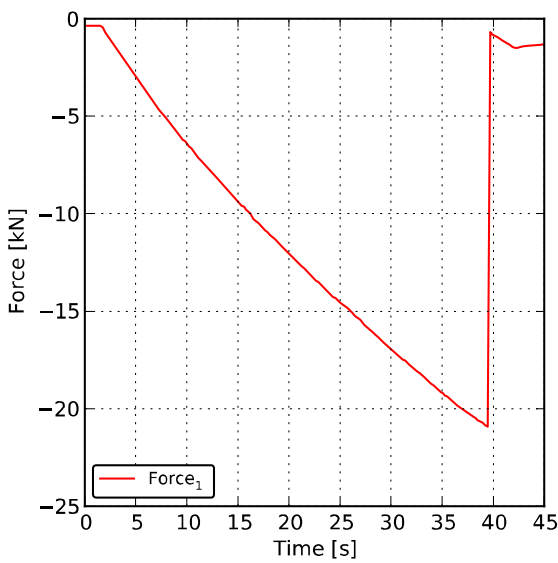
Test results for specimen: DW07R08

Channel	Maximum	Minimum	at max. Force
Force <sub>1</sub> [kN ]	0.49	-44.17	-44.17
Displ. <sub>1</sub> [mm]	-75.61	-77.22	-77.15
$\epsilon_{1,0^\circ}$ [ $\mu\epsilon$ ]	239	-17374	-16973
$\epsilon_{2,0^\circ}$ [ $\mu\epsilon$ ]	399	-19056	-19056
$\sigma_1$ [MPa]	8.3	-747.3	-747.3
Temperature	Maximum	Minimum	Average
Temp. <sub>2</sub> [ ° C]	-39.3	-40.1	-39.7
$E_{1c}$ [MPa]	38303	Young's Modulus front (comp.)	
$E_{2c}$ [MPa]	38866	Young's Modulus back (comp.)	



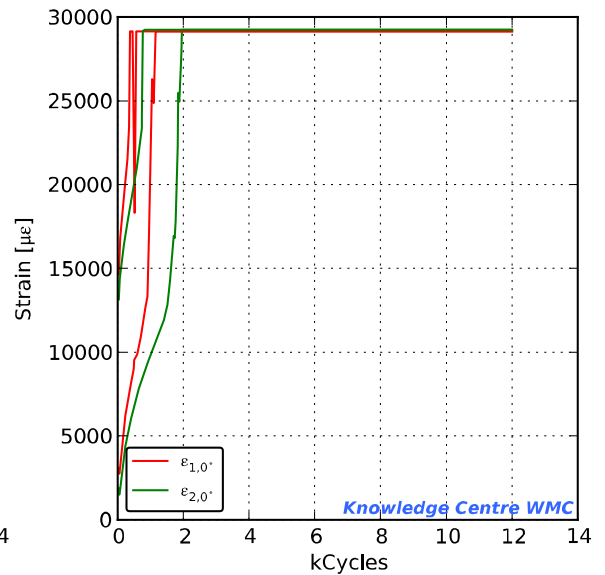
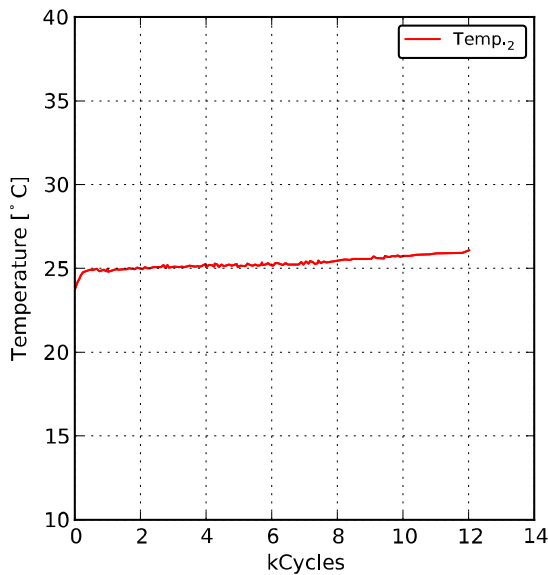
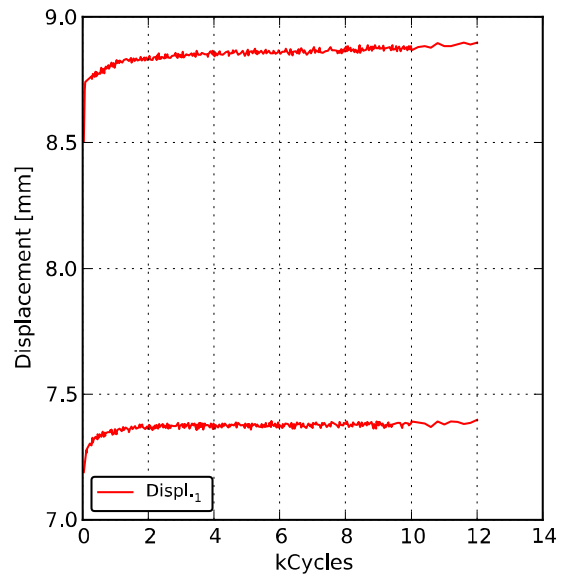
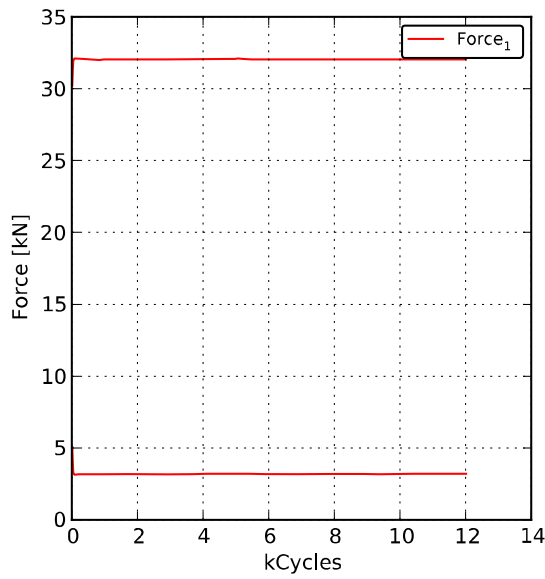
Test results for specimen: ET10R08

Channel	Maximum	Minimum	at max. Force
Force <sub>1</sub> [kN]	-0.35	-20.99	-20.99
Displ. <sub>1</sub> [mm]	-57.65	-58.37	-58.30
$\epsilon_{1,0^\circ}$ [ $\mu\epsilon$ ]	-167	-10339	-10339
$\epsilon_{2,0^\circ}$ [ $\mu\epsilon$ ]	57	-9543	-9543
$\sigma_1$ [MPa]	-5.7	-346.8	-346.8
Temperature	Maximum	Minimum	Average
Temp. <sub>2</sub> [°C]	59.9	59.5	59.7
$E_{1c}$ [MPa]	34475	Young's Modulus front (comp.)	
$E_{2c}$ [MPa]	35161	Young's Modulus back (comp.)	



Test results for specimen: CB03R08

Channel	Mean Maximum	Mean Minimum	Maximum	Minimum
Force <sub>1</sub> [kN ]	31.98	3.18	32.12	3.12
Displ. <sub>1</sub> [mm]	8.84	7.36	8.90	7.19
$\epsilon_{1,0^\circ}$ [ $\mu\epsilon$ ]	28774	27454	29148	2685
$\epsilon_{2,0^\circ}$ [ $\mu\epsilon$ ]	28556	26206	29240	1426
$\sigma_1$ [MPa]	522.3	51.9	524.5	51.0
Temperature	Maximum	Minimum	Average	
Temp. <sub>2</sub> [ ° C]	26.1	23.8	25.3	
Number of Cycles	12006			

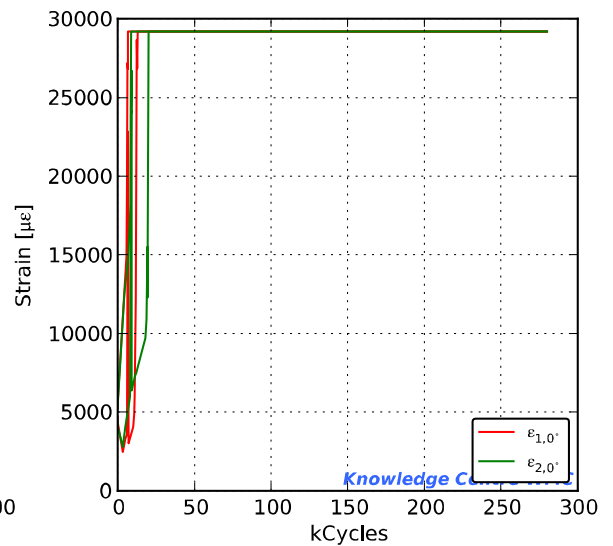
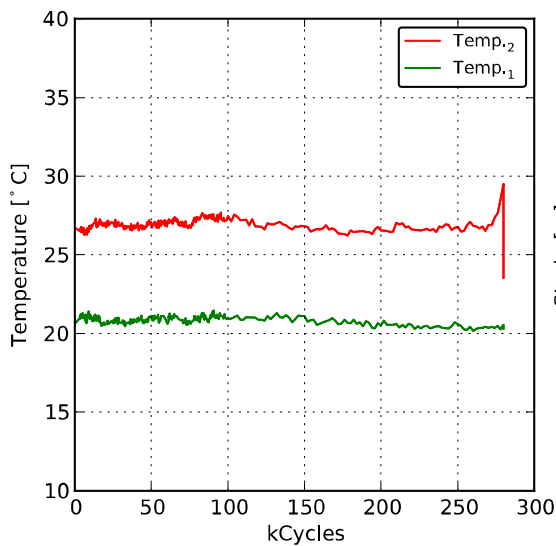
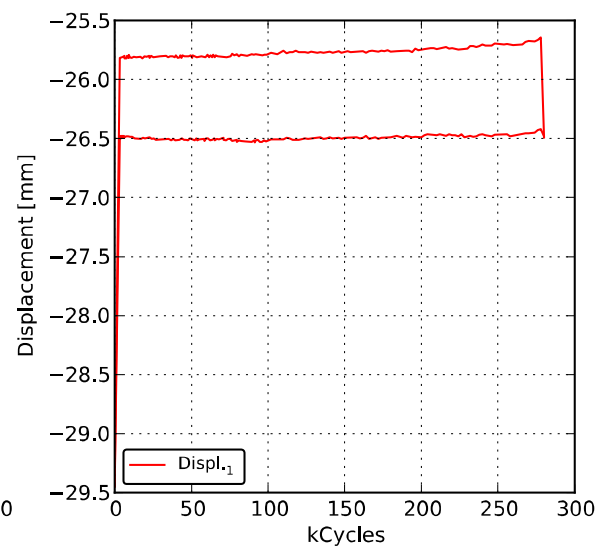
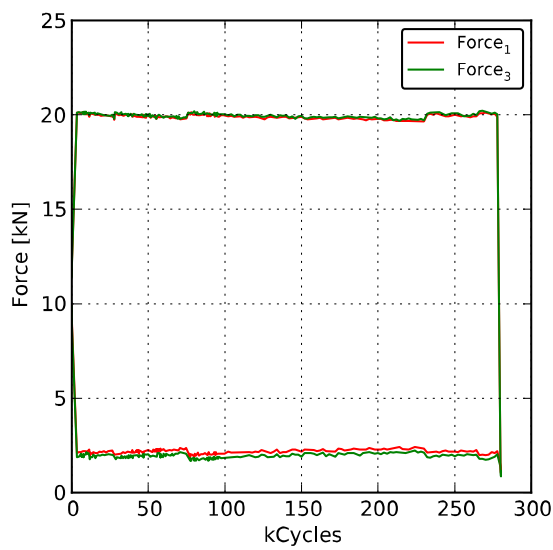


Knowledge Centre WMC



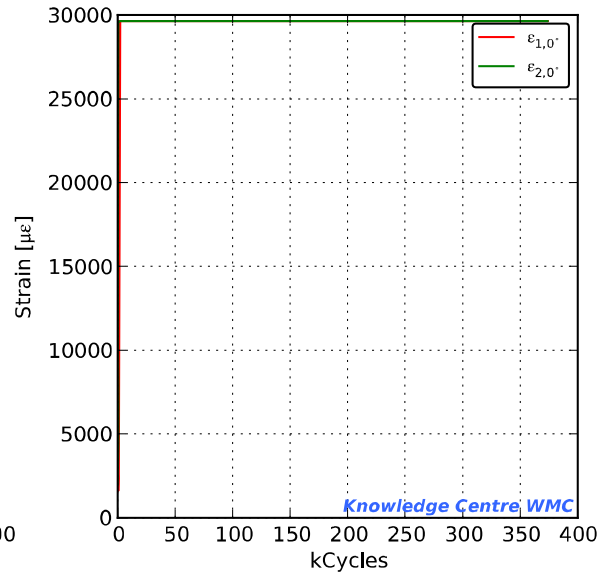
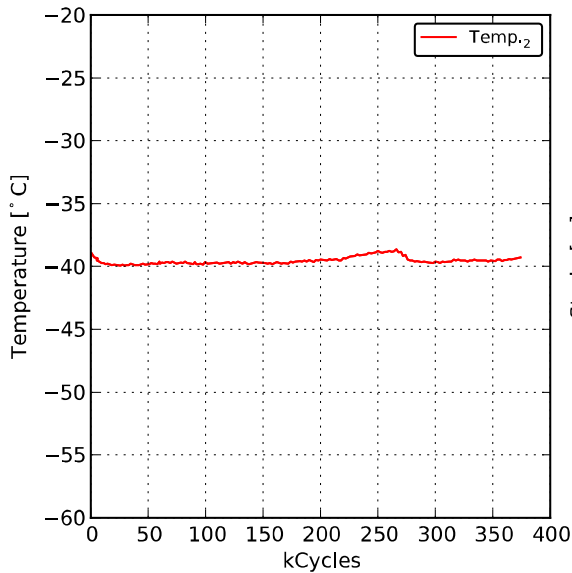
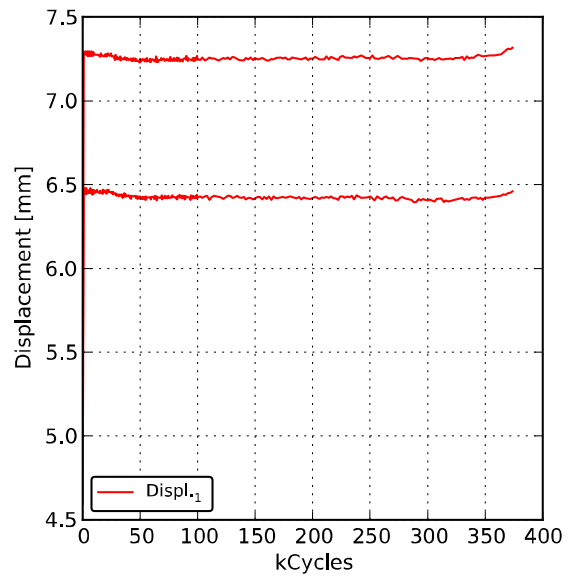
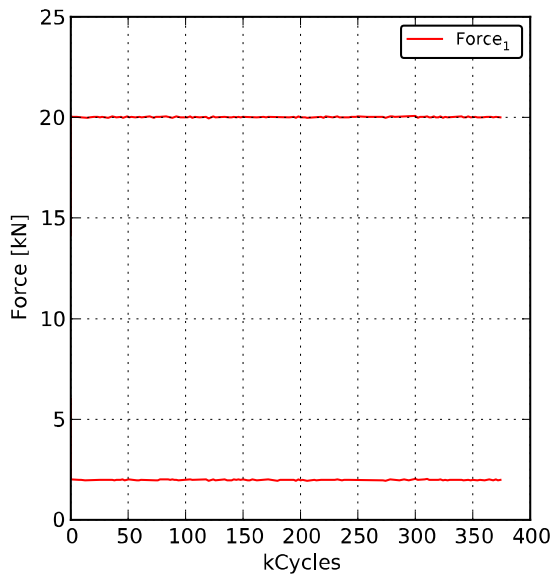
Test results for specimen: DD22R08

Channel	Mean Maximum	Mean Minimum	Maximum	Minimum
Force <sub>1</sub> [kN ]	19.76	2.18	20.18	1.03
Displ. <sub>1</sub> [mm]	-25.77	-26.49	-25.64	-29.45
Force <sub>3</sub> [kN ]	19.82	1.96	20.22	0.87
ε <sub>1,0'</sub> [με]	28795	28125	29182	2461
ε <sub>2,0'</sub> [με]	28714	27650	29190	2778
σ <sub>1</sub> [MPa]	322.6	35.6	329.5	16.7
Temperature	Maximum	Minimum	Average	
Temp. <sub>2</sub> [ ° C]	29.5	23.5	26.9	
Temp. <sub>1</sub> [ ° C]	21.5	20.2	20.7	
Number of Cycles	280213			



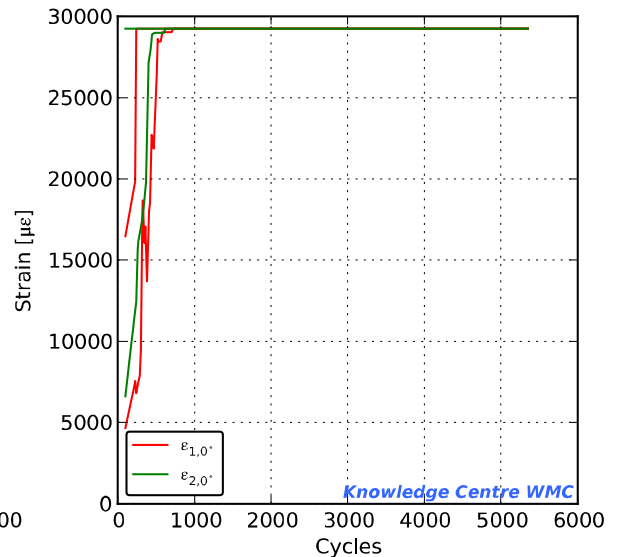
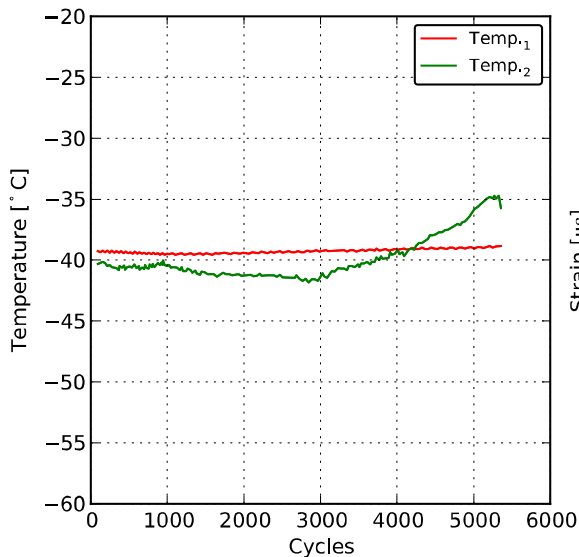
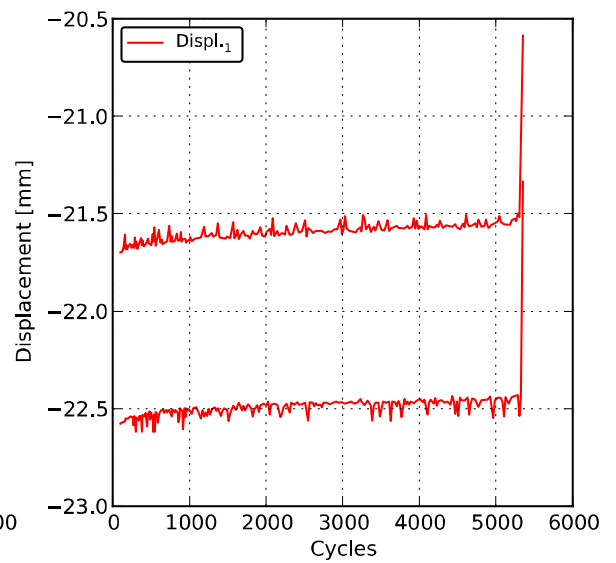
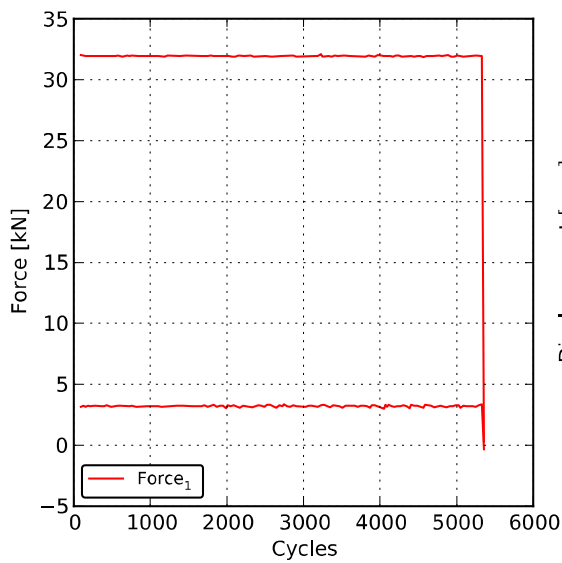
Test results for specimen: CW25R08

Channel	Mean Maximum	Mean Minimum	Maximum	Minimum
Force <sub>1</sub> [kN ]	20.02	1.98	20.09	1.90
Displ. <sub>1</sub> [mm]	7.26	6.42	7.32	4.59
$\epsilon_{1,0^\circ}$ [ $\mu\epsilon$ ]	29591	29518	29644	1547
$\epsilon_{2,0^\circ}$ [ $\mu\epsilon$ ]	29628	29608	29649	470
$\sigma_1$ [MPa]	324.5	32.1	325.6	30.8
Temperature	Maximum	Minimum	Average	
Temp. <sub>2</sub> [° C]	-38.6	-40.0	-39.5	
Number of Cycles	374004			



Test results for specimen: DQ21R08

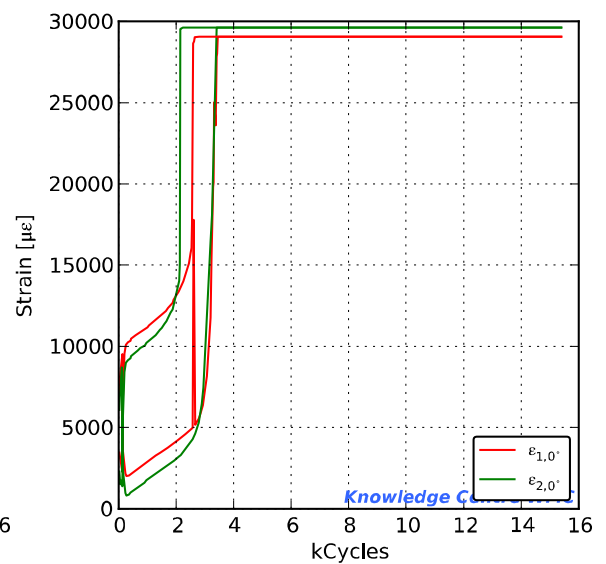
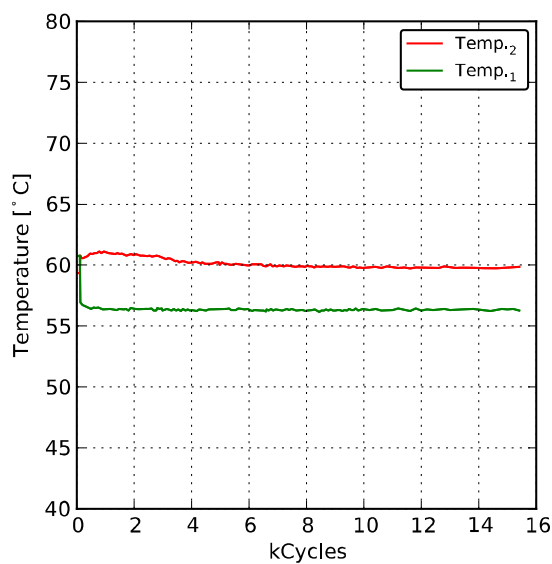
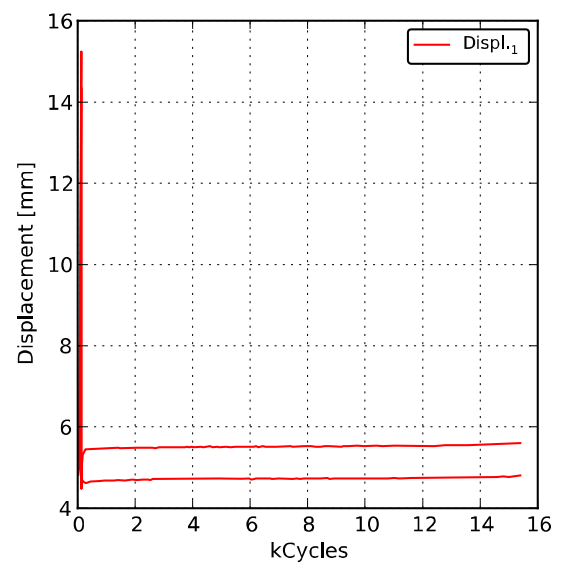
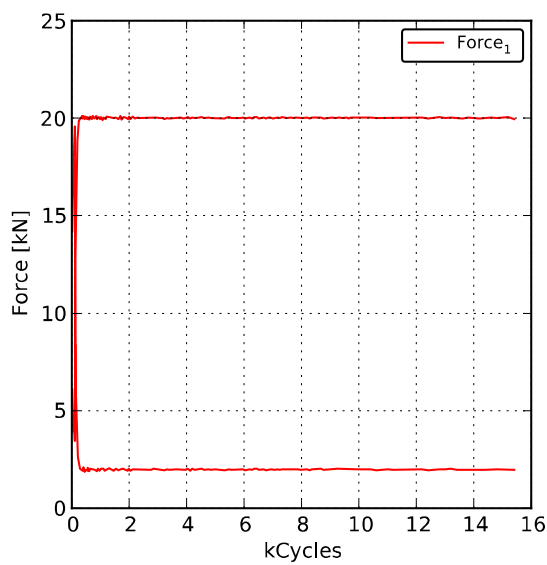
Channel	Mean Maximum	Mean Minimum	Maximum	Minimum
Force <sub>1</sub> [kN ]	31.20	3.13	32.10	-0.33
Displ. <sub>1</sub> [mm]	-21.19	-22.07	-20.59	-22.62
$\epsilon_{1,0^\circ}$ [ $\mu\epsilon$ ]	28444	27472	29245	4672
$\epsilon_{2,0^\circ}$ [ $\mu\epsilon$ ]	28711	27868	29246	6634
$\sigma_1$ [MPa]	509.4	51.2	524.1	-5.4
Temperature	Maximum	Minimum	Average	
Temp. <sub>1</sub> [° C]	-38.8	-39.6	-38.5	
Temp. <sub>2</sub> [° C]	-34.7	-41.8	-39.2	
Number of Cycles	5355			



Knowledge Centre WMC

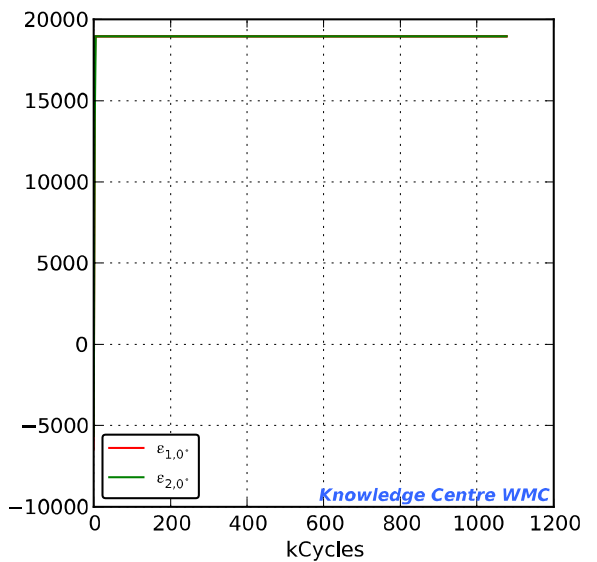
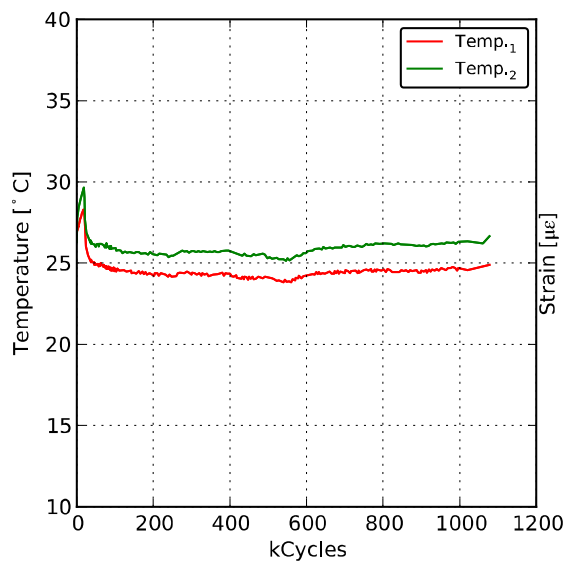
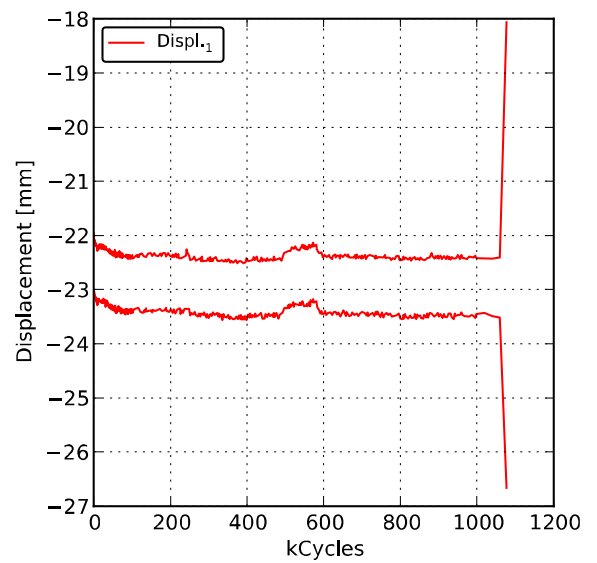
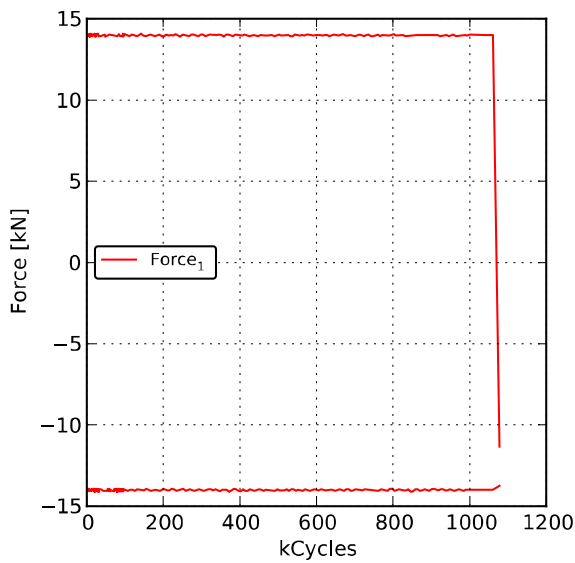
Test results for specimen: DD03R08

Channel	Mean Maximum	Mean Minimum	Maximum	Minimum
Force <sub>1</sub> [kN ]	19.95	2.01	20.16	1.85
Displ. <sub>1</sub> [mm]	5.53	4.74	15.25	4.48
$\epsilon_{1,0}$ [ $\mu\epsilon$ ]	26185	23803	29050	1963
$\epsilon_{2,0}$ [ $\mu\epsilon$ ]	26981	24107	29634	781
$\sigma_1$ [MPa]	320.3	32.2	323.6	29.7
Temperature	Maximum	Minimum	Average	
Temp. <sub>2</sub> [° C]	61.1	59.3	60.0	
Temp. <sub>1</sub> [° C]	60.9	56.1	56.3	
Number of Cycles	15402			



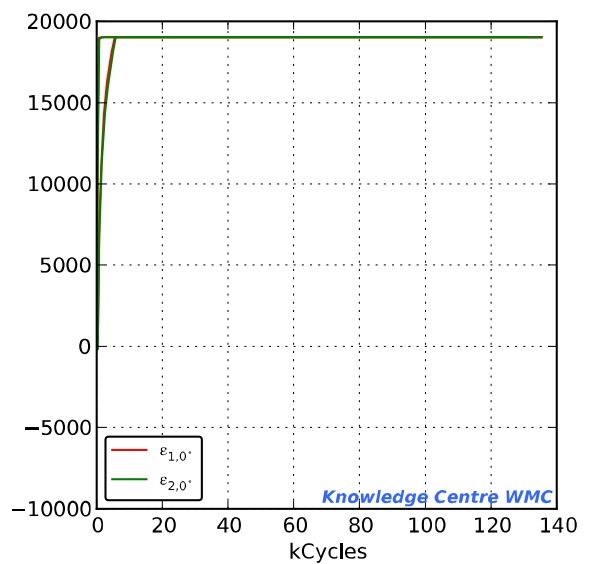
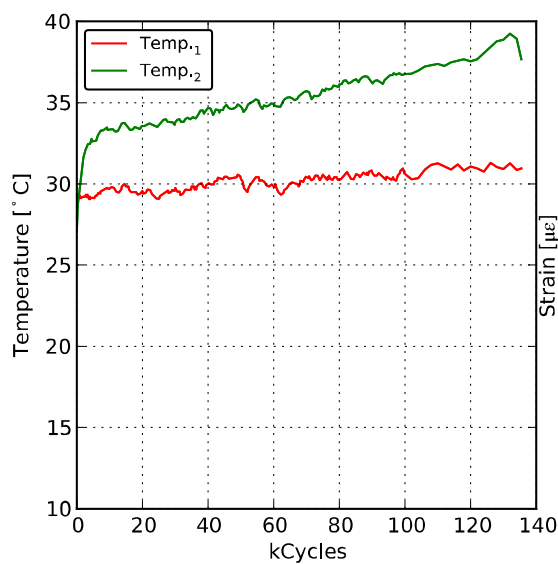
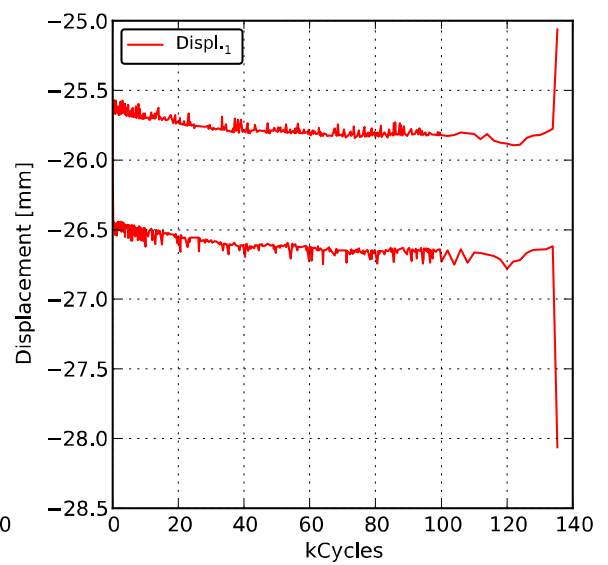
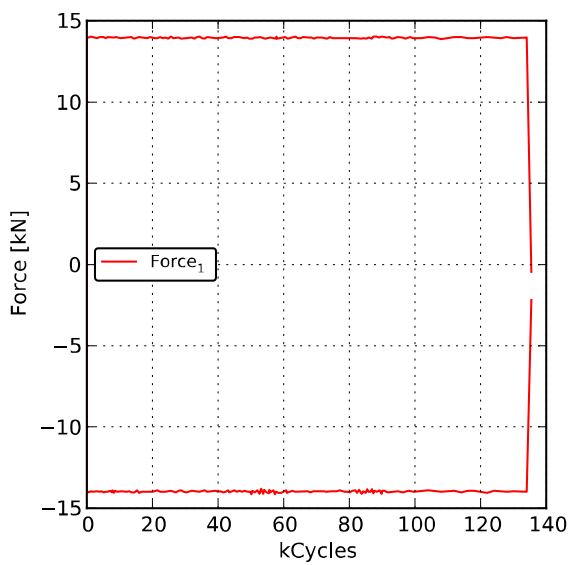
Test results for specimen: LN05R08

Channel	Mean Maximum	Mean Minimum	Maximum	Minimum
Force <sub>1</sub> [kN ]	13.57	-14.01	14.10	-14.16
Displ. <sub>1</sub> [mm]	-22.32	-23.48	-18.06	-26.66
$\epsilon_{1,0^\circ}$ [ $\mu\epsilon$ ]	18961	18945	18963	-6486
$\epsilon_{2,0^\circ}$ [ $\mu\epsilon$ ]	18963	18938	18966	-5645
$\sigma_1$ [MPa]	248.5	-256.5	258.2	-259.3
Temperature	Maximum	Minimum	Average	
Temp. <sub>1</sub> [° C]	28.4	23.8	24.5	
Temp. <sub>2</sub> [° C]	29.7	25.1	25.9	
Number of Cycles	1077612			



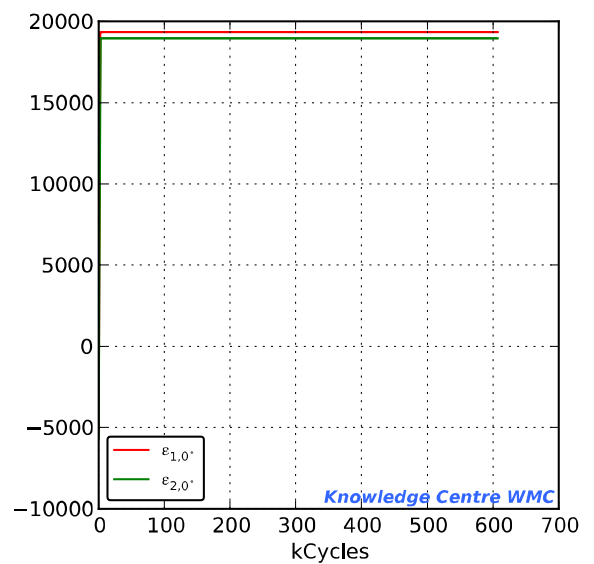
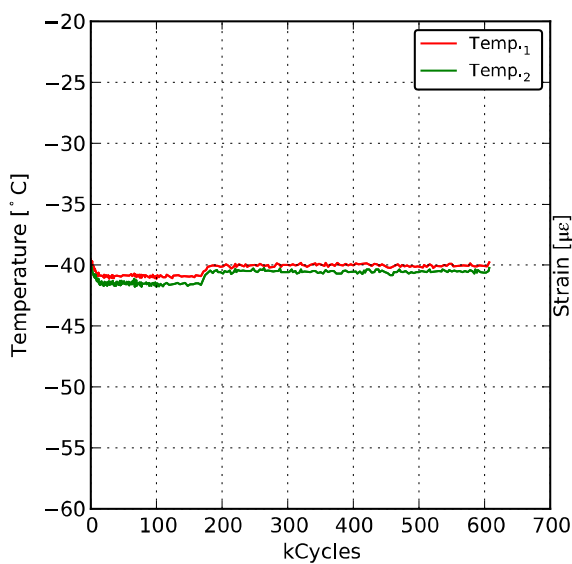
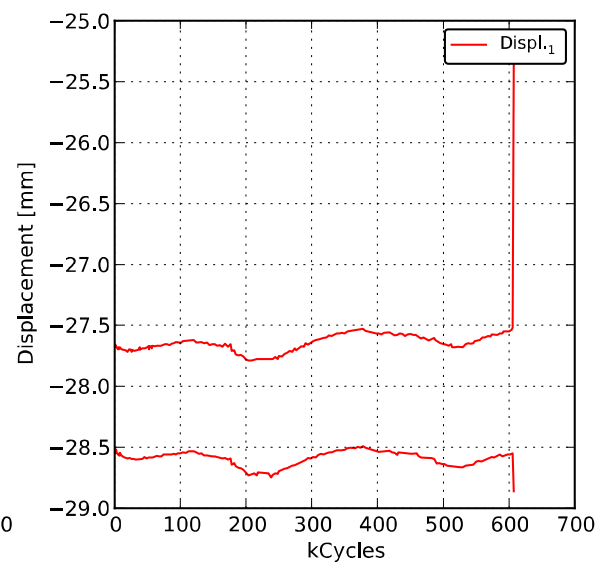
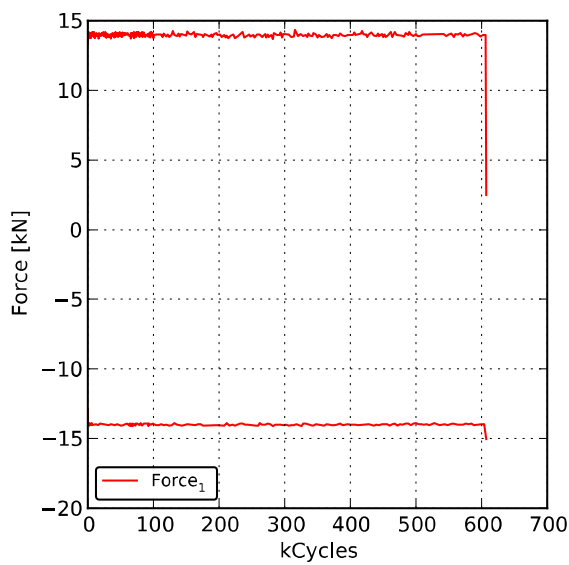
Test results for specimen: DQ25R08

Channel	Mean Maximum	Mean Minimum	Maximum	Minimum
Force <sub>1</sub> [kN ]	13.81	-13.86	14.06	-14.15
Displ. <sub>1</sub> [mm]	-25.78	-26.64	-25.06	-28.06
$\epsilon_{1,0^\circ}$ [ $\mu\epsilon$ ]	18997	18805	19019	-5113
$\epsilon_{2,0^\circ}$ [ $\mu\epsilon$ ]	18990	18779	19019	-5281
$\sigma_1$ [MPa]	227.8	-228.5	231.8	-233.3
Temperature	Maximum	Minimum	Average	
Temp. <sub>1</sub> [° C]	31.3	29.0	30.2	
Temp. <sub>2</sub> [° C]	39.2	27.0	35.5	
Number of Cycles	135385			



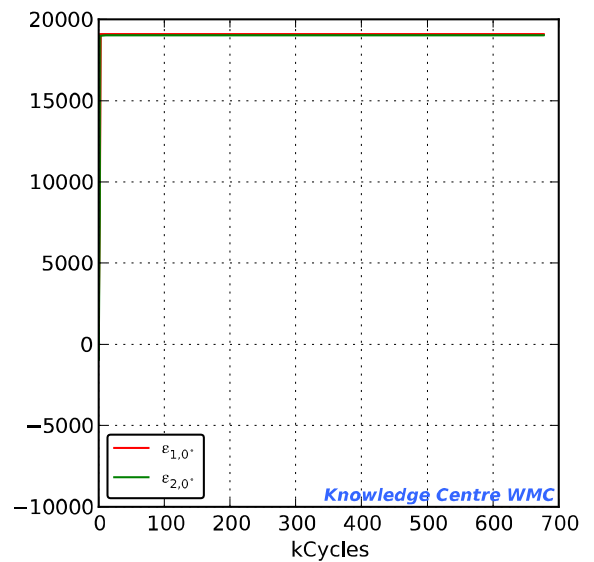
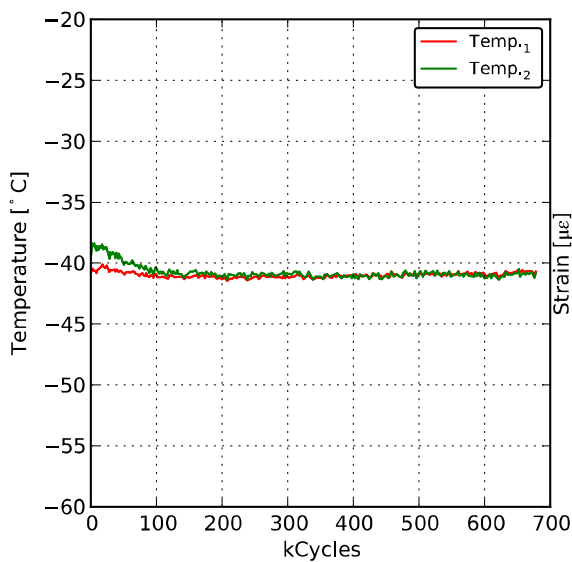
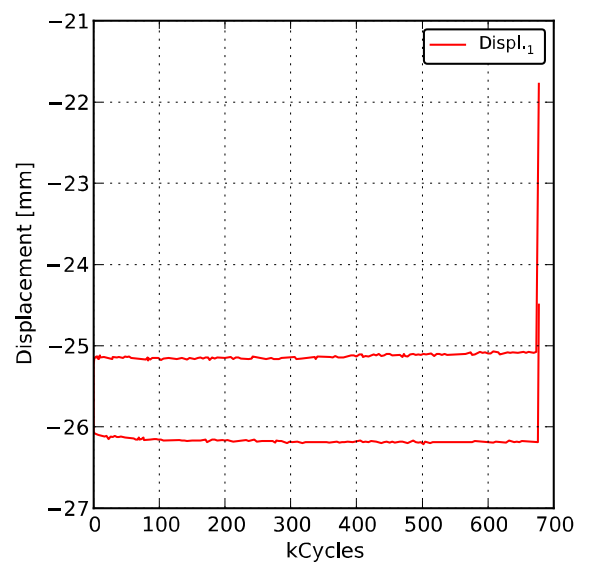
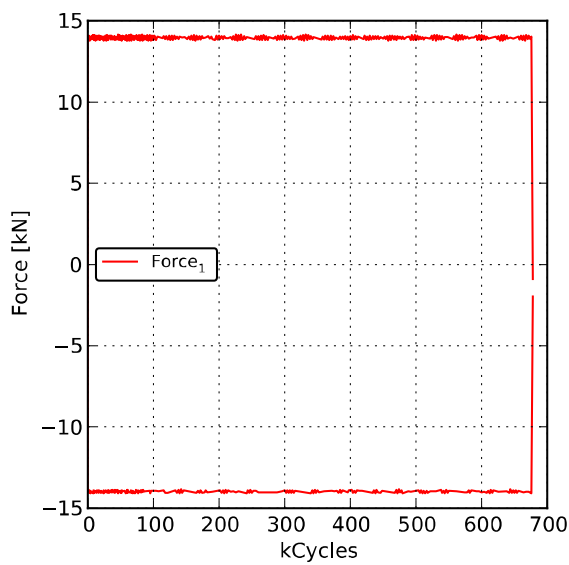
Test results for specimen: DV11R08

Channel	Mean Maximum	Mean Minimum	Maximum	Minimum
Force <sub>1</sub> [kN]	13.95	-14.00	14.33	-15.03
Displ. <sub>1</sub> [mm]	-27.64	-28.59	-25.36	-28.86
ε <sub>1,0°</sub> [με]	19327	19299	19331	-5438
ε <sub>2,0°</sub> [με]	18954	18920	18959	-5820
σ <sub>1</sub> [MPa]	232.2	-233.0	238.5	-250.1
Temperature	Maximum	Minimum	Average	
Temp. <sub>1</sub> [°C]	-39.4	-41.1	-40.3	
Temp. <sub>2</sub> [°C]	-39.8	-41.8	-40.8	
Number of Cycles	607278			



Test results for specimen: DV29R08

Channel	Mean Maximum	Mean Minimum	Maximum	Minimum
Force <sub>1</sub> [kN]	13.92	-13.95	14.16	-14.12
Displ. <sub>1</sub> [mm]	-25.12	-26.17	-21.78	-26.21
$\epsilon_{1,0^\circ}$ [ $\mu\epsilon$ ]	19079	19046	19085	-3848
$\epsilon_{2,0^\circ}$ [ $\mu\epsilon$ ]	19009	18977	19016	-5795
$\sigma_1$ [MPa]	229.4	-230.0	233.4	-232.7
Temperature	Maximum	Minimum	Average	
Temp. <sub>1</sub> [°C]	-40.1	-41.4	-41.0	
Temp. <sub>2</sub> [°C]	-38.2	-41.4	-40.8	
Number of Cycles	677803			

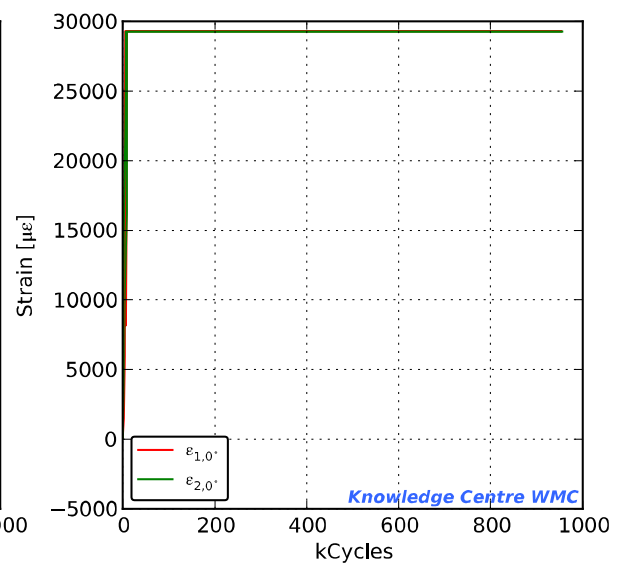
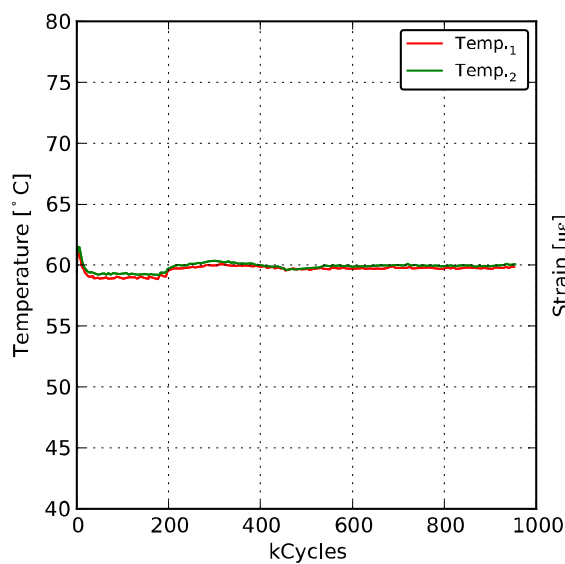
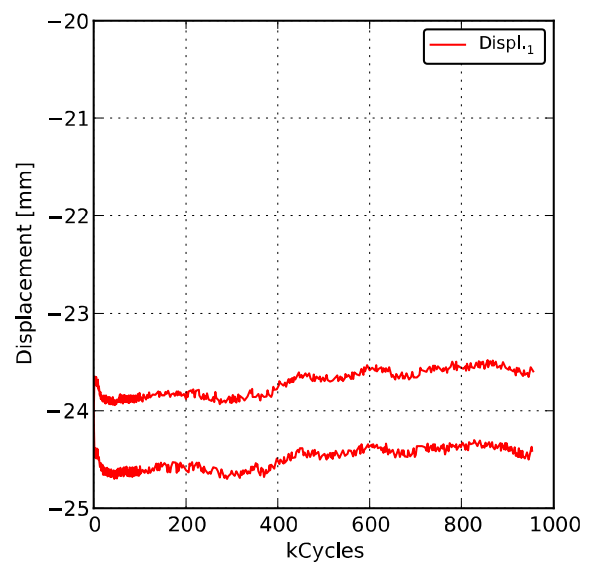
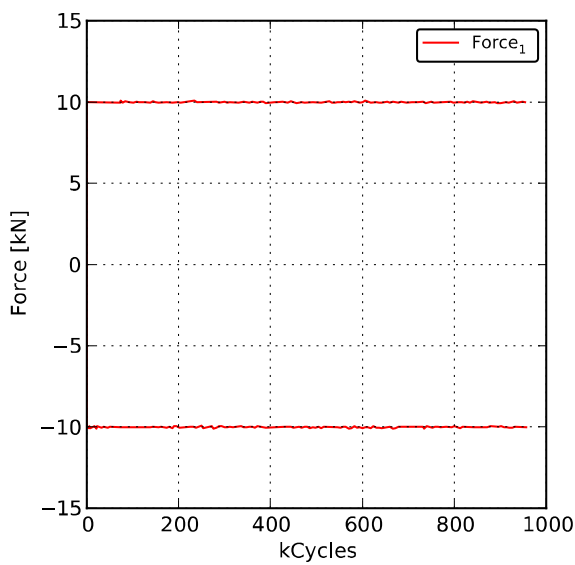


Knowledge Centre WMC

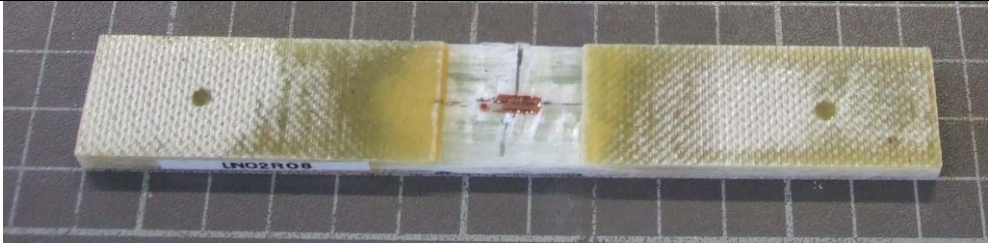
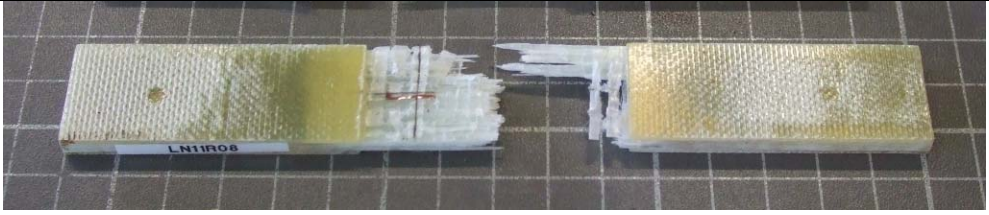


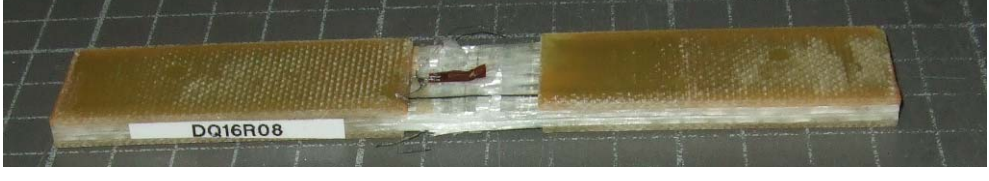



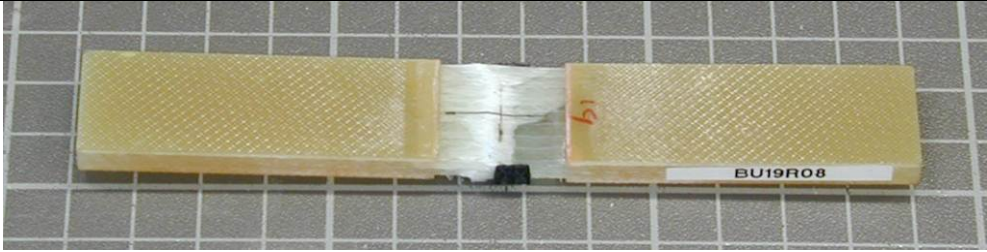
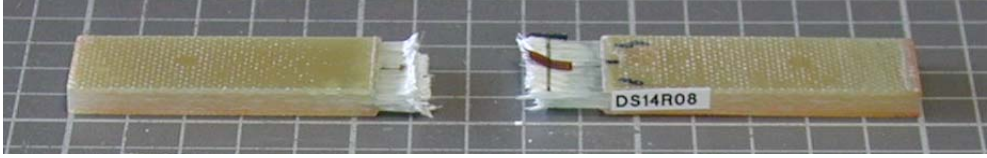


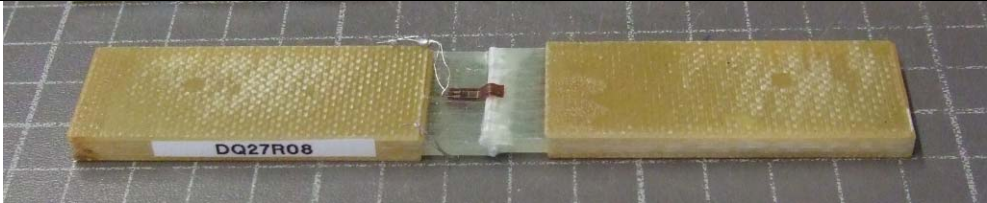
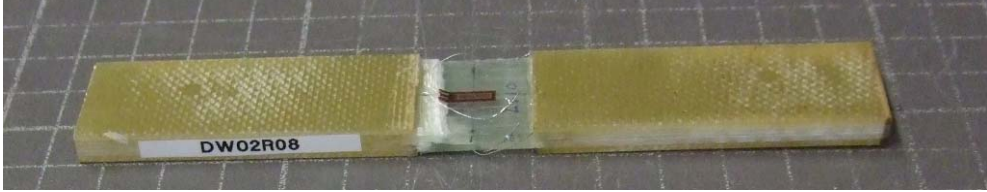
Test results for specimen: DW20R08

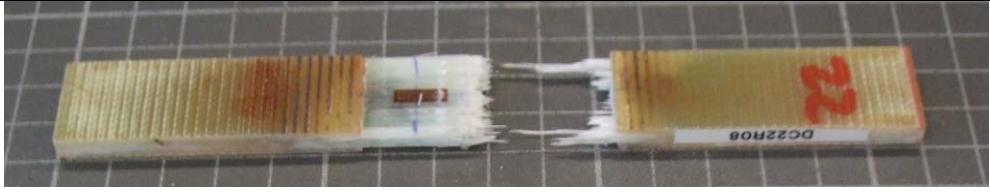





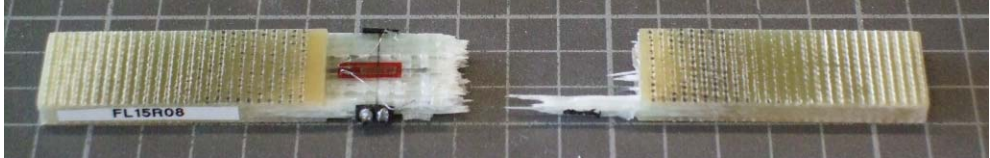
Channel	Mean Maximum	Mean Minimum	Maximum	Minimum
Force <sub>1</sub> [kN ]	9.99	-10.01	10.10	-10.12
Displ. <sub>1</sub> [mm]	-23.71	-24.49	-23.48	-24.70
ε <sub>1,0°</sub> [µε]	29238	29125	29323	-4140
ε <sub>2,0°</sub> [µε]	29194	29091	29270	-4746
σ <sub>1</sub> [MPa]	165.4	-165.9	167.2	-167.7
Temperature	Maximum	Minimum	Average	
Temp. <sub>1</sub> [ ° C]	61.2	58.8	59.6	
Temp. <sub>2</sub> [ ° C]	61.6	59.2	59.9	
Number of Cycles	956005			

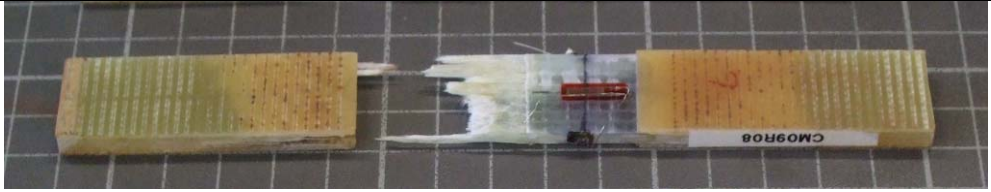

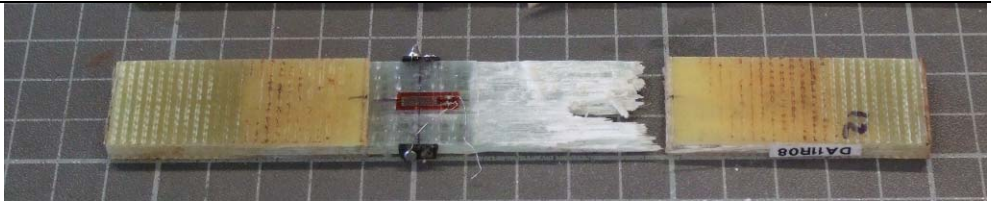






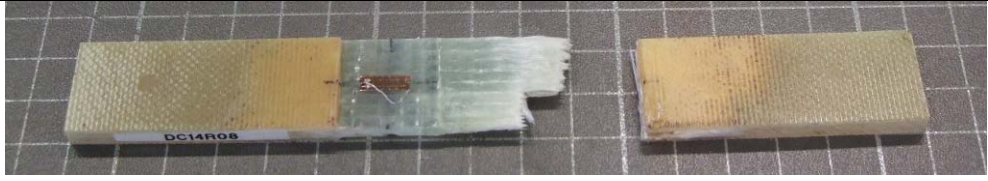
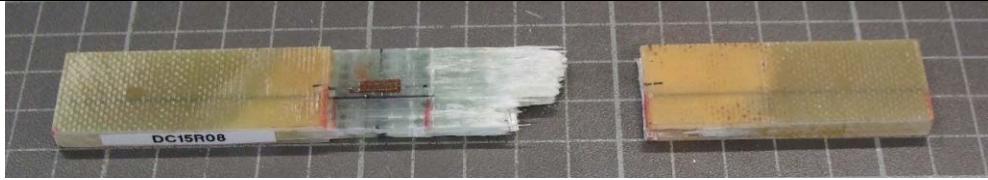
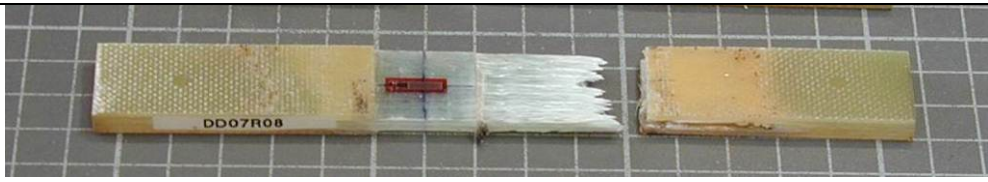
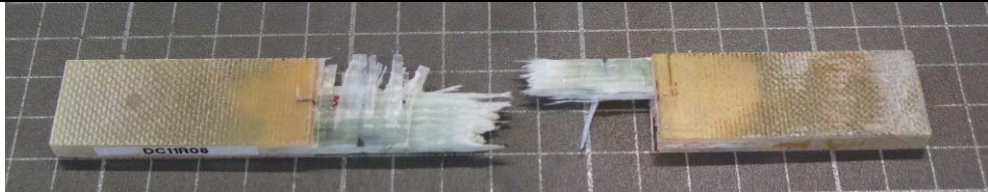
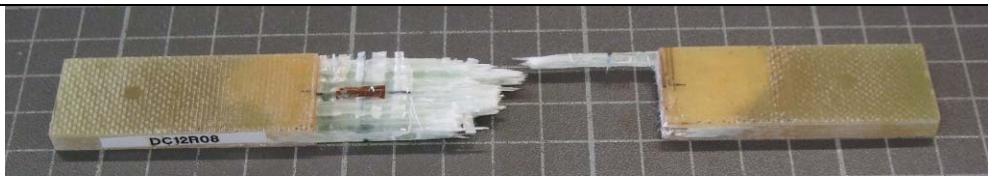

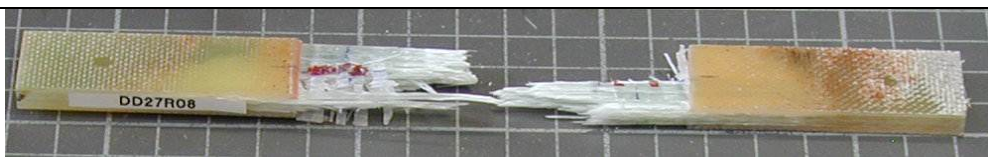
**ANNEX C Selected specimen pictures after testing**

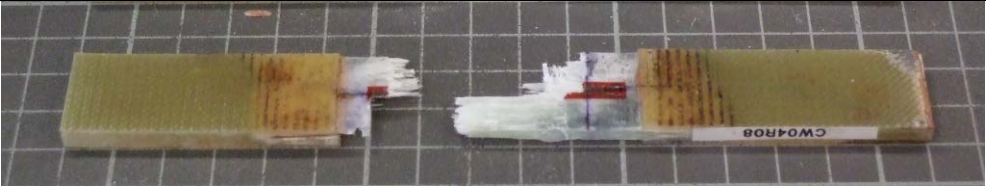

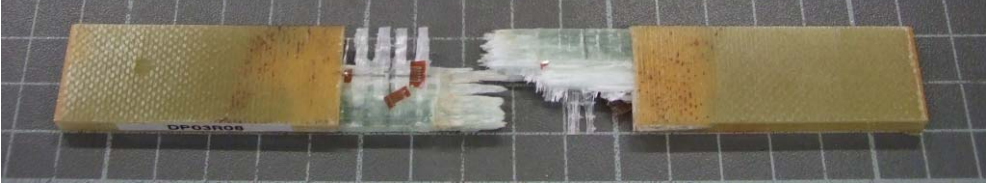
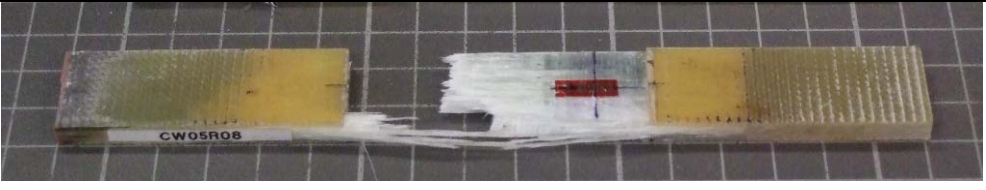
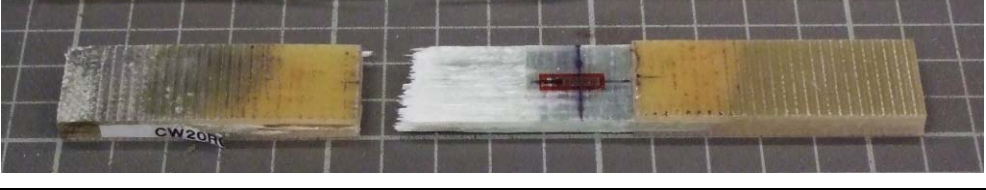
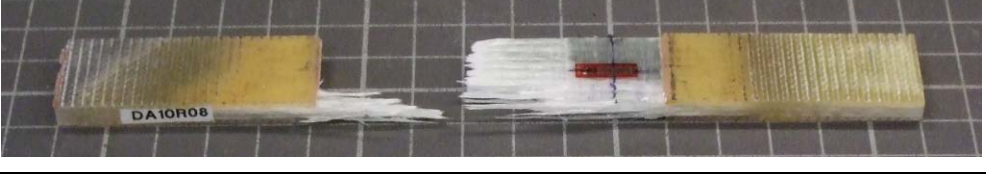
Static tension; 23 °C	
LN02R08	
LN11R08	
Static tension; -40 °C	
ET20R08	
EV24R08	
Static tension; 60 °C	
DQ16R08	
DV25R08	

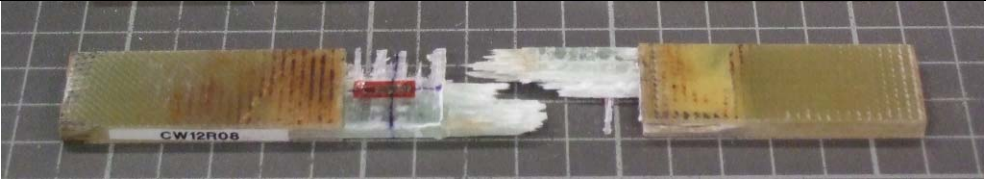
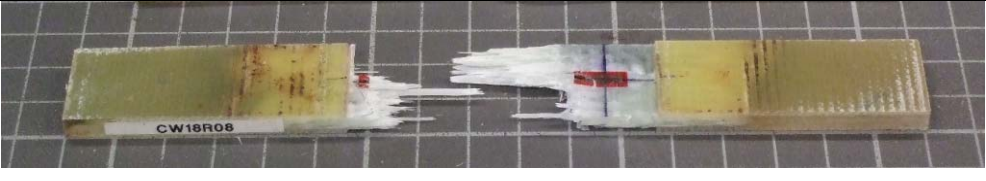
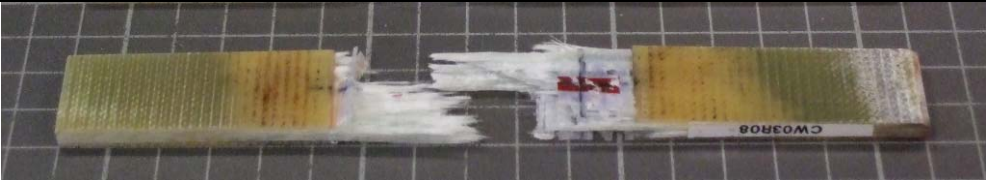
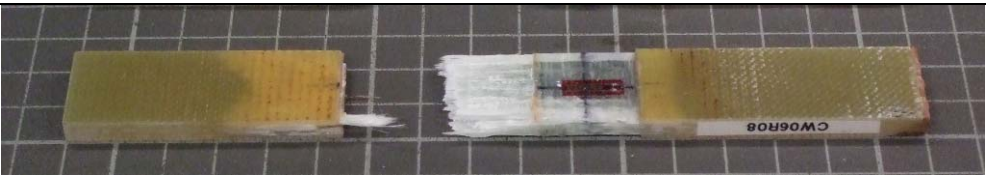
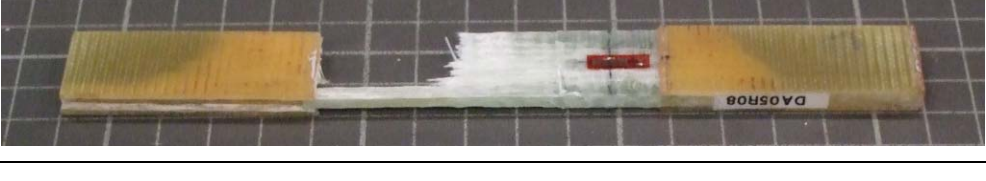
Static compression; 23 °C	
BU19R08	
DS14R08	
Static compression; -40 °C	
DP26R08	
DV21R08	
Static compression; 60 °C	
DQ27R08	
DW02R08	

R=0.1; 23 °C; CA; 2-20 kN	
D22R08	
DV20R08	
DV22R08	
R=0.1; 23 °C; CA; 3.2-32 kN	
CB03R08	
DQ06R08	
DQ23R08	
FL15R08	


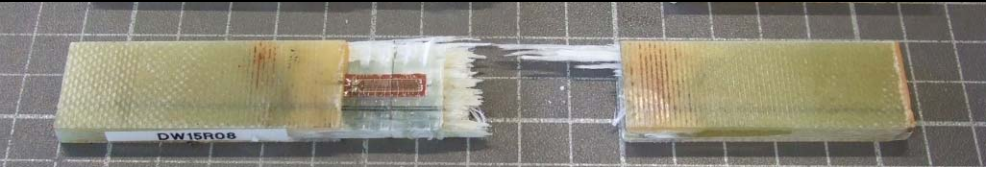

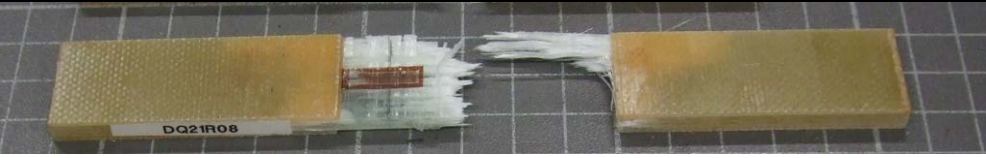


R=0.1; 23 °C; CAM; 2-20 kN	
CM09R0 8	
DA07R08	
DA11R08	
R=0.1; 23 °C; CAM; 3.2-32 kN	
CB11R08	
CB15R08	
CB21R08	
CB29R08	

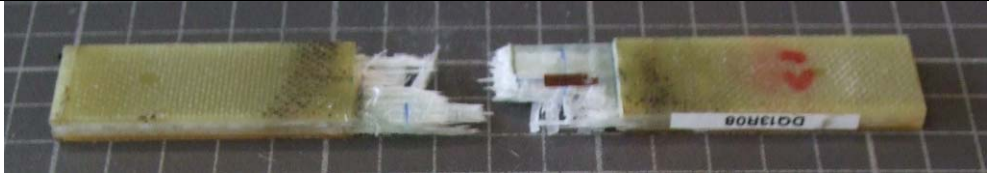

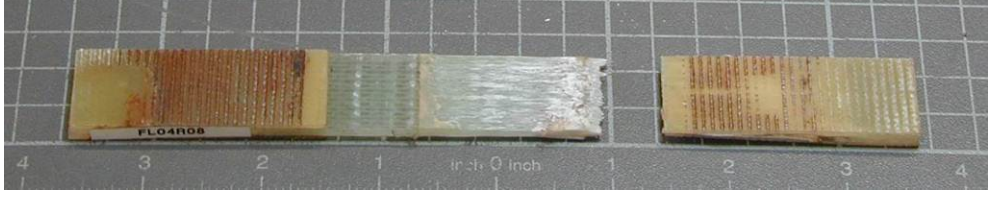
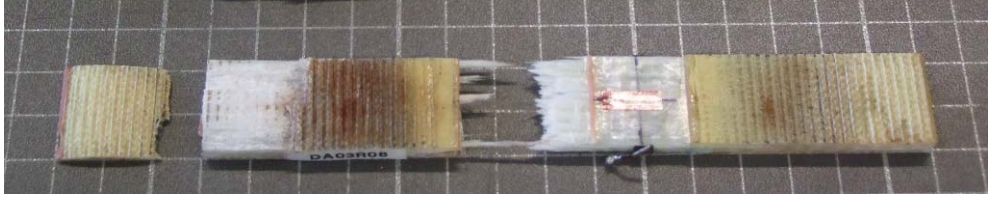

R=0.1; 23 °C; CAH; Low load	
Dc14R08	
DC15R08	
DD07R08	
R=0.1; 23 °C; CAH; High load	
DC11R08	
DC12R08	
DD21R08	
DD27R08	





R=0.1; -40 °C; CA; 2-20 kN	
CW04R08	
CW09R08	
DP03R08	
R=0.1; -40 °C; CA; 3.2-32 kN	
CW05R08	
CW20R08	
DA10R08	

R=0.1; ; -40 °C; CAM; 2-20 kN	
CW12R08	
CW18R08	
R=0.1; -40 °C; CAM; 3.2-32 kN	
CW03R08	
CW06R08	
DA05R08	



R=0.1; -40 °C; CAH; 2-20 kN	
DQ07R08	
DW15R08	
DW17R08	
R=0.1; -40 °C; CAH; 3.2-32 kN	
DQ21R08	
DW03R08	
DW06R08	

R=0.1; 60 °C; CA; 2-20 kN	
DQ13R08	
DW26R08	
FL04R08 (1.8-18 kN)	
R=0.1; 60 °C; CA; 3.2-32 kN	
DA03R08	
DD09R08	

R=-1; 23 °C; CA; ±14 kN	
Dc016R0 8	
LN05R08	
LN14R08	
LN20R08	

R=-1; 23 °C; CA; ±24 kN

DC05R08



DC08R08



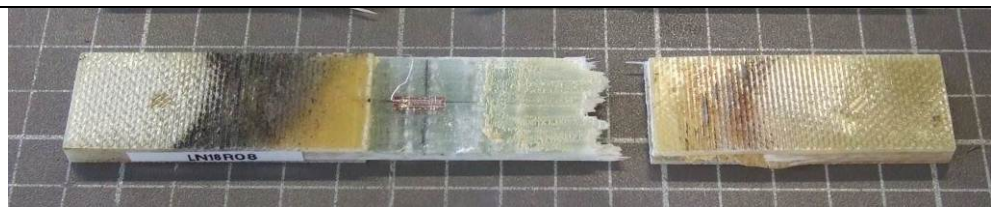
DC19R08


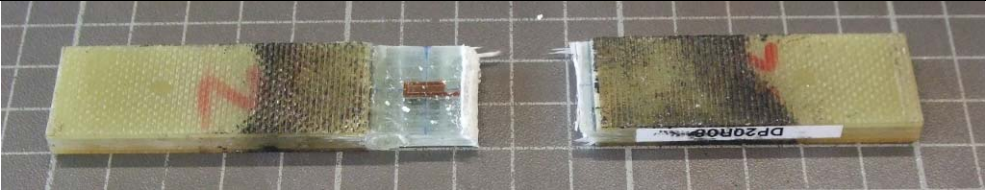












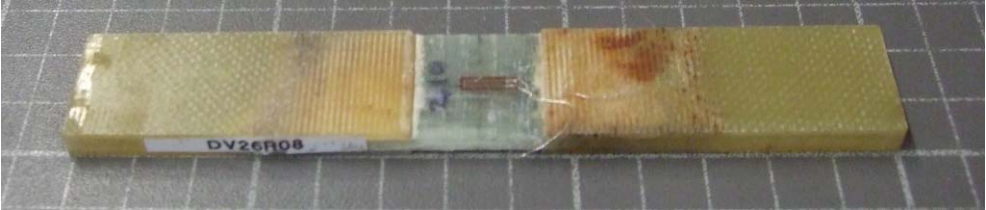

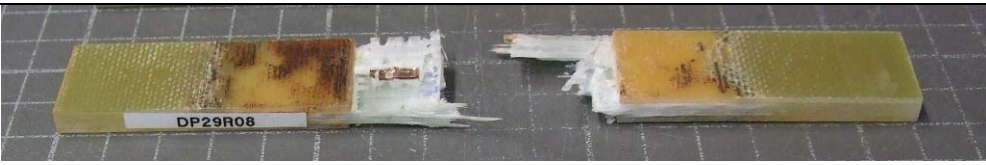

LN15R08















LN18R08






R=-1; 23 °C; CAH; ±14 kN	
DP17R08	
DP20R08	
DQ25R08	
R=-1; 23 °C; CAH; ±24 kN	
DP12R08	
DV06R08	
DW16R08	
DW16R08	



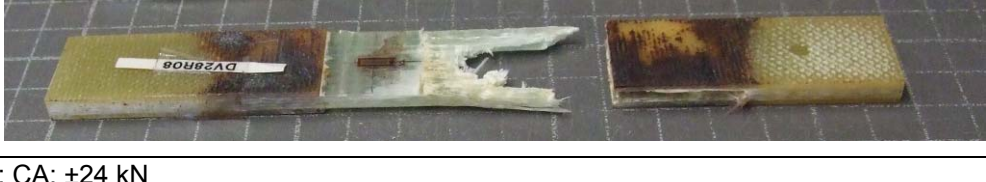
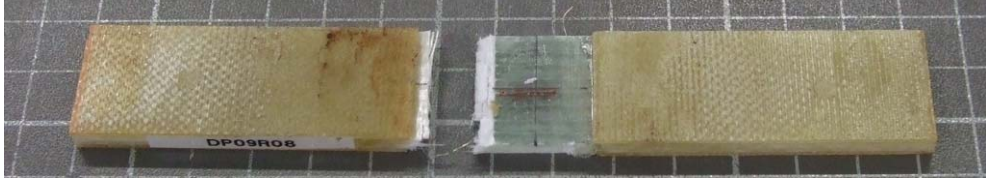
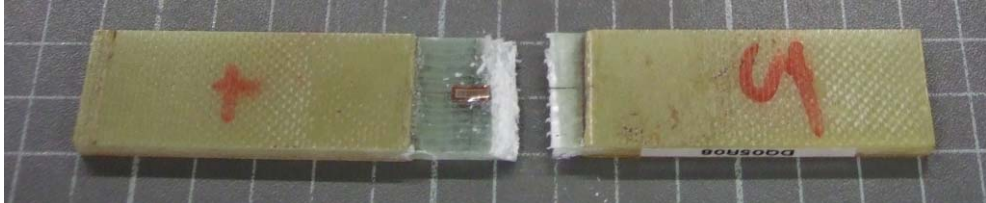

R=-1; -40 °C; CA; ±14 kN	
DP25R08	
DQ14R08	
DQ20R08	
DV11R08	
DV12R08	
DV26R08	
DW30R08	
R=-1; -40 °C; CA; ±24 kN	
DP29R08	
DQ17R08	

DV01R08	
DW04R08	
DW27R08	

R=-1; -40 °C; CAH; ±14 kN	
DP21R08	
DQ19R08	
DQ26R08	
DV29R08	
DW01R08	
DW21R08	
R=-1; -40 °C; CAH; ±24 kN	
DP24R08	
DQ03R08	
DV05R08	



DV18R08	
DW19R08	
DW25R08	

R=-1; 60 °C; CA; ±14 kN	
DP11R08	
DV16R08	
DV28R08	
R=-1; 60 °C; CA; ±24 kN	
DP09R08	
DQ05R08	
DV23R08	
DV28R08	